Contents

1 Project Summary

Understanding the effects of fusion neutron irradiation on the mechanical properties of structural materials is undoubtedly pivotal to the successful development of reliable, safe and economical fusion energy sources. Recent advances in computer modeling and simulations of the mechanics of materials at the nano- and micro- scales are providing unprecedented opportunities for the fusion materials program. The *Multiscale Modeling of Materials (MMM)* approach, which relies on a systematic, yet rigorous reduction of the degrees of freedom at natural length scales is a cornerstone of the present proposal. Connections between such scales are achieved either by a parameterization or a coarse-graining procedure. Parameters that describe the system at a lower length scale are obtained from computer simulations, verified experimentally, and passed on to upper scales. The main motivation behind this proposal is to provide the science underpinnings for the design of radiation-resistant structural materials, and to plan for meaningful experiments that can be understood through physical models of deformation and fracture phenomena.

The objective of this proposal is to develop a range of hierarchical models for the post-elastic deformation, fracture and failure of fusion structural materials. The proposed multiscale modeling approach is based on rigorous mathematical, physical, and computational methods at the forefront of computational materials science. At the fundamental and smallest length scale (nm-μm), we plan to continue our development of advanced rate theory and Monte Carlo approaches to model microstructure evolution, non-equilibrium phase transformations, and dislocation-defect interactions. Microscopic and mesoscopic models of radiation hardening, ductile-to-brittle-transition, post-elastic deformation, plastic instabilities, and fracture processes will be based on Dislocation Dynamics (DD) and Grain Growth Dynamics (GGD) . At the continuum level, we will focus on modeling fracture and failure mechanisms for Virtual Integrated Testing (VISTA), and for understanding the limits of both materials-by-design versus structural component design. We will use meshfree, parallel FEM, and coupled FEM-DD methodologies to predict failure modes, lifetimes and reliability of critical First Wall/ Blanket components. The proposed research is strongly coupled with the U.S. national experimental program to ascertain and verify the range of investigated phenomena. The following tasks are proposed for the five-year duration of the project:

1. KMC & Rate Theory Modeling of Microstructure Evolution;
2. Radiation-Induced Phase Transitions;
3. Dislocation-Defect Interaction Mechanisms;
4. Radiation Hardening & Plastic Instabilities;
5. High-Temperature Helium Embrittlement;
6. Modeling Fracture Processes;
7. Modeling the Ductile-to-Brittle Transition;
8. Participation and co-development of VISTA: a Virtual Integrated Test Assembly;
9. Development of The Digital Fusion Materials Database & Constitutive Equations.

2 Significance and Background

2.1 Deformation & Fracture: the Key to First Wall Survival

The environmental and operational conditions of First Wall/ Blanket (FW/B) structural materials in fusion energy systems are undoubtedly amongst the harshest in any technological application. These materials must operate reliably for extended periods of times without maintenance or repair. They must withstand the assaults of high particle and heat fluxes, as well as significant thermal and mechanical forces. Rival conditions have not been experienced in other technologies, with possible exceptions in aerospace and defense applications. Moreover, the most significant dilemma here is that the actual operational environment cannot be experimentally established today, with all of the synergistic considerations of neutron spectrum, radiation dose, heat and particle flux, and gigantic FW/B module sizes. Because of these considerations, we may rely on a purely empirical and incremental boot-strapping approach (as in most human developments so far), or an approach based on data generation from non prototypical setups (e.g. small samples, fission spectra, ion irradiation, etc.), or a theoretical/ computational methodology. The first approach would have been the most direct had it not been for the unacceptable risks in the construction of successively larger and more powerful fusion machines, learning from one how to do it better for the next. The last approach (theory and modeling alone) is not a very viable option, because we are not now in a position to predict materials behavior in all its aspects from purely theoretical grounds. The empirical, extrapolative approach has also proved itself to be very costly, because we cannot practically cover all types of material compositions, sizes, neutron spectra, temperatures, irradiation times, fluxes, etc.. Major efforts had to be scrapped because of our inability to encompass all of these variations simultaneously. While all three approaches must be considered for the development of fusion materials, the Multi-scale Materials Modeling (MMM) framework that we propose here can provide tremendous advantages if coupled with experimental verification at every relevant length scale.

A wide range of structural materials has been considered over the past 25-30 years for fusion energy applications (Zinkle and Ghoniem, 2000). This list includes conventional materials (e.g. austenitic stainless steel), low-activation structural materials (ferritic/martensitic steels, V-4Cr-4Ti, and SiC/SiC composites), oxide dispersion strengthened (ODS) ferritic steels, conventional high temperature refractory alloys (Nb, Ta, Cr, Mo, W alloys), titanium alloys, Ni-based super alloys, ordered intermetallics (TiAl, Fe_3Al, etc.), high-strength, high-conductivity copper alloys, and various composite materials (C/C, metal-matrix composites, etc.). Numerous factors must be considered in the selection of structural materials, including material availability, cost, fabricability, joining technology, unirradiated mechanical and thermophysical properties, radiation effects (degradation of properties), chemical compatibility and corrosion issues, safety and waste disposal aspects (decay heat, etc.), nuclear properties (impact on tritium breeding ratio, solute burnup, etc.).

Strong emphasis has been placed within the past 10-15 years on the development of three reduced-activation structural materials: ferritic/ martensitic steels containing 8-12%Cr, vanadium base alloys (e.g. V-4Cr-4Ti), and SiC/SiC composites. Recently there also has been increasing interest in reduced-activation ODS ferritic steels. Additional alloys of interest for fusion applications include copper alloys (CuCrZr, Cu-NiBe, dispersion-strengthened copper), tantalum-base alloys (e.g. Ta-8W-2Hf), niobium alloys (Nb-1Zr), molybdenum, and tungsten alloys.

It has been established, especially during the past decade, that the most important considerations in structural material selection, increasing the useful operating temperature-dose design window, and component lifetime or reliability are all governed by deformation and fracture phenomena. In the following, we give a brief analysis of the most limiting mechanical properties based on our earlier work (Zinkle and Ghoniem, 2000).

2.1.1 Lower operating temperature limits

The lower temperature limits for FW/B structural materials (i.e. excluding copper alloys) are strongly influenced by radiation effects. For body-centered cubic (BCC) materials such as ferritic-martensitic steels and the refractory alloys, radiation hardening at low temperatures can lead to a large increase in the Ductile-To-Brittle-Transition-Temperature (DBTT)(Hishinuma, Kohyama, Klueh, Gelles, Dietz and Ehrlich, 1998; Cox and Wiffen, 1973; Klueh and Alexander, 1995; Odette and Lucas, 1983; Rieth, Dafferner and Röhrig, 1998). For SiC/SiC composites, the main concerns at low temperatures are radiation-induced amorphization (with an accompanying volumetric swelling of ∼11%) (Snead, Zinkle, Hay and Osborne, 1998) and radiation-induced degradation of thermal conductivity. The radiation hardening in BCC alloys at low temperatures ($0.3T_M$) is generally pronounced, even for doses as low as ∼1 dpa (Rieth et al., 1998; Wiffen, 1973; Maksimkin, 1995; Snead, Zinkle, Alexander, Rowcliffe, Robertson and Eatherly, 1997; Zinkle and et al., 1998). The amount of radiation hardening typically decreases rapidly with irradiation temperature above $0.3\ T_M$, and radiation-induced increase in the DBTT may be anticipated to be acceptable at temperatures above $\sim 0.3T_M$. A Ludwig-Davidenkov relationship (Cox and Wiffen, 1973; Odette and Lucas, 1983) between hardening and embrittlement was used to estimate the DBTT shift with increased irradiation dose. In this model, brittle behavior occurs when the temperature dependent yield strength exceeds the cleavage stress. It is worth noting that operation at lower temperatures (i.e. within the embrittlement temperature regime) may be allowed for some low-stress fusion structural applications (depending on the value of the operational stress intensity factor relative to the fracture toughness).

Numerous studies have been performed to determine the radiation hardening and embrittlement behavior of ferritic-martensitic steels. The hardening and DBTT shift are dependent on the detailed composition of the alloy. For example, the radiation resistance of Fe-9Cr-2WVTa alloys appears to be superior (less radiation hardening) to that of Fe-9Cr-1MoVNb (Zinkle, Robertson and Klueh, 1998a; Robertson, Shiba and Rowcliffe, 1997). The radiation hardening and DBTT shift appear to approach saturation values following low temperature irradiation to doses above 1-5 dpa, although additional high-dose studies are needed to confirm this apparent saturation behavior. At higher doses under fusion conditions, the effects of He bubble accumulation on radiation hardening and DBTT need to be addressed. Experimental observations revealed brittle behavior (K_{IC} ∼30 MPa-$\sqrt{m}$) in V-(4-5)%Cr-(4-5)%Ti specimens irradiated and tested at temperatures below 400°C (Zinkle, Snead, Rowcliffe, Alexander and Gibson, 1998b; Gruber, Galvin and Chopra, 1998). From a comparison of the yield strength and Charpy impact data of unirradiated and irradiated V-(4-5)%Cr-(4-5)%Ti alloys, brittle fracture occurs when the tensile strength is higher than 700 MPa. Therefore, 400°C may be adopted as the minimum operating temperature for V-(4-5)%Cr-(4-5)%Ti alloys in fusion reactor structural applications(Zinkle and et al., 1998). Further work is needed to assess the impact (if any) of fusion-relevant He generation rates on the radiation hardening and embrittlement behavior of vanadium alloys.

Very little information is available on the mechanical properties of irradiated W alloys. Tensile elongation of ~ 0 have been obtained for W irradiated at relatively low temperatures of 400 and 500°C (0.18-0.21 T_M) and fluences of $0.5 - 1.5 \times 10^{26}$ n/m^2 ($\prec$2 dpa in tungsten) (Wiffen, 1984; Steichen, 1976; Gorynin and et al., 1992). Severe embrittlement (DBTT $\geq$ 900°C) was observed in un-notched bend bars of W and W-10%Re irradiated at 300°C to a fluence of 0.5×10^{26} n/m^2 ($\prec$ 1 dpa)(Krautwasser and Derz, 1976). Since mechanical properties data are not available for pure tungsten or its alloys irradiated at high temperatures, an accurate estimate of the DBTT versus irradiation temperature cannot be made. The minimum operating temperature which avoids severe radiation hardening embrittlement is expected to be 900 ± 100°C.

2.1.2 Upper operating temperature limits

The upper temperature limit for structural materials in fusion reactors may be controlled by four different mechanisms (in addition to safety considerations): Thermal creep, high temperature helium embrittlement, void swelling, and compatibility: corrosion issues. Void swelling is not anticipated to be significant in ferritic-martensitic steel (Gelles, 1996) or V-Cr-Ti alloys (Loomis and Smith, 1992) up to damage levels in excess of 100 dpa, although swelling data with fusion-relevant He:dpa generation rates are needed to confirm this expectation and to determine the lifetime dose associated with void swelling. The existing fission reactor database on high temperature (Mo, W, Ta) refractory alloys (e.g. (Wiffen, 1984)) indicates low swelling ($\prec$2%) for doses up to 10 dpa or higher. Radiation-enhanced recrystallization (potentially important for stress-relieved Mo and W alloys) and radiation creep effects (due to a lack of data for the refractory alloys and SiC) need to be investigated. Void swelling is considered to be of particular importance for SiC (and also Cu alloys, which were shown to be unattractive fusion structural materials (Zinkle and Ghoniem, 2000)).

An adequate experimental database exists for thermal creep of ferritic-martensitic steels (Shiba, Hishinuma, Tohyama and Masamura, 1997) and the high temperature (Mo, W, Nb, Ta) refractory alloys (Goldberg, 1969; Conway, 1984; McCoy, 1986). Oxide-dispersion-strengthened ferritic steels offer significantly higher thermal creep resistance compared to ferritic-martensitic steels (Ukai, Nishida, Okuda and Yoshitake, 1998; Maziasz and et al., 1999), with a steady-state creep rate at 800°C as low as 3×10^{-10} s^{-1} for an applied stress of 140 MPa (Maziasz and et al., 1999). The V-4Cr-4Ti creep data suggest that the upper temperature limit lies between 700 and 750°C, although strengthening effects associated with the pickup of 200-500 ppm oxygen during testing still need to be examined. The predicted thermal creep temperature limit for advanced crystalline SiC-based fibers is above 1000°C (Youngblood, Jones, Morscher and Kohyama, 1997).

One convenient method to determine the dominant creep process for a given stress and temperature is to construct an Ashby deformation map (Ashby, 1972). Using the established constitutive equations for grain boundary sliding (Coble creep), dislocation creep (power law creep) and self-diffusion (Nabarro-Herring) creep, the dominant deformation- mode regimes can be established (Zinkle and Ghoniem, 2000)

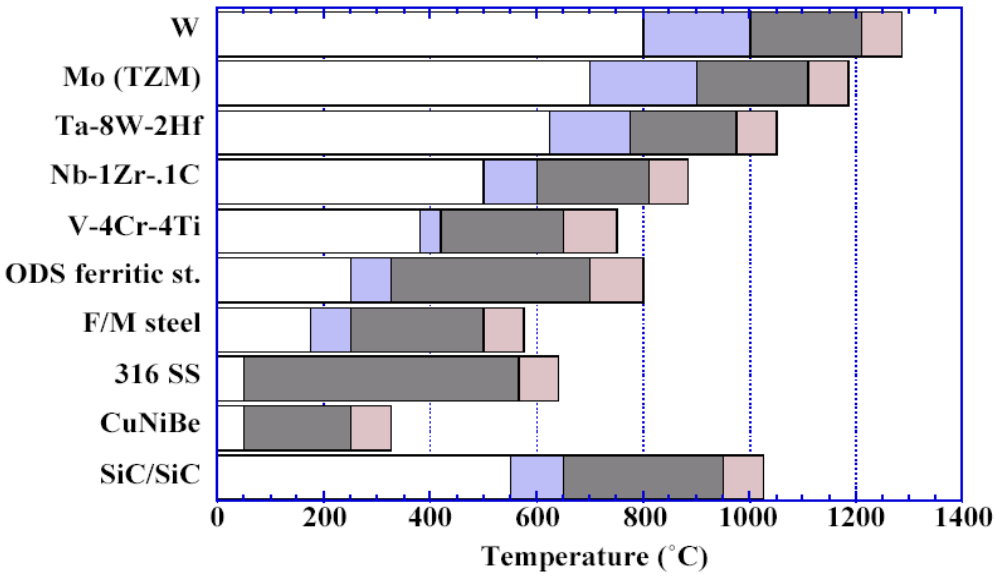

Figure 1: Operating temperature windows (based on radiation damage and thermal creep considerations) for refractory alloys, Fe-(8-9%)Cr ferritic-martensitic steel, Fe-13%Cr oxide dispersion strengthened ferritic steel, Type 316 austenitic stainless steel, solutionized and aged Cu-2%Ni-0.3%Be, and SiC/SiC composites. The light shaded bands on either side of the dark bands represent the uncertainties in the minimum and maximum temperature limits.

2.1.3 Operating Temperature Windows

Figure (1) summarizes the operating temperature windows (based on thermal creep and radiation damage considerations) for nine structural materials considered by Zinkle and Ghoniem (2000). The temperature limits for Type 316 austenitic stainless steel are also included for sake of comparison. In this figure, the light shaded regions on either side of the dark horizontal bands are an indication of the uncertainties in the temperature limits. Helium embrittlement may cause a reduction in the upper temperature limit, but sufficient data under fusion-relevant conditions are not available for any of the candidate materials. Due to a high density of matrix sinks, ferritic/martensitic steel appears to be very resistant to helium embrittlement (Hishinuma et al., 1998; Schroeder and Ullmaier, 1991). An analysis of He diffusion kinetics in vanadium alloys predicted that helium embrittlement would be significant at temperatures above 700∘C (Ryazanov, Manichev and van Witzenburg, 1996). As discussed in Subsection 2.1.1, the lower temperature limits in Figure (1) for the refractory alloys and ferritic:martensitic steel are based on fracture toughness embrittlement associated with low temperature neutron irradiation. An arbitrary fracture toughness limit of 30 MPa-$\sqrt{m}$ was used as the criterion for radiation embrittlement. Further work is needed to determine the minimum operating temperature limit for oxide dispersion strengthened (ODS) ferritic steel (Hishinuma et al., 1998). The value of 290 ± 40°C used in Figure (1) was based on results for HT-9 (Fe-12Cr ferritic steel) (Rowcliffe and et al., 1998). The minimum operating temperature for SiC/SiC was based on radiation-induced thermal conductivity degradation, whereas the minimum temperature limit for CuNiBe was simply chosen to be near room temperature. The low temperature fracture toughness radiation embrittlement is not sufficiently severe to preclude using

copper alloys near room temperature (Alexander, Zinkle and Rowcliffe, 1999; Tatinen, Pyykkoen, Karjalainen-Roikonen, Singh and Toft, 1998), although there will be a significant reduction in strain hardening capacity as measured by the uniform elongation in a tensile test. The high temperature limit was based on thermal creep for all of the materials except SiC and CuNiBe. Due to a lack of long-term (10,000 h), low-stress creep data for several of the alloy systems, a Stage II creep deformation limit of 1% in 1000 h for an applied stress of 150 MPa was used as an arbitrary criterion for determining the upper temperature limit associated with thermal creep. Further creep data are needed to establish the temperature limits for longer times and lower stresses in several of the candidate materials.

2.2 The Multiscale Modeling Approach as a New Paradigm

Computational modeling of materials behavior is becoming a reliable tool of scientific investigation, complementary to traditional theory and experimentation. The Multiscale Materials Modeling (MMM) approach reflects the realization that continuum and atomistic analysis methods are complementary. Understanding materials behavior acknowledges the dual nature of the structure of matter: being continuous when viewed at large length scales and being discrete when viewed at an atomic scale. At meso-scales (i.e. *in between* continuum and atomistic), continuum approaches begin to break down, and atomistic methods reach inherent time and length-scale limitations. Mesoscopic simulation methods are developed to bridge the gap between length scale extremes. Recently, a number of factors may have led the scientific community to seriously consider the MMM approach as a reasonable strategy for understanding the mechanical behavior of materials, and hence as a potential approach to material system design.

The power of analytical theory lies in its ability to reduce the complex collective behavior of the basic ingredients of materials (e.g. atoms and electrons, if one admits tight coupling between nucleons) into insightful relationships between cause and effect. For example, the relationship between the magnitude of an externally applied force and the position of *all atoms* in an isotropic elastic material requires knowledge of only two elastic constants. When the applied force is large, such simple description is not possible, and one requires more parameters to obtain such relationship. A description of material deformation beyond the elastic regime is usually summarized in engineering *constitutive equations*, which are relationships between the stress, strain, temperature, strain rate, and other additional environmental factors. The description is empirical, and relies on extensive experimental database. Its extrapolation beyond the database is always uncertain, requiring sometimes large safety factors in engineering designs. Inclusion of these relationships within the continuum mechanics framework constitutes the theory of plasticity, with the inherent assumption that materials are statistically homogeneous. Nevertheless, many experimental observations on the mechanical behavior of fusion materials cannot be readily explained within the continuum mechanics framework: dislocation patterns in fatigue and creep, surface roughening and crack nucleation in fatigue, the inherent inhomogeneity of plastic deformation under irradiation, the statistical nature of brittle failure, plastic flow localization in shear bands, and the effects of size, geometry and stress state on yield and failure properties.

Recently, the interest in materials-by-design for the development of radiation resistant structural materials is challenging the scientific community to analyze, develop and design materials and structures via direct computer simulations. Many examples of current research interests show the need for a physically-based approach to performance analysis and design of FW/B structures. The

challenge is great, because traditional continuum methods of analysis are quite limited, and the appropriate simulation method should be selected with caution. Theory and modeling are playing an ever increasing role in this area, because of the need to interpret experimental data and at the same time reduce the development time before full-scale manufacturing proceeds. The few examples discussed here will illustrate the role of MMM in the development of radiation-resistant FW/B materials.

In high-payoff, high-risk technologies, such as the design of large-structures in the aerospace and nuclear energy industries (including fusion), the effects of aging and severe environments on failure mechanisms cannot be left to conservative factor-of-safety approaches. The complexity of the environment and the large size of FW/B components demand increasing efforts to focus on the utilization of the MMM approach. An example of applying this strategy to the development of large components surrounding the plasma core of a fusion energy system is shown in Figure (2).

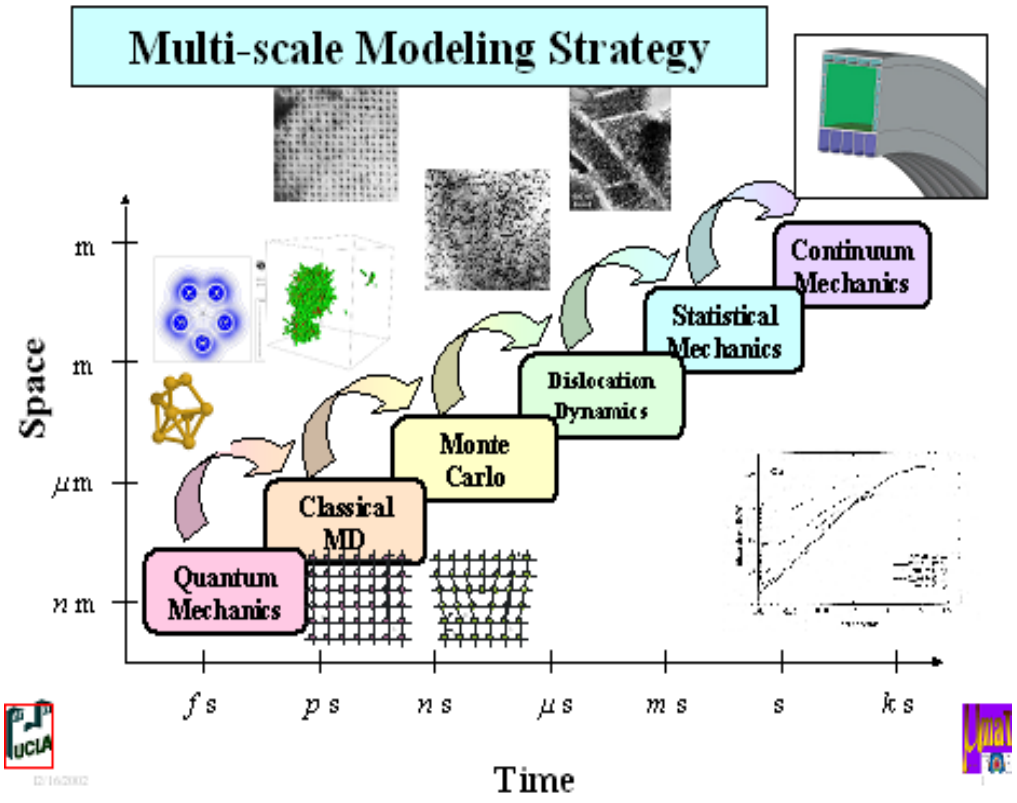

Figure 2: Illustration of the multiscale modeling approach to the design of radiation-resistant materials for fusion energy structures

Although experimental observations of the fact that plastic deformation is rather heterogeneous have been around for some time, the significance of these facts has not been addressed till very recently. Surprisingly regular patterns of localized zones of high deformation, surrounded by vast material volumes, which contain little or no deformation, are frequently seen in unirradiated (Mughrabi, 1983; Mughrabi, 1987; Amodeo and Ghoniem, 1988) and irradiated alloys (Singh, Foreman and Trinkaus, 1997). Nevertheless, the spacing between these patterns (e.g. a typical size of a dislocation cell, the ladder spacing in Persistent Slip Bands (PSB's), dislocation channels in irra-

diated materials, or the spacing between coarse shear bands) appears to control the strength and ductility of plastic deformation, and to be dictated only by external thermodynamic forces. The basic reasons for this important and intrinsic material length scale, and the relationship with material deformability have been subjects of recent great intellectual and practical challenges. Unlike most approaches on the elastic properties of composite materials, the overall plastic response of even single phase materials cannot be conveniently "homogenized' in an average sense. Therefore, new methods of investigation are needed to resolve these two basic effects of plastic deformation: the presence of an intrinsic length scale, and the existence of a dependence on the material size. In all of these examples of deformation at the *meso* length scale, neither atomistic simulations nor continuum theory are adequate.

The factors discussed above can be considered as intrinsic issues that have resulted in a greater emphasis on the MMM approach as an essential tool for the development of radiation-resistant structural materials. However, the tremendous growth and sophistication of computer hardware and software has made large-scale computing far more accessible than ever before. Such accessibility has become by itself a driving force for the development of efficient numerical methods within the MMM framework. Moreover, and as will be realized in this proposal, there is considerable room for improvements. It is expected that new concepts, theory, simulation techniques, and computer software will be developed to achieve truly seamless multiscale simulations of the mechanical behavior of FW/B materials in a fusion environment.

3 Research Objectives

Recent progress and advances in computer hardware, architectures, algorithms, and computational methods have vitalized materials theory and have enabled direct simulations of properties based on fundamental and physical principles. The prospects of materials-by-design have become tantalizingly within reach, with enormous implications on manufacturing and design. Advances in modeling tools, such as Molecular Dynamics (MD), Kinetic Monte Carlo (KMC), Dislocation Dynamics (DD), Grain Growth Dynamics (GGD), Parallel Finite Element Methods (P-FEM), Meshless Galeriken Methods (MGM) are providing exciting new opportunities for fusion materials development when coupled with the US national experimental program. We propose to develop here a hierarchy of Multiscale Materials Modeling (MMM) tools for investigation of the mechanical behavior of FW/B materials. Two basic interfaces of our proposed approach will enhance its reach and range of validity. First, we rely on the numerous activities in the US program on atomistic Ab-initio or MD modeling of the primary damage structure, defect energetics, and dislocation-defect interactions. Such activities provide some of the necessary and key parameters for our MMM hierarchy of models. Second, we must integrate our proposed MMM approach with the US national experimental program in such a way as to suggest key experiments, validate models, measure key parameters, and extrapolate to the complex operational conditions of FW/B modules.

The proposed five-year program will focus on plastic deformation, fracture and mechanical failure phenomena in the main structural materials considered for applications in FW/B modules of Magnetic Fusion Energy (MFE) devices. The proposed research is cross-cutting in its application to BCC and FCC metallic alloys, including vanadium, iron, copper, and tungsten alloys. The primary phenomena to be investigated here are: (1) nucleation and growth of helium-filled voids (bubbles); (2) irradiation-induced phase transformations; (3) microstructure evolution (i.e. dislocations, bubbles and vacancy clusters, precipitates, and SIA clusters); (4) formation of dislocation channels and plastic instability; (5) radiation hardening dependence on neutron dose, temperature and initial microstructure; (5) the DBTT shift with the neutron dose; (6) the effects of alloy microstructure (e.g. precipitates, cold-work, etc.) on the DBTT; (7) crack stability and growth for complex 3-D geometry; (8) high-temperature helium embrittlement and creep rupture; (9) the effects of helium on grain boundary crack nucleation and growth; (10) fatigue crack growth in BCC metals and alloys; (11) development of constitutive mechanical equations for FEM modeling of FW/B components; (12) development and applications of parallel FEM simulation techniques for complex 3-D FW/B geometry and multi-physics conditions; (13) development of a Web-based database for the properties of fusion materials, design rules, and constitutive models.

To achieve this wide range of goals, the proposed research is conveniently planned in three major groups of models: one at the nano-scale, a second at the mesoscale (in between nano- and macroscopic), and a third at the macro-scale. To develop full computational description of plasticity, fracture and failure phenomena, we plan to continue our development and applications of Advanced Rate Theory, Kinetic Monte Carlo (KMC), and Dislocation Dynamics (DD) models of microstructure evolution, irradiation-induced phase transitions, and dislocation-defect interaction mechanisms. The input parameters to this group of models (e.g. defect energetics, or partitioning in collision cascades, etc.) are very few, and will be derived from on-going Ab-initio or MD models, or directly from experimental measurements. The results of these models will also be directly compared to experimental data, for example the heterogeneous distribution of Self-Interstitial Atom (SIA) clusters, dislocation decoration, loop raft formation, vacancy-helium cluster density and size,

types and temperature dependence of irradiation-induced phases, critical stresses required to free dislocations from defect clusters, precipitates, etc.

The next level of models will be aimed at simulations of plasticity and fracture mechanisms at length scales that are not accessible by atomistic simulations or by continuum mechanics. Methodologies for this *meso-scale* will be aimed at material volumes that are in the 1-30 μm range, and would require extensive computer simulations of the collective behavior of significant statistical representation of the microstructure. We have been advancing two new approaches in this area. The first is a significant modification of the standard KMC simulation technique. The key new development here is the ability to include, for the first time, the effects of the internal elastic field on the heterogenous evolution of the microstructure. This approach will be applied to the simulation of large-scale microstructure evolution and collective aspects of defect-dislocation interactions. Although the KMC and DD methods will be used in both the first and second group of models, the distinction lies in the level of detail. At the nano-scale, problems of a single dislocation-defect, or multiple defects will be pursued, while collective behavior (i.e hundreds to thousands of microstructure features) will be emphasized. DD simulations will focus on radiation hardening (or softening), plastic instabilities in dislocation channels or shear bands, and detailed 3-D models of the DBTT in irradiated BCC metals and alloys.

To connect our models at the nano- and meso-scales to engineering design, we plan to pursue the development of a number of coupled discrete-continuum models of fracture and failure processes. We have succeeded in the development of a coupled FEM-DD method for the simulation of the DBTT in irradiated materials. We plan to extend this work in two new directions: (1) applications to predictions of the onset of brittle fracture in irradiation testing, as well as realistic FW/B geometry; (2) modeling fatigue crack growth in BCC alloys (especially Fe and W) under irradiation conditions. A new revolutionary approach for polycrystalline plastic deformation of fusion materials is also proposed. This approach is based on a variational Galeriken formulation of Gibbs free energy for dislocations, grain boundaries and the grain matrix itself. A set of equations is derived for degrees of freedom representing with dislocation motion, grain boundary motion, and material motion. The model will tightly couple DD, GGD and the meshfree computational methods. The presence of inhomogeneous plastic strain in the form of dislocation channels and slip bands (in fatigue) will require the utilization of meshfree methods, since FEM implementations are notoriously inaccurate in modeling localization phenomena and fracture processes. On the applications side, we plan to continue our recent efforts in the Virtual International Test Assembly (VISTA) collaboration. This will involve three main aspects: (1) damage function development; (2) 3-D FEM model development; (3) virtual module performance evaluation and testing. In addition, we will also continue our effort on the construction of a community-shared Web-based fusion materials database. In the following, we outline our research plan, and describe how we will accomplish the various proposed tasks.

4 Research Plan

4.1 KMC & Rate Theory Modeling of Microstructure Evolution

4.1.1 Kinetic Monte Carlo Simulation of Defects

So far in all KMC simulation codes, the elastic interaction between defects, and between defects and other microstructure (e.g. dislocations) have been ignored. For example, the simulations of ALSOME (Heinisch, 1990; Heinisch, 1995; Heinisch and Singh, 1996; Jaraiz, Gilmer, Poate and de la Rubia, 1997; Heinisch and Singh, 1997) or BIGMAC (Soneda and Diaz de la Rubia, 1998; Caturla, Soneda, Alonso, Wirth, Diaz de la Rubia and Perlado, 2000) do not explicitly take the effects of the internal stress field into consideration. However, the elastic interaction between dislocations and point defects that result from collision cascades play a key role in determining the effects of irradiation on mechanical properties. Any simulation methodology must also address the many diffusional pathways available, and reveal the dependence on temperature and dose so as to compare to experiments. In order to carry out KMC simulations for the evolution of defect distributions, several kinetic data are required: activation energy and prefactors for the motion of vacancies, self interstitial atoms (SIAs), vacancy and SIA clusters, the stand-off distance of dislocations, and the atomic details of cluster-cluster interactions. These parameters can be obtained from MD or Molecular Statics (MS) simulations that are on-going within the US fusion materials program.

The jump frequency for a possible jump of a cluster, i, to take place is given by:

$$r_i = \omega_0 \exp(-\frac{E_i}{k_B T}) \tag{1}$$

where ω_0 is the pre-exponential factor of the defect cluster, k_B the Boltzmann constant, E_i the 'effective' activation energy for jumps of the cluster, and T is the absolute temperature. The values of E_i for interstitials and vacancies can be obtained from MD calculations.

In many applications of the MC method, such as the equilibration of atomic positions in a defected crystal, the space of possible configurations that the system can assume is continuous. Therefore, there exists (in theory) an infinite number of new configurations available to the system at any MC step. However, since we are simulating defects in a volume of $finite$ size which evolves according to a $finite$ set of physical or mechanical mechanisms, the number of new configurations available at any MC step is $finite$ and *enumerable*. This configuration space is discrete. In other words, at each MC step, we can determine all of the potential changes that the system can possibly undergo. Therefore, instead of attempting a random change to the system at each simulation step and then accepting or rejecting that change based on some criterion (e.g., the Metropolis MC method(Metropolis, Rosenbluth, Rosenbluth, Teller and Teller, 1953)), we choose and execute one change from the list of all possible changes at each simulation step. The choice is made based on the relative rates at which each change can occur (i.e., the probability of choosing one particular reaction instead of another is proportional to the rate at which the reaction occurs relative to the rates of the other reactions).

Thus, simulation of microstructure evolution of cascade-induced damage is accomplished by a KMC procedure in which one reaction is executed at one site during each time step. The first step in KMC simulations is to tabulate the rate at which an event (i) will take place anywhere

in the system, r_i. The probability of selecting an event is simply equal to the rate at which the event occurs relative to the sum of all possible event rates. Once an event is chosen, the system is changed appropriately, and the list of events that can occur at the next KMC step is updated. Therefore, at each KMC step, one event denoted by m is randomly selected from all possible M events, as follows:

$$\frac{\sum_{i=0}^{m-1} r_i}{\sum_{i=0}^{M} r_i} < \xi_1 < \frac{\sum_{i=0}^{m} r_i}{\sum_{i=0}^{M} r_i} \tag{2}$$

where r_i is the rate at which event i occurs ($r_0 = 0$) and ξ_1 is a random number uniformly distributed in the range $[0, 1]$. The way in which the M events are labeled (i.e., by specifying which events correspond to $i = 1, 2, 3, \ldots, m, \ldots, M$) is arbitrary. After an event is chosen and executed, the total number of possible events, M, and the sequence in which the events are labeled, will change.

The reciprocal of an atomic jump probability per unit time is the residence time for a defect cluster that moves by that specific type of jump. Since the jump probabilities of all the different types of jumps are independent, the overall probability per unit time for the system to change its state by any type of jump step is just the sum of all the possible specific jump type probabilities, and so the residence time that would have elapsed for the system in a specific configuration is the reciprocal of this overall jump probability:

$$\Delta t = \frac{1}{\sum_{i=0}^{M} r_i} \tag{3}$$

which is independent of the chosen transition. It may also be important to include the appropriate distribution of escape times. For random uncorrelated processes, this is a Poisson distribution. If ξ_2 is a random number from 0 to 1, the elapsed time for a particular transition is given by

$$\Delta t = \frac{-\ln \xi_2}{\sum_{i=0}^{M} r_i} \tag{4}$$

The system is then advanced to the final state of the chosen transition and the process is repeated. The expression for Δt in Eq. 4 is rigorous (Bortz, Kalos and Lebowitz, 1975), and a derivation is also provided by Battaile and Srolovitz (1997).

A cascade is introduced into the simulation box at a random position in terms of a certain damage production rate. The point defects produced by the cascade then instantly interact with each other, and lead to recombination and clustering. The set of atoms in the simulation system is then be monitored for diffusional modification prior to the arrival of the next cascade, i.e. in the time T_C. When a jump is made, a time equal to the net residence time (calculated using Eqn. 4) is subtracted from T_C so that there is less time remaining for further jumps in the allotted time period. This process is iterated until the time of making any jump is greater than the remaining time. Whenever a jump is to be made, the specific one is determined by random choice based on the relative probabilities of all potential jumps as described above. When the remaining time reaches zero, the clock is turned ahead by T_C and another cascade is then introduced. An implementation algorithm of this cascade damage simulation is described next.

4.1.2 Elastic Interactions between Point Defects

The concept of KMC simulation provides a powerful tool in the study of atomic point defects distribution process of irradiation damage, which can be experimentally verified (e.g.. by TEM (Yamakawa and Shimomura, 1988)). As a result, physical mechanisms for most of individual point defect motions are extremely difficult to obtain under real observations. For example, the phenomena of loop raft formation, dislocation decoration and dislocation wall formation rely heavily upon the properties of defects and the elastic interactions between them. Very little experimental results on the magnitude of these interactions exists. However, so far, all KMC computer simulations for microstructure evolution under irradiation have not considered the influence of the internal and applied stress fields on defect motion (for example Soneda and Diaz de la Rubia (1998), Caturla et al. (2000), Soneda and Diaz de la Rubia (2001)). We propose here to continue our development of KMC simulations, where the elastic interactions between SIA/vacancy clusters themselves, SIA and vacancy clusters, and SIA/vacancy clusters and dislocations are explicitly accounted for.

4.1.3 Implementation of KMC Algorithm

SIA clusters are directly produced on the periphery of collision cascades, and they may contain from a few atoms up to tens of atoms in the near vicinity of the cascade (Bacon and Diaz de la Rubia, 1994). Such clusters are extremely mobile, and migrate predominantly along highly-packed crystallographic directions, with migration energies of less than 0.1 eV (Bacon and Diaz de la Rubia, 1994; Soneda and Diaz de la Rubia, 1998). Small SIA clusters may also spontaneously change their Burgers vector, and thus have the flexibility to translate along various crystallographic directions if their motion is not obstructed by internal strain fields. Since MD simulations have shown that the majority of SIA clusters have the form of mobile (glissile) perfect dislocation loops, in this work, we represent SIA clusters as small prismatic, rigid and circular dislocation loops. As for vacancies, small spherical voids are employed to approximate single vacancies and vacancy clusters.

The temperature dependence of the jump frequency of defect clusters diffusion is given by Equation(1). In our KMC simulation, the elastic interaction is incorporated. The influence of other defects and the external stress on one SIA or vacancy cluster is given by the stress field σ_{ij}. By applying the infinitesimal dislocation loop approximation for SIA clusters , the work necessary to form the loop characterized by normal n, Burgers vector b and area δA in the stress field σ_{ij} is SIA cluster interaction energy E_{int}, and is given by

$$E_I = \int_V \sigma_{ij}^{(1)} \varepsilon_{ij}^{(2)} dV \tag{5}$$

in which $\sigma_{ij}^{(1)}$ is the stress arising from the first dislocation and $\varepsilon_{ij}^{(2)}$ the strain originating in the other. For the present study, if the second loop (defect cluster) is assumed to be infinitesimal, the interaction energy can be simplified to (Kroupa, 1966)

$$E_I = \delta A^{(2)} n_i^{(2)} \sigma_{ij}^{(1)} b_j^{(2)} \tag{6}$$

where $n_i^{(2)}$ is the unit normal vector to the defect cluster habit plane of area $\delta A^{(2)}$. The total cluster activation energy is then given by:

$$\tilde{E}_m = E_m + \Delta E_{\text{int}} \tag{7}$$

where E_m is the activation energy in a perfect crystal structure and can be obtained by either experiments or MD simulations, and ΔE_{int} the difference in the interaction energy of an defect cluster placed at two neighboring equivalent position in the crystal. This includes the effects of forces and moments on the virtual loop or microvoid motion.

The implementation can be demonstrated in detail through a cascade damage flowchart, simply described below. With the initiation of dislocation distribution, cascade damage rate and matrix temperature as well as the initial calculation and summation of atomic jump rates, the key steps lie in the execution of the thermal diffusion loop and can be described as follows:

1. Select a jump path at random weighting by individual rate;
2. Make the jump;
3. Update and sum up jump rates;
4. Turn ahead simulation clock;
5. Iterate step 1 through 4 until designated damage dose (in terms of the number of cascades) is achieved.

Selection of the jump path by a linear search is represented by a cumulative and conditional probability process, shown in Figure (3). Suppose that there are three jumping atoms, the first has two jump paths and the second and third each have three. The eight available jump paths have probabilities p_{11}, p_{12}, p_{21}, p_{22}, p_{23}, p_{31},p_{32} and p_{33} respectively.

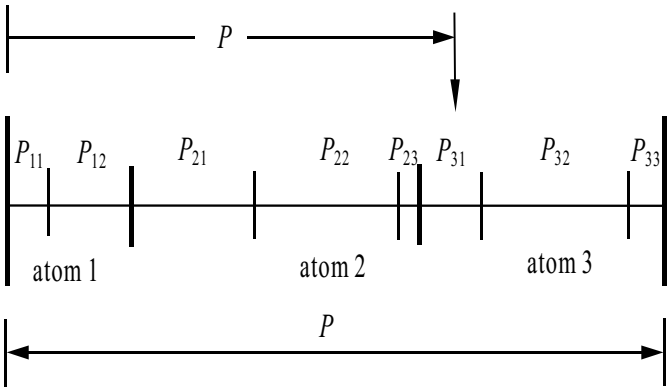

Figure 3: A schematic illustration of the linear procedure used to select the jump path. Path p_{31} is a randomly chosen event on a line segment of length P.

Suppose now that the jump path, p_{31}, has been randomly selected. This is equivalent to: $\xi < (p_{11} + p_{12} + p_{21} + p_{22} + p_{23} + p_{31})/P$, where P is the total length of the segment and ξ is a random number over the interval $[0, 1]$. For a large system, the relationship for selecting the process can be written as

$$\xi < \sum_{i=1}^{K} \sum_{j=1}^{n_i} p_{ij} / \left(\sum_{i=1}^{N} \sum_{j=1}^{n_i} p_{ij} \right) \tag{8}$$

where p_{ij} is the jump rate for the i-th particle at the j-th jump path, $n(i)$ is the total number of jump paths for the i-th particle, N is the total number of particles. Eq. 8 indicates the K-th particle is selected with $K < N$.

4.1.4 Diffusion of Glissile SIA Clusters

The fact that SIA and vacancy clusters are produced directly in the high-energy displacement cascades has significant effect on damage accumulation behavior, and thus physical and mechanical properties of materials under cascade damage conditions. The 1-D motion of small SIA clusters is especially important, because of their influence on dislocation decoration (Stiegler and Bloom, 1971; Singh, Horsewell, Toft and Edwards, 1995b), and formation of rafts of dislocation loops(Singh, Evans, Horsewell, Toft and Edwards, 1995a). In addition, the restriction of diffusion of SIA clusters to 1-D leads to a reduction in the reaction rate with other defects because one dimensionally moving clusters are able to travel in the atmosphere of randomly distributed lattice defects through larger distances than those 3-D moving ones, and consequently the possibility that such SIA clusters annihilate at extended sinks such as pre-existing dislocations and grain boundaries increase. At the same time lattice defects affect the motion of one dimensionally diffusing clusters in a more substantial way than they influence the motion of vacancies since one dimensionally moving clusters have less chances to avoid obstacles by changing their direction of diffusion (Dudarev, 2000). As a consequence, a diffusion bias is established during steady-state irradiation whereby the vacancy concentration can greatly exceed that of SIAs. In addition to the 1-D diffusion of SIA clusters, the motion of a single SIA is also of interest. In order to investigate the migration mechanism of interstitial clusters, Fig. 4 shows the trajectories of the centers of mass of an SIA cluster containing 6 interstitials for diffusion at 300 K with different activation energies of direction change of its Burgers vector. The transition from 1-D motion to 3-D diffusion is clearly dependent on this activation energy, which must be determined by MD or MS simulations.

4.1.5 Accumulation of Radiation Damage

Due to the low activation energies of SIAs and SIA clusters (< 0.1 eV), a typical diffusion event related to SIAs can occur on the order of 10^{12} (or even more) times per second at room temperature, and would typically be important in the time evolution of the system. However, the accumulation of radiation damage occurs over hundreds to millions of seconds. A direct classical dynamics simulation which necessarily has to faithfully track all this vibrational motion would take thousands of years of computer calculations on the fastest present day computer before a single transition can be expected to occur! It is clear that meaningful studies of irradiation damage evolution cannot be carried out by simply simulating the classical dynamics of defect clusters. It is essential to simulate the system on a much longer time scale. This time scale problem is one of the important challenges in computational research on atomic scale systems, and we plan to tackle this problem as described next.

Since it is almost impossible to study a continuous cascade damage process by tracing every fast event of SIAs, an alternative has to be found to track the fates of all defect species and provide a prediction of the microstructural evolution under irradiation. As a matter of fact, the Monte Carlo simulation method for particle transport has been extensively used in present day understanding of radiation damage phenomena. In this method, sampling is conducted from a

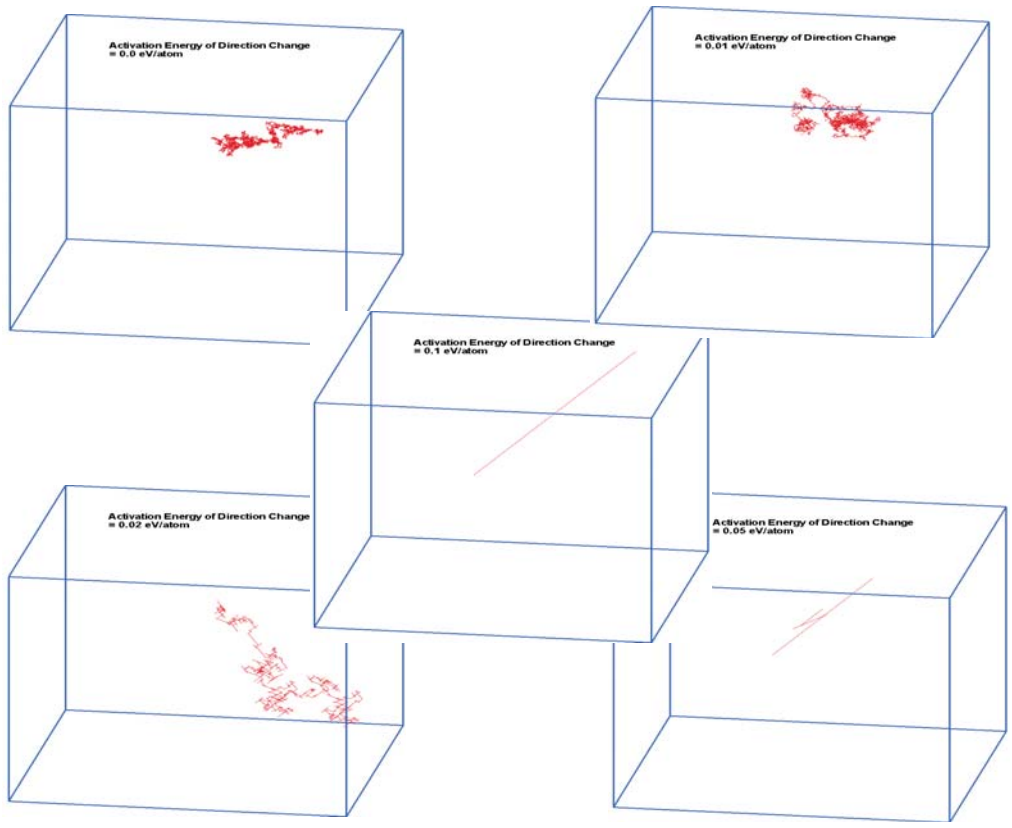

Figure 4: Center-of-mass trajectories of a SIA cluster containing 6 interstitials migration for 10,000 consecutive KMC steps at 300K with different reorientation activation energies. The units are in lattice constants. All the straight line segments are oriented along the $< 111 >$ directions.

probability distribution according to relevant physical laws. For a small glissile SIA cluster, the possible event that could happened to it is either getting trapped in the strain field of another defect cluster such as cavities and small dislocation loops or line defects such as dislocations, or traveling one-dimensionally in the crystal. Statistically, the fraction of absorbed clusters depends on the strength of sinks.

There are two important aspects in the kinetics of one-dimensionally diffusional defects in comparison to the kinetics of three-dimensionally diffusional defects: (1) the range of free migration and (2) absorption once the defect is trapped in the strain field of another defect (including pre-existing defects) (Trinkaus, Singh, and Foreman, 1997a). The existing treatment of interactions between mobile SIA clusters and lattice defects is based on the mean-field approach, where the effective range of motion of clusters in the material is characterized by the mean free path λ. For a defect of configuration i migrating one-dimensionally in a crystal containing a number density c_j of defects of configuration j with effective interaction cross section $\sigma_{ij} = \pi r_{ij}^2$ and a line density ρ of dislocations with effective interaction diameter d_i the reciprocal mean free path $\Pi_i = \lambda_i^{-1}$ is given by (Trinkaus, Singh and Woo, 1994)

$$\Pi_i = \lambda_i^{-1} = \sum_j \sigma_{ij} c_j + d_i \hat{\rho} \tag{9}$$

where $\hat{\rho} = \frac{\pi\rho}{4}$ is the dislocation line length per unit volume projected on a plane perpendicular to the migration direction. σ_{ij} and d_i are determined by the mutual elastic defect interaction.

The probability of a defect getting absorbed at a sink after moving a distance Δl in the computation box is then given by

$$P = 1 - \exp\left(-\frac{\Delta l}{\lambda_i}\right) \tag{10}$$

Because the MC method is used to determine the eventual fate of a cluster in terms of probabilities of a certain number of events, this scheme is so-called "Event Monte Carlo" (EMC).

In a long-time-scale simulation, since the trajectories of defects cannot be faithfully followed in all its details, a scheme coupling KMC and EMC is a reasonable compromise. KMC can be used to capture strong space-time correlations in the system, and EMC can provide the means to extrapolate from small damage dose levels to larger values. This hybrid scheme is similar to the *predictor-corrector* integration method, and is described as follows:

1. Select a simulation box, say 0.5 μm on the box edge, and distributed some dislocation loops in terms of a designed dislocation density;
2. Choose a starting point at some low dose damage level, say 10^{-6} dpa. The total number of cascades and corresponding SIA clusters can be readily obtained by using the empirical relationship between the number of Frenkel pairs and the kinetic energy of the PKA (Bacon, Gao and Osetsky, 2000). The corresponding size distribution of clusters can also be acquired from MD simulation results;
3. Perform KMC simulation for a short time, which can be taken as the time required for one SIA cluster to cross the simulation box several times;
4. Terminate the KMC simulation;
5. Perform *quasi-equilibrium* EMC calculation for each and every mobile SIA clusters to approximate the long-term redistribution of defects;
6. Use EMC to accumulate defect damage, with the corresponding size distribution, and use the data as a new starting point at a higher dose (e.g. 10^{-5} dpa);
7. Repeat steps (3) to (6) to the desired dose level.

4.1.6 The Role of Advanced Rate Theory

Advanced Rate Theory refers to considerations of a number of processes and phenomena that have been shown by either MD or KMC, and were not considered in the original development of the *Standard Rate Theory*. These are: (1) simultaneous nucleation and growth of vacancy-helium clusters without artificial separation of regimes, (2) the asymmetric split of defects into sessile and glissile portions, following the cascade event; the so-called production bias, (3) the transition in defect diffusional kinetics from 1-D to 3-D, and the ensuing effects on microstructure evolution; (4) cascade-induced dynamic events, such as precipitate re-solution and secondary bubble nucleation. We plan to continue the development of our Advanced Rate theory code (Sharafat and Ghoniem,

2000) that has been calibrated with recent experiments to include these four aspects of the theory. Moreover, we will use the code to check on the global features of damage evolution by the KMC method, as described before. The main value of KMC/EMC simulations will be the ability to determine the conditions of spatial segregation of defects. The influence of such segregation on the mechanical properties can be studied by DD simulations, as will be explained in Subsection **??**. The specific topics that will be addressed in this area are:

1. Self-consistent formulation of the distribution of clustered and freely migrating point defects, in the presence of simultaneous helium clustering with vacancies under conditions of high helium production rates;
2. Incorporation of helium transport mechanisms by pipe diffusion in dislocation cores, by dislocation drag under stress, and by bubble mobility.
3. Coupled moment equations and re-construction of the size distribution of helium-vacancy clusters.
4. Simultaneous evolution of non-equilibrium phases, and coupling between helium cluster and phase evolution (see below on phase evolution).
5. Coupled rate equations for helium-vacancy cluster evolution on grain boundaries for coupling with the creep rupture modeling efforts.
6. Applications of the models to experimental analysis and alloy design.

4.1.7 Radiation-Induced Phase Transitions

Phase transitions under irradiation are generally non-equilibrium, as they are influenced by a number of mechanisms: enhanced diffusion, solute segregation, and radiation-induced dissolution of new phases by disordering and ballistic displacements. We plan to develop kinetic models for the non-equilibrium precipitate phases in both ferritic steels and vanadium. In particular, we will focus on oxide-dispersoids in ODS steels (e.g. Y_2O_3), and on Ti-oxy-carbo-nitrides in vanadium. The methods developed here will be readily transferable to other irradiation-induced phase transformations. Ultra-fine non-equilibrium phases, which are homogeneously distributed as nano-scale coherent solute clusters, will be modeled, building on our most recent work on cluster dynamics and kinetic modeling of non-equilibrium phase evolution (Demetriou, Ghoniem and Lavine, 2002c; Demetriou, Ghoniem and Lavine, 2002b; Demetriou et al., 2002c; Demetriou et al., 2002b).

Demetriou, Ghoniem and Lavine (2002a) developed a CALPHAD algorithm to compute the metastable W-C phase diagram in the vicinity of the metastable reactions involving the carbides by reproducing the equilibrium boundaries using optimized free energy data obtained from (Gustafson, 1986), and by extending the stable boundaries into regions of metastability as suggested by (Perepezko and Boettinger, 1983). The computed stable phase equilibria are in excellent agreement with those computed by (Gustafson, 1986), which closely resemble experimental phase equilibrium data presented by (Rudy, 1969). Modeling non-equilibrium phases under irradiation will be based on our recent efforts in this area, and will be closely tied to our microstructure evolution models described earlier, and will include the interaction of interstitial solutes (i.e., C, N, O) with extended defects.

4.2 Modeling Plasticity of Irradiated Materials

4.2.1 Radiation Hardening & Plastic Instabilities

Many experimental observations have shown that neutron irradiation of metals and alloys at temperatures below recovery stage V causes a substantial increase in the upper yield stress (radiation hardening), and beyond a certain dose level, induces a yield drop and plastic instability. Furthermore, the post-deformation microstructure of a specimen showing the upper yield point has demonstrated two significant features. First, the onset of plastic deformation is generally found to coincide with the formation of "cleared"channels, where practically all plastic deformation takes place. The second feature refers to the fact that the material volume in between cleared channels remains almost undeformed (i.e. no new dislocations are generated during deformation). In other words, the initiation of plastic deformation in these irradiated materials occurs in a very localized fashion. This specific type of plastic flow localization is considered to be one of many possibilities of plastic instabilities in both irradiated and unirradiated materials.

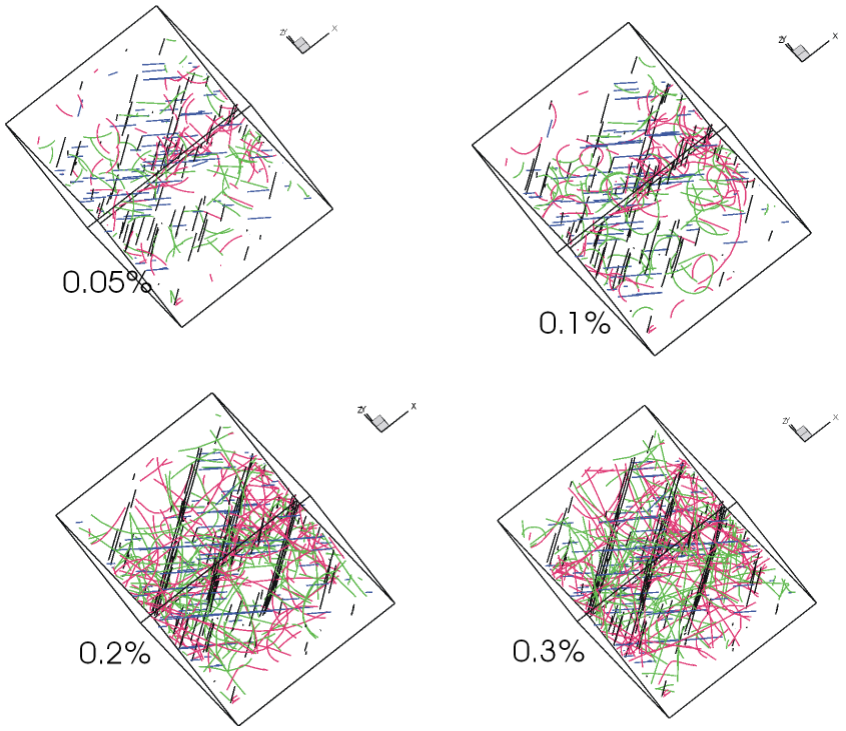

Figure 5: Results of computer simulations for dislocation microstructure deformation in copper deformed to increasing levels of strain (shown next to each microstructure
(After Wang, Ghoniem, LeSar and Sriram (2003))

In this part of the investigation, we plan to continue the development of our parametric DD to assess the physical mechanisms, which are responsible for the initiation of plastic instability in irradiated FCC and BCC metals. The computational capabilities of our method are very substantial now, and realistic simulations of small material volumes (e.g. several microns in size) can be routinely carried out, as can be seen in Figure (5). We plan to investigate the mechanisms of dislocation unlocking from defect clusters in the form of Stacking Fault Tetrahedra, SIA clusters,

microvoids, and ultra-fine radiation-induced precipitates. We will also investigate the mechanisms of structural softening in flow channels as a consequence of dislocation interaction with these defect features.

One of the main problems that have faced the simulation community is the enormous density of defect clusters contained in micron-size simulation boxes. A direct numerical simulation of the interaction between dislocations and radiation-induced defects is very limited. We plan to develop a new statistically-based DD simulation method, where the details of the interaction between dislocations and small-size defects are represented by statistical power spectra, modeled as time series. Invoking the concept of ergodicity, we can perform a limited number of detailed simulations between single dislocations and statistical distributions of defects, from which we can determine the details of dislocation-defect interaction forces. These statistical fluctuating components of the Peach-Kohler force will be added to the deterministic counterpart computed from the local stress and self-force. Therefore, we plan to modify the main equations of motion of the Parametric DD, so as to include stochastic fluctuations from defect fields and thus represent thermally-activated processes aS well. The procedure will be similar to Langevin Dynamics in particle simulation techniques, as opposed to classical MD simulations.

4.2.2 A Self-consistent Meso-mechanics Variational Formulation

It is immediately noted that the variational principle for power dissipation in dislocation dynamics is quite similar to the variational form used for grain growth dynamics. Our plan is then to develop a self-consistent and more general variational form that accounts for power dissipation by motion of *both* the grain boundaries and the interior dislocations. We will follow the thermodynamics formulation of Ghoniem, Singh, Sun and Diaz de la Rubia (2000a), where the components of the Gibbs free energy will include relevant contributions from the dislocation microstructure as well as the grain boundaries. We also plan to generalize the grain boundary meso-dynamics to 3-D, where GBs are modeled as parameterized surfaces rather than parameterized space curves. Consider the virtual motion of all elements of the dislocation and GB microstructure in 3-D space. Following Ghoniem et al. (2000a), we have the following forms of the Gibbs free energy rate:

$$
\begin{aligned}
\delta\dot{G} = \; & - \sum_{I=1}^{I=N_{loop}} \oint_{\Gamma_d} (\mathbf{f}_S + \mathbf{f}_O + \mathbf{f}_{PK}) \cdot \delta\mathbf{v}_d \mid d\mathbf{s} \mid \\
& - \sum_{J=1}^{J=N_{GB}} \int_{\Gamma_{GB}} \left[\gamma(\frac{\partial \bar{v}^s_{gb}}{\partial s} + \frac{\bar{v}^n_{gb}}{R}) + \frac{1}{2}((\sigma^+ : \epsilon^+ + E^+_{self}) - (\sigma^- : \epsilon^- + E^-_{self}))\delta\bar{v}^n_{gb} \right] d\Gamma_{GB} \\
& - \int_{\Omega} \frac{1}{2}\delta(\sigma : \dot{\epsilon}) d\Omega + \int_{\Gamma_{GB}} \delta\mathbf{v} \cdot \mathbf{h} d\Gamma_{GB} + \int_{\Omega} \delta\mathbf{v} \cdot \mathbf{b} d\Omega
\end{aligned}
\tag{11}
$$

where the first three terms (first line in the equation) are for the rate of Gibbs free energy due to the dislocation microstructure, N_{loop} is the total number of dislocation loops in the system, Γ is a specific parameterized line contour representing each dislocation loop, $\mathbf{f}_S$ is the force associated with self-energy of a dislocation loop, $\mathbf{f}_O$ is an *osmotic* force on a dislocation due to point defect absorption, $\mathbf{f}_{PK} = \sigma \cdot \mathbf{b} \times \mathbf{t}$ is the *Peach-Kohler* force (where the stress tensor includes applied

and internal stress sources from other dislocations and GBs, $\mathbf{b}$ is Burgers vector and $\mathbf{t}$ the tangent vector), and $\mathbf{v}_d$ is the dislocation velocity vector. Terms in the second line is from contributions from GB motion, and the third line is for contributions by the applied forces at the material boundary and the body forces. Note that this variational equation contains line integrals for dislocations, surface integrals for GBs and volume integrals for body forces and internal stresses. Also, the free energy terms for dislocations are coupled with both matrix and GB energy terms, because the self energy of dislocations must be computed from both sides of a grain boundary (+ and -) to determine an effective driving force for GB motion. In addition, GBs will act as sources and sinks for dislocation loops, and thus influence their populations. In the previous equation, three different velocities for three different types of Degrees of Freedom (DOF) will have to be simultaneously determined. These are velocities assigned to DOF on dislocation lines, denoted by $\mathbf{v}_d$, velocities assigned to DOF on GBs, denoted by $\bar{\mathbf{v}}_{gb}$, and velocities of material points that can be determined by the mesh-free method, and those are denoted by $\mathbf{v}$.

The second law of thermodynamics dictates that Gibbs free energy given by EQN. 11 must continuously decrease for the irreversible process of microstructure evolution as a consequence of the increase in the total system entropy. The dissipation of this free energy is described phenomenologically by considering all microscopic dissipative processes during dislocation and GB motion, as:

$$\delta G^t = -\sum_{I=1}^{I=N_{loop}} \oint_{\Gamma} B_{\alpha k} V_\alpha \delta r_k \mid d\mathbf{s} \mid - \sum_{J=1}^{I=N_{GB}} \int_{\Gamma_{GB}} \frac{1}{2\mu} v_{gb}^2 ds \tag{12}$$

The first integral is for the dissipation of free energy by dislocation motion, where the resistivity matrix can have three independent components (two for glide and one for climb), depending on the crystal structure and temperature. It is expressed as:

$$[B_{\alpha k}] = \begin{bmatrix} B_1 & 0 & 0 \\ 0 & B_2 & 0 \\ 0 & 0 & B_3 \end{bmatrix} \tag{13}$$

The second integral is for the dissipation by motion of grain boundaries, where μ is the grain boundary mobility. Equating EQN. 11 to EQN. 12, and performing parameterized discretiztion, we obtain a set of equations for the DOF for the entire system. This set is composed of three coupled sets of equations, one describing the motion of nodes on dislocation lines, the second set describes the motion of nodes on GB surfaces, and the third set for material point motion that require solution by mesh-free methods. We thus have formulated a self-consistent method that can describe the simultaneous evolution of dislocation loops, GBs and material points.

One key idea is that the microstructure can be re-created from the statistics of the spatial distribution of the nodes. One can think of these nodes as particles suspended in 3-D space with statistical distribution properties (e.g. density, spatial correlation functions, etc.). Thus, solution of the dynamical equations for a relatively small volume of dislocation loops can be used to statistically re-generate equivalent dislocation loop microstructure in various grains (of course with some limitation on stress variations from grain to the next). Similarly, the GB microstructure can be statistically regenerated from the information obtained in small volumes.

4.3 Modeling Fracture Processes

Understanding the DBTT in fusion structural materials requires two main steps. First, we plan to model simple crystals that do not contain other initiation sites for micro-cracks ahead of a main crack. In this case, the controlling factors of the DBTT are at the nano-scale, and are determined by the nucleation conditions or or by various effects on dislocation mobility ahead of cracks. So far, there has been no development in the lkiterature for modeling full 3-D conditions of cracks of arbitrary shapes with emitted dislocations. All research reported so far is for simpolistic 2-D analysis. Second, in alloys containing micro-crack initiation sites (e.g. ferritic/ martensitic steels), the behavior is dominated by the distribution of such initiating sites (carbides or triple-point junctions). In this second area, we plan to extend the Master Curve approach of Odette and co-workers (Odette and He, 2002) by developing a computational analog that combines 2-D DD with 2-D FEM simulations of crack-tip plasticity. This will be explained in the next section.

In the first area of modeling fracture processes, future research will focus on the following aspects related to the DBT behavior:

- Effects of dislocation pinning ahead of crack tip as a result of their interaction with radiation induced defects, precipitates or solute atoms;
- Effects of stress triaxiality;
- Effects of prior dislocation microstructure (pre-deformed);
- Large scale simulation of Crack-Dislocation ensemble in the transition region.

In the following sections, we will briefly describe our proposed research plan.

4.3.1 Effects of Nano-scale Impurities and Defect Clusters

It has been shown that impurities have strong effect on the DBTT for Cr-based alloys. Understanding of the effects of impurities and solutes on the DBTT is critical to the development of alloys that are resistant to embrittlement. In our previous work (Huang and Ghoniem, 2002), the density of sessile interstitial atom (SIA) clusters was found to greatly affect the Critical Resolved Shear Stress(CRSS) for dislocation motion. The question arise then, what's the effect of these clusters if they are located near the crack tip. The CRSS of each dislocation loop will be changed, it is expected that they will influence the back stress on the crack, and hence will influence on material ductility? Our objective is to understand the effect of these SIA clusters, microvoids, precipitate inclusions, and interstitial impurities on the DBTT. This will hopefully enable us to design more embrittlement-resistant alloys.

4.3.2 Pre-deformed microstructure

Sharp DBTT transitions can only occur in well prepared dislocation-free crystals. Thus, a pre-existing dislocation microstructure will change the DBT. FIG. 6 shows an illustration of different densities of randomly distributed dislocations that will be placed ahead of 3-D crack tips. We plan

to determine the mechanisms by which the pre-existing dislocation microstructure influence emitted dislocation motion, and hence the transition behavior from brittle to ductile. One possibility is that with a high density of dislocation, dipoles and junctions are easily formed, so higher stress are needed to break these strong interactions, causing immobility of these dislocations, and hence higher stress field near crack tip. The effect of different densities of initially distributed dislocations will be studied in our future work.

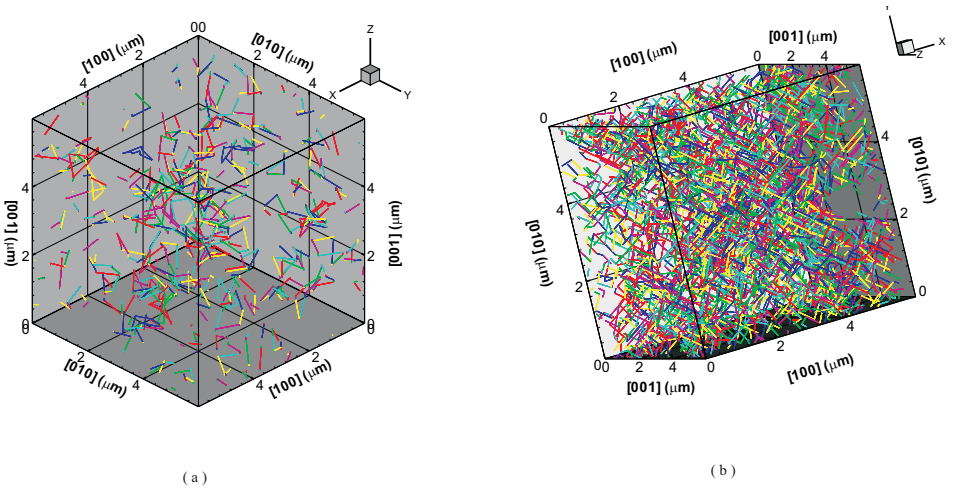

Figure 6: Illustration of different dislocation densities within one single cube. (a) low density (b) high density

4.3.3 Effects of stress triaxiality

Three-dimensional surface and embedded cracks are usually encountered in engineering structures at varies temperatures, thus it is necessary to understand the ductility of the material at varies temperatures. A large effort has been invested on the solution of the stress field of 3-D cracks. Sih and coworkers (Hartranft and Sih, 1969; Hartranft and Sih, 1977; Kassir and Sih, 1966; Sih and Chen, 1981) performed a thorough study of three-dimensional crack problems. The analytical forms of the stress field near crack crack surface is obtained (Kassir and Sih, 1966) if the stress intensity factor K is known. But the problem is how can we obtain these Ks when cracks are interacting with dislocations? Here our future objective is to avoid these crack stress calculations in 3-D. We plan to develop an extension of the earlier representation of cracks with dislocation distributions to the more challenging case of fully 3-D cracks of arbitrary shape. We believe that this will represent an important step in the realistic modeling of crack tip plasticity of practical materials.

IIt is known that the image force due to crack free surface can be obtained in analytical forms ((Lin, Lin, Chen and Chang, 1997; lin Pan, 1995; Wang and Lee, 1998)) in the 2-D case. However, for 3-D problems, the shielding effect of dislocations is still unknown. The Finite element method has been used to solve some simple cases (Jr., 2000), but for the shielding effect on cracks, the FEM will be very time-consuming and impractical. Here, we will introduce the notion of *3-D crack dislocation loop distribution* to avoid the painstaking iterative calculations in FEM approaches.

As discussed in literature (Lardner, 1974), a crack can be represented by a series of so called

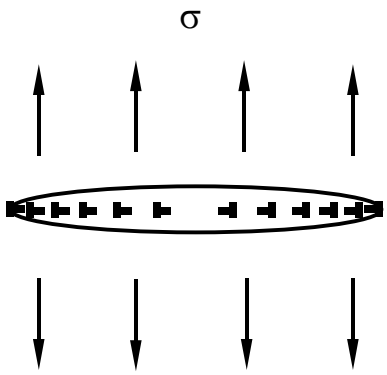

Figure 7: A Plain crack in infinite domain is represented by an array of edge dislocations

crack dislocation as shown in FIG. 7. The stress field of these distributed edge dislocations is the same as that generated by a crack. Thus the crack problem can be transformed to solve the distribution of the dislocations, and as if there is no crack in the material. For a simple 2-D case, the crack can be represented by n edge dislocations, by solving equation set:

$$\sum_{l \neq k} -\frac{\mu b}{2\pi(1-\nu)} \frac{1}{x_l - x_k} + \sigma = 0, k = 1, 2, ...n \tag{14}$$

However, it is difficult to get the analytical solution for EQN. 14. First suggested by Leibfried(Lardner, 1974), and later modified by other researchers, a continuum distribution of dislocation with density $f(x)$ is introduced. For the case of uniformed tensile loading, $f(x)$ is found to be (Lardner, 1974):

$$f(x) = -\frac{2(1-\nu)\sigma}{\mu b} \frac{x}{\sqrt{a^2 - x^2}} \tag{15}$$

The stress of each point near the crack tip can be obtained by the integral of the stress generated by these continuum dislocations. So far, most of the solutions for 2-D crack problem can be easily obtained by way of crack dislocations (Lardner, 1974). Here, our objective is to extend this concept to solve general 3-D crack problem.

For the 3-D crack problem, these crack dislocations are expected not to be straight and infinitely long. This is due to the fact that the stress field along the crack front is no longer uniform, and dislocations tend to be curved as shown in FIG. 8. Instead of solving a similar equation set EQN. 14, we plan to use our dislocation dynamics method to dynamically simulate the equilibrium configuration of discrete dislocations. Here, we assume that crack dislocation are emitted from one side and move toward the crack front as shown in the figure under the external driving force. Due to the interactions of these dislocations, they will pileup near the crack front and finally reach an equilibrium state. This procedure is an extension to the earlier work of Amodeo and Ghoniem on 2-D pile-up dynamics.

As discussed earlier, direct calculation of image stresses due to the crack free surface is a painful process. We will treat here the stress field of those *real* crystal dislocations as those of an external load. Thus the combined effects of external load, emitted crystal dislocations and the mutual interactions of crack dislocations makes an equilibrium state for each of the crack dislocations. The

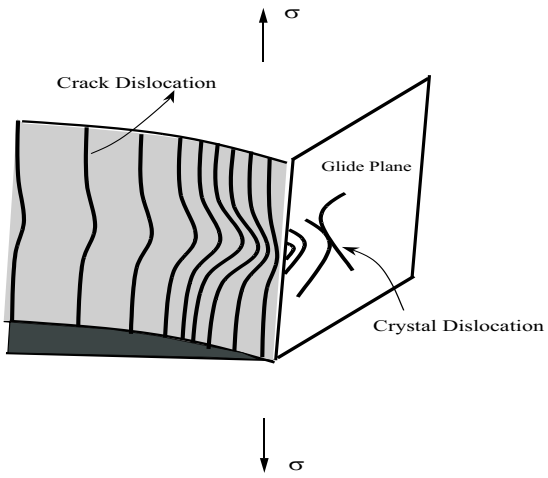

Figure 8: Opening crack with curved 3-D dislocation representation

final stress field near the crack tip will be the sum of the stresses from all the crack dislocations and all the crystal dislocations plus the external loads. Calculation of image forces and stress due to the external load can be unified to solve a dislocation pileup problem. No image stress calculation is needed. dislocation.

As an application of crack dislocations, we plan to use closed loop crack dislocations to simulate penny shaped cracks as illustrated in FIG.9. Compared with the open crack, all boundary conditions can be fully satisfied. Our preliminary calculations of the Crack Opening Displacement (COD) and the stress fields around crack tips are extremely encouraging, and will be published shortly. An example of a re-constructued 3-D crack at the hexagonal grain boundary surface in between two grains is shown in Figure (10), which shows a hexagonal grain boundary crack subject internal helium pressure p. The outermost dislocation loop are chosen as the periphery of the grain boundary. A total of 15 dislocations are fitted within the crack surface, excluding the outermost bounding one. As shown in the figure, due to the interaction with the boundary, the shape of the loop are more like hexagon, this is more obvious in the outer dislocation loops. The stress contour due to this distribution is also obtained in FIG. **??**b, due to symmetry of the problem, only the shaped parts is given. It is shown that due to the effect of 3-D, when the distance to the tip is very small, the stress decays as $1/\sqrt{r}$, but is much faster at longer distances.

4.3.4 Large-scale simulation of Crack Tip Plasticity

After solving the pileup process, the whole problem can be unified to large scale simulation of dislocation interactions, no crack will enter the calculation. All dislocations can be classified into two groups, one is the *crack dislocations* which is related to the crack tip stress and image stress fields, the other is the crystal dislocations, emitted from the crack tip, whose effect will influence both the distribution of crack dislocations and the total stress field around the crack tip. With known crack tip stress, and applying the Griffith's theory, a final simulation of the DBTT will be done. So our problem now can be simplified as the problem of dislocation interactions, and no crack is needed! We plan to investigate the computational issue associated with 3-D parallel dislocation dynamics code on the 160-node ISIS computational cluster at UCLA

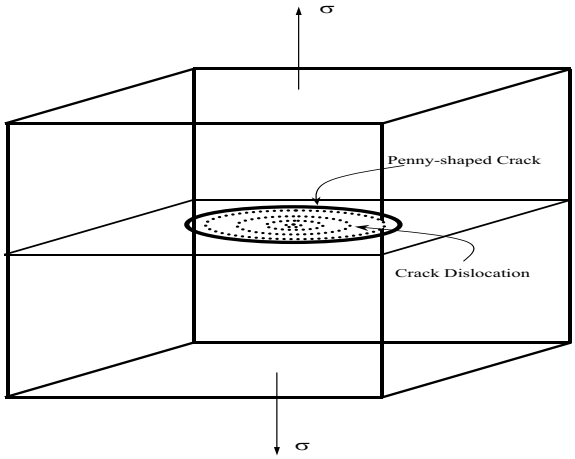

Figure 9: Representation of the openning of a penny-shaped crack

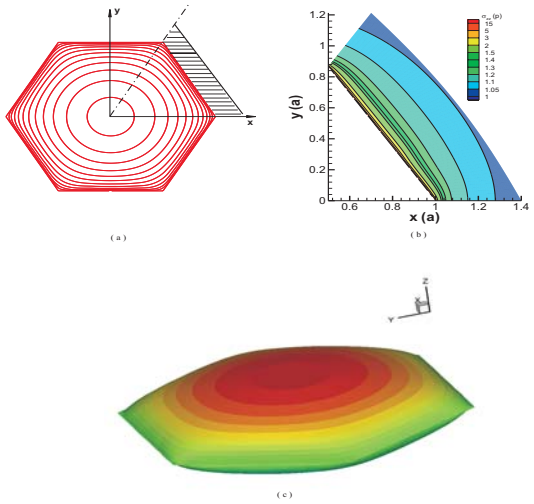

Figure 10: Shape of a 3-D grain boundary crack computed by our PDD method

4.3.5 High-Temperature Helium Embrittlement

The data base on helium embrittlement and corresponding models were developed almost entirely for austenitic alloys. It is generally believed that F-M alloys are less sensitive to helium embrittlement than austenitic alloys. However, creep strength is likely to be more limiting than creep rupture for conventional F-M alloys. The combined effects of helium and the high matrix strength of ODS systems are not known. While in principle, vanadium alloys have high thermal creep strength, simple solid solution variants are almost certainly very vulnerable to low rupture time and ductility due to high helium concentrations in grain boundary bubbles. This research will address all of these issues, but will primarily focus on the effects of high helium concentrations. At service stress levels, creep rupture generally occurs by the nucleation, growth and coalescence of grain boundary cavities . The nucleation stage is often rate controlling and for a variety of reasons, usually involves heterogeneous cavity formation at grain boundary precipitates. However, this may be effectively short-circuited by the conversion of stressed helium bubbles to rapidly growing cavities. Helium not only reduces creep cavity incubation times, but also increases cavity number densities on boundaries and the fraction of cavitated boundaries; all three of these responses to higher helium levels have very deleterious effects on creep rupture. Even without helium, creep rupture times would be very low if cavity growth took place by unconstrained boundary diffusion. However, in useful alloys growth rates are decreased by many orders-of-magnitude by both grain boundary phases that lower effective boundary diffusion rates and creep accommodation of local dilations around heterogeneous distributions of cavitated boundary facets due to grain boundary cavity growth.

In this Task we propose do develop creep rupture models that self-consistently account for: a) nucleation, including bubble-to-cavity conversions; b) cavity growth by restricted local boundary diffusion; and c) creep accommodation of material surrounding local dilations of cavitating boundary facets by stress redistribution. This will closely link to the previous task on the transport and fate of helium. Furthermore, the critical role of matrix creep strength will be integrated in this model. Generally, high creep strength increases rupture times, although the effects of interconnected soft boundary zones must also be considered. In the ODS systems, the nature of dislocation-obstacle interaction is key to providing high levels of creep strength, and will be modeled in detail for various dispersiods. The thermal and irradiation creep models of Ghoniem and co-workers will be integrated in this comprehensive effort. In these models, rate equations are developed for various dislocation populations (e.g. mobile, slow moving and boundary dislocations), and are coupled to nucleation/growth equations for dislocation sub-boundaries, dislocation cells, and irradiation-produced point defects. Extensions of this formulation to model the behavior of ODS systems will be particularly emphasized. While semi-analytical treatments of creep-accommodated cavity growth are available, FEM simulation methods will be used to better quantify this process. The effect of irradiation creep on accommodation will also be treated. Various parallel and sequential multi-mechanism creep and creep rupture processes will be represented as Ashby-type maps (creep, creep rupture and creep ductility), both for close interfacing with experiment and as a convenient design tool.

Coupled with microstructural simulations, which will help guide management of helium flows to the grain boundaries, our creep rupture models will provide an important material design tool. We plan to assess factors, which can be effectively used to optimize competing effects. These are: grain boundary design (e.g. phases which enhance nucleation and retard growth of cavities), high matrix creep strength (longer creep rupture time, lower ductility), fine matrix dispersions, grain size

effects, dislocation cell size effects, and the effects of alloying on creep rates and helium transport.

4.4 Modeling the Ductile-to-Brittle Transition

4.4.1 Recent Physical Models of DBTT

There is a range of structural materials, mostly mutiphase materials (e.g. steels) in which microcracks ahead of the macrocrack control the fracture toughness of the materials, see eg. (Rosenfield, Shetty and Skidmore, 1983; Veistinen and Lindroos, 1983) and references therein. It is now well-established fact that the microcracks in brittle precipitates (originated by slip in the matrix); situated ahead of notch or pre-crack is detrimental in the fracture behavior of ferritic steels. Conventionally, this is modelled by a critical tensile stress criterion at some distance ahead of the macrocrack tip. Since the original attempt by Ritchie, Knott and Rice (RKR) (Ritchie, Knott and Rice, 1973) to quantify the characteristic distance in relation to grain size, there has been an upsurge in the literature (for a recent review see (Knott, 2000)). Now a commonly assumed relation that ferrite grains are grown out of austenite by the rejection of carbon. Thus if there are more ferrite grains (finer grain size) the carbides will be thinner when adjacent grains impinge on each other. The RKR model or its variants were successful in explaining the lower-shelf fracture behavior, but fails at the transition region. Wallin *etal* extended the modelling with some success to the transition region by considering variation of effective surface energy $(\gamma_s + \gamma_p)$(where γ_s the true surface energy and γ_p the plastic work done during propagation) with temperature(**?**). This eventually lead to the Master Curve (MC) Hypothesis which predicts that brittle-ductile transition of all ferritic steels follows a universal curve. The data from different irradiation conditions or microstructure can be 'mapped' into a single curve by shifting it with a 'reference temperature' T_0 (Wallin, 1993; McCabe, Merkle and Wallin, 2000). Irrespective of the fact that Master curve hypothesis is an empirical relation, it is now widely used to check the reliability of structures under irradiation in the nuclear industry(ASTM, 2002). The ultimate goal of the project is to derive the physical parameters involved in the Ductile-Brittle transition from fundamental (dislocation level and atomistic) processes.

Hirsch-Roberts Model for Brittle-Ductile Transition

The dislocation dynamics model developed by Hirsch and Roberts (HR)(Hirsch, Roberts and Samuels, 1989; Hirsch and Roberts, 1991) was quite successful in predicting the fracture toughness of many single crystalline materials. In this model plastic zone around the crack-tip is modelled as a dynamic array of dislocations. As the load is increased, dislocations are emitted from a source near the crack-tip. The emitted dislocation impedes further emission due to its back stress at the source position, the back stress decreases as the dislocation moves away. The plastic zone thus generated shields the crack-tip from external load and enhances the fracture toughness. When the crack-tip stress intensity reaches a critical value (usually the Griffith value), fracture is assumed to occur. Since with increasing temperature dislocation velocity increases, more dislocations are emitted and the fracture toughness increases. Experimentally obtained dislocation velocities are mostly used.

Lately the model used friction stress controlled dislocation velocity law, which is appropriate for BCC metals and alloys. Using a friction stress $\tau_f = \sigma_y/\sqrt{3}$, where σ_y is the uniaxial yield stress (here τ_f is equivalent to the shear yield stress when von Mises yield criterion is assumed) the pre-

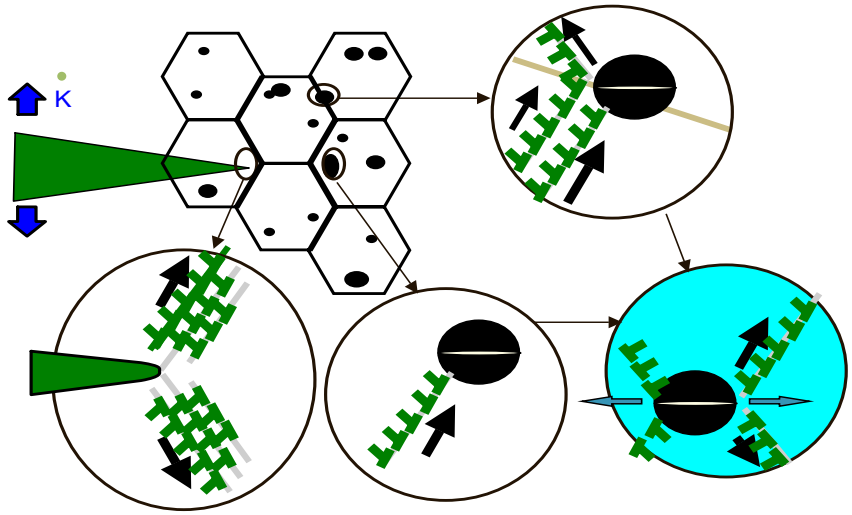

Figure 11: A schematic of the microstructural details of the crack-system we are modelling

dicted plastic zone size and crack opening displacements compares well with analytical results. And the stress field ahead of the crack matches with that obtained analytically by HRR (Hutchinson, 1968; Rice and Rosengren, 1968) for small scale yielding in power-law hardening materials. Using the critical stress ahead of crack criterion this model was successfully extended to predict the lower shelf fracture toughness behavior of Ferritic steels (Hirsch and Roberts, 1997).

Recent Modeling of Cleavage Initiation in Ferritic Steels

To account the microstructural details in the fracture prediction of ferritic steels, recently we modelled the low temperature (lower shelf) fracture behavior of Ferritic Steels (Roberts, Noronha, Wilkinson and Hirsch, 2002; Noronha, Roberts, Wilkinson and Hirsch, 2003) as follows. The cleavage fracture in cracked-carbide particle was represented as a slit crack capable of emitting dislocations when loaded. The basic relation of stresses used were derived by Wang and Lee(Wang and Lee, 1990). To simulate the behavior of crack in a plastic zone, beyond yield (i.e $\sigma_{applied} > \sigma_{yield}$, modified relations were used. They are obtained by subtracting the far-field of applied stress and adding in the far-field at yield, or in other words keeping the non-K-field constant at σ_{yield}. This represents a triaxial stress state ahead of crack of a perfectly plastic materials. With the approximation that crack plane is perpendicular to the loading direction and dislocations are emitted from the crack-tip along inclined and perfectly aligned slip planes it predicts the fracture stress invariance found experimentally in ferritic steels. Also it enables to make a theoretical prediction of the plastic work done during crack-propagation (γ_p). But steels are hardening materials, and this assumed triaxiality is far less than an approximation. Now we used the triaxial condition appropriate for a hardening material, with exponents $n = 0.1 - 0.3$, the typical hardening exponents for ferritic steels.

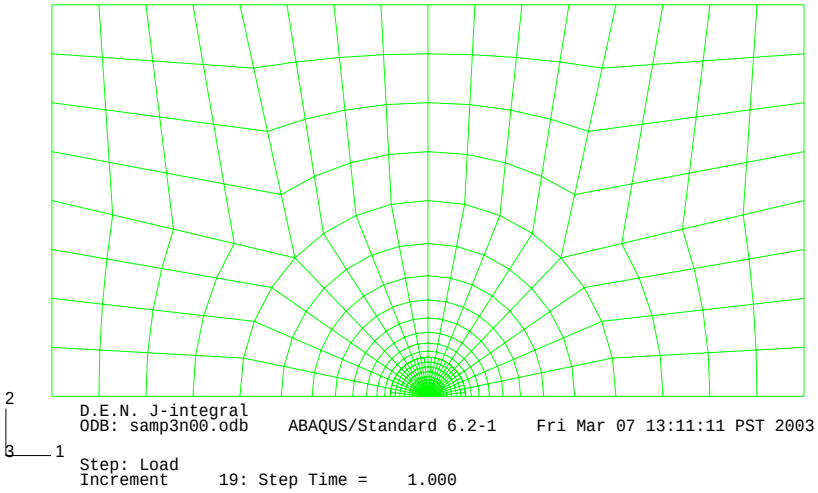

Figure 12: Typical mesh used in the Finite Element simulation of the primary crack

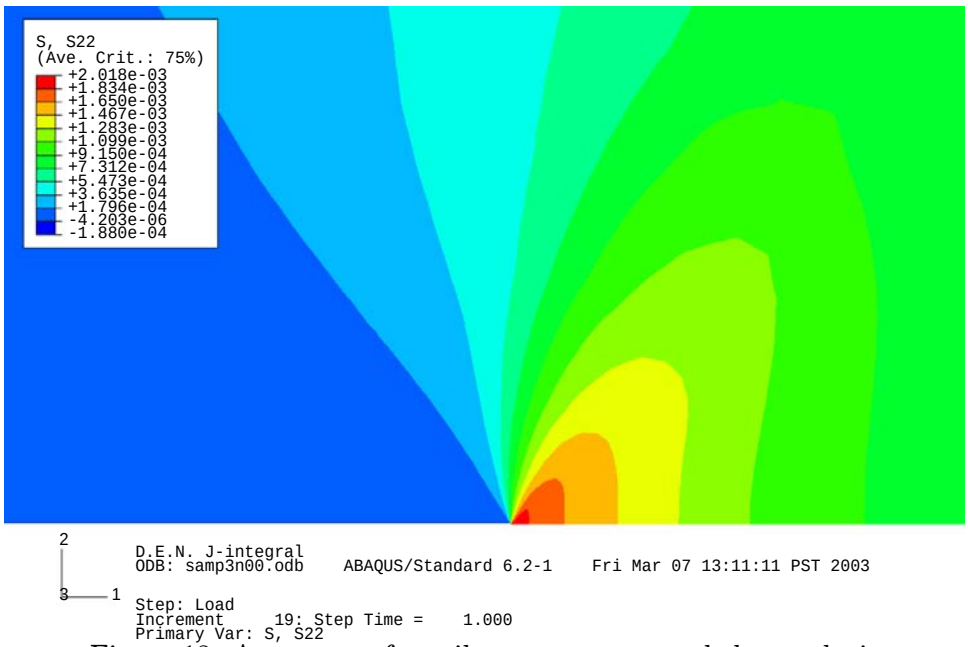

Figure 13: A contour of tensile stress σ_{22} around the crack-tip

.

4.4.2 Recent work at UCLA

Model and method of calculation

The system we model involves, a primary (macro) crack (which is the precrack in experimental samples) or surface cracks in practical structures. And a secondary crack which are usually cracked brittle particles situated in the plastic zone of the primary crack (See Figure (13).

We model the macrocrack as finite element elastic-plastic crack in power-law hardening material and the secondary crack originated from brittle particle as a slit-crack capable of emitting discrete dislocations. The microcracks are in the field of finite element (FE)-crack, the coupling is unidirectional, meaning the presence of free-surface due the microcracks are not accounted for the FE-simulation (it is negligible due the small size of these cracks when compared to the primary crack).

Two dimensional finite element simulations were performed using the general purpose FE code

ABAQUS(*Abaqus V6.2*, 2001). A typical mesh used for the calculation is shown in figure 2. The initial radius of the crack-tip is taken to be 10^{-5} times the width of the specimen. Accordingly, the dimensions of the refined mesh near the crack-tip was about 10^{-5} of the coarsest mesh. In the simulation of a half specimen 1544 nodes and 1407 4-node linear elements were used. Elastic-plastic constitutive equations $\sigma = \sigma_0 + K\epsilon^n$ with K=400 MPa, σ_0 is the yield stress and n the hardening exponent were used. Figure 3 shows the stress contour of tensile stress σ_{22} around the crack tip along the loading direction.

The secondary crack (micro crack) is represented as a finite through-thickness crack, capable of emitting dislocations. Its plastic zone is represented by edge dislocations on slip planes oriented at an angle to the crack plane, emanating from sources near the crack tips. These dislocations shield the crack (i.e. reduce the crack tip stress intensity) through the compressive stresses exerted by them on the crack. For each positive dislocation emitted, a negative one moves into the crack. In the simulations, applied stress is increased according to the stress series obtained at the 'particle' by FE-simulation. At each time step the dislocation array is equilibrated and a dislocation nucleation criterion, is evaluated to decide whether a dislocation will be emitted. The nucleation of dislocations reduces the local stress intensity at the crack tip such that further dislocation nucleation is impeded. In the time step immediately before a new dislocation is nucleated, the local stress intensity is at its maximum. This maximum increases steadily in magnitude as the applied stress is increased according to the stress series obtained by FEM simulations. Finally, in the microcracks that fail the local stress intensity k at the crack tip exceeds the critical value for fracture (here taken as $1MPa\sqrt{m}$). The applied stress (tensile) at this stage defines the stress at fracture (σ_F) at the microcrack. In these simulations, the dislocations move against a friction stress (which is taken as $\tau_f = \sigma_y/\sqrt{3}$). The obtained fracture toughness values can be mapped to temperature using the experimentally determined variation of yield stress (σ_y) with temperature. Knowing the tensile stress at the microcrack at fracture σ_F we find the J-integral value at that applied load. This is the J_c from which we obtain $K_{Jc} = \sqrt{EJ_{Ic}}/(1-\nu^2)$.

4.4.3 Results

Figure (14) shows a Brittle to ductile transition (BDT) curve we obtained by using the method. The fracture toughness values calculated as a function of friction stress (or yield stress) is mapped using the σ_y versus temperature data for high nitrogen mild steel reported in (Ritchie et al., 1973). Carbides in the range of $0.1-10\mu m$ with normal size distribution is used in the calculation. For yield stresses (corresponding to each temperature) Finite Element analysis is done with the appropriate constitutive laws and the stress at a point ($1.2\mu m$) is recorded as the load is increased. This stress series is then applied to each microcrack and the corresponding microscopic cleavage fracture stress is found (If the microcrack does not fail they are considered as impotent cracks and will not contribute to the fracture toughness of the specimen). As we can see by varying one parameter itself a scatter in the fracture toughness values is reproduced. More more work is in progress looking the effect of position and orientation of the crack.

4.4.4 Future directions/Project Plan

Work in progress

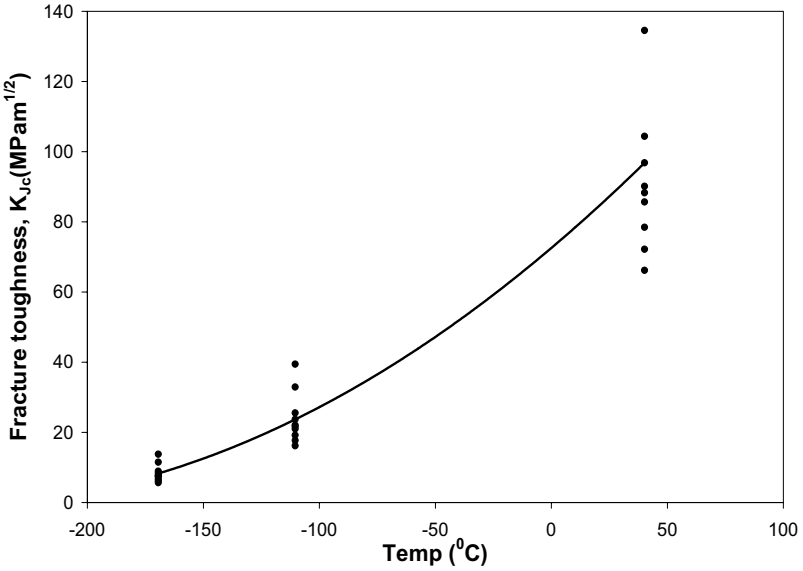

Figure 14: The fracture toughness versus temperature curve obtained from our computation for a high-nitrogen mild steel

- **Effect of Mixed Mode Loading**
  Almost always secondary cracks are modeled as if they are parallel to and situated at the crack-plane ahead of the macrocrack. But there were experimental observations that these secondary cracks could be located at some angle to the primary crack plane (**?**). We intend to study the effect of mixed mode loading by obtaining different stress component series by FE simulation at random off-crack plane positions, especially along different relevant angles like $45^0, 70.5^0$ etc. These stress series will then be used in the discrete dislocation simulation of crack-tip as described above. This will enable us in exploring the combined effect of size and position of carbides.

- **Crack Growth**
  Irrespective of the fact that stable crack-growth has been observed around the ductile-brittle transition temperature, most modelling so far has been done considering only the unstable cleavage. This could be one of the reasons why most models predict the fracture behavior well at the lower shelf, whereas it fails to predict the transition. Here we intend to extend the model to include the crack-growth. In the DD simulation this demands having dynamic multiple slip planes along which dislocations can be emitted as the crack propagates. We have already implemented the multiple slip plane, see (**?**). Now we intend to simulate the crack growth using the following relation between crack velocity and crack-tip stress intensity factor (**?**).

$$v_c = bM_c(\frac{K}{A\sqrt{2\pi b}})^{\eta} \tag{16}$$

  where v_c is the velocity of crack, M_c the crack mobility, b the Burgers vector of the dislocations involved and η is is taken to be 3. $A = \mu/2\pi(1-\nu)$ for mode I crack, where μ is the shear modulus and ν is the Poisson's ratio. Thus while the dislocation are emitted crack can also

extend. Including the crack growth should enable us to simulate (and predict) the Brittle to ductile (BDT) transition curve all the way to transition temperature and beyond by a fundamental formulation.

- **Effect of Dislocation nucleation**
  In our recent simulations of microcracks we found that the number of dislocations being emitted and the size of the plastic zone is much larger than that we anticipate from experimental observations. The reason for this discrepancy could be the fact that in our simulations the stress required for dislocation nucleation is taken to be equivalent that for the dislocation motion. But it has been shown that dislocation nucleation even from the most easiest emission configuration (emission from ledges) has shown to require a much higher energy (Xu, Argon and Ortiz, 1997). We recently attempted to couple (externally by passing-on parameters) atomistic and dislocation simulation of crack-tips(Noronha and Farkas, 2002). We intend to do a more detailed atomistic simulation of microcracks originating from carbides and propagating to ferrite matrix, with ledges and other imperfection along the crack-front.

- **Extending the model to predict the fatigue growth**
  Once the crack growth is included into our computational scheme, it could be extended to use the fatigue crack growth. There has been some attempts to study the Mode II fatigue crack growth(Wilkinson, Roberts and Hirsch, 1998), but more practically relevant Mode I has never been studied. In our simulations the rate of crack growth will be a function of difference in dislocations emitted at maximum stres and minimum stress at each loading cycle. We ill use this approach to study the fatigue around the threshold and the Paris-law regime. According to Paris-law,
  $$\frac{da}{dN} = C_P(\Delta K)^m \tag{17}$$
  da/dN is the rate of crack growth, ΔK is the difference between K_{max} and K_{min}, C_P is proportionality constant dependent on the load ratio (K_{max}/K_{min}) and m is an exponent depends on the material. We can check the estimated exponent m with that obtained from experiments. Also we intend to compare it with the values obtained by Deshpande *et al* (**?**) using another discrete dislocation simulation. When compared our method the timescales they can simulate is very less.

- **Specimen Size Effecst on the DBTT**
  Small specimen test-techniques are widely used in the determining the structural integrity of nuclear reactor vessels (Crowin and et al, 1993). The standard fracture toughness procedures (which are specified to have highly constrained specimens) overestimate the structural performance. There were several attempts to quantify the constraint loss and make corrections in the data (Odette and He, 2002). Dislocation simulation methods have not yet been used to quantify the constraint loss. We intend to use our FEM-DD simulation scheme to study the effect of constraint loss in these specimens by bringing in the variables like specimen size into the model.

- **Coupled Macro-micro crack tip dislocation models**
  We propose to develop a fully coupled dislocation dynamics scheme with a macrocrack and several microcracks. In this representation the coupling between the macrocrack and secondary cracks will be complete and dynamic. The dislocations emitted from every crack will interact with every other. Once developed this should be a very powerful computational

tool in fracture prediction since microstructural details (like carbide distribution and grain size effects) can be built-in. To start with we intend to implement the dislocation dynamics code with solutions obtained by Shiue *et al* (**?**) for the plain strain case of a macro and micro with dislocations. This will be a computationally intensive calculation since we take into account the mutual interaction between every dislocations. We will implement this in our computational cluster (Beowulf Cluster) using MPI. Odette *et al*(Odette, 2000) extended the Master Curve methodology to include the geometric effects; so that it could be used to develop fracture toughness data base from small test specimens(Odette, 2002). This new method enable us to account for the shift in temperature due to the loss of constraint in small test specimens(**?**; G. R. Odette and Lucas, 2002). The ultimate goal of the project is to derive the physical parameters involved in the Ductile-Brittle transition from fundamental (dislocation level and atomistic) processes .

- Fracture Prediction

  To determine the structural integrity probabilistic methods are widely used. They all are based on the weakest-link theory, and either use the Weibull distribution for the probability of fracture (Beremin model) (**?**) or end up in similar expression starting from a carbide distribution (**?**). In both these models, the stress field ahead of the crack is obtained from Finite Element solutions. In the BEREMIN model for each volume element ΔV_j the maximum principal stress $\sigma_{1,j}$ is calculated and a probability of failure is assigned. The total probability of failure is then obtained by summing over the whole plastic zone. The cumulative probability of failure $p_f$is given by

$$p_f = 1 - exp\{\sum_j (\frac{\sigma_{1,j}}{\sigma_u})^m \frac{\Delta V_j}{V_u}\} \tag{18}$$

  Both Weibull modulus m, and the scale parameter σ_u are assumed to be characteristic material parameters which are independent of temperature, geometry and mode of loading. The parameter V_u is a characteristic volume such that $V_u \approx 1/N_v$, where N_v is the number of critical inclusions per unit volume. Currently the parameters m and σ_u are used in this model are obtained by best-fit to experimental data. There is very little understanding of their meaning or relation of such basic microstructural and material properties as the carbide size and strength distribution and the fracture and flow properties of the matrix.

  We propose to derive the material parameters m and σ_u from dislocation model and compare with the experimental data. The influences of temperature and strain rate will be assessed to investigate the influence of these parameters on cleavage toughness.

4.5 VISTA: Virtual International Structural Test Assembly

The primary goal of VISTA (Virtual International Structural Test and Analysis Facility) is to facilitate the development and implementation of advanced and fully integrated integrity and lifetime assessment methods by:

1. Providing a methodology and physical basis to evaluate relations between research on material properties, failure paths and structural integrity assessment methods related to
   - various properties, and
   - the performance and lifetime limits of fusion structures.

2. Inserting a much higher degree of realism in so called design studies with respect to:
   - Geometric realization
   - Multi-physical loading conditions
   - Interaction of different sources of loading and damage.
3. Facilitating the development and implementation of advanced and fully integrated integrity and lifetime assessment methods.

VISTA is a modelling tool in a very broad sense. The aim goes well beyond establishing new models, new codes or analyzing a particular blanket concept. Rather the objective is to combine wide range of models including constitutive and damage laws, Finite Element models, geometrical configurations and loading conditions, to perform "virtual experiments" over a wide range of conditions, to carry out sensitivity studies and to evaluate a range of potential interactions and failure paths. The preparatory stages for development of VISTA have been categorized into three Phases.

- ***Phase-I (December 2002 - April 2003)***consists of acquisition and setting up the necessary hardware and software for modeling and running FEM codes and programs on the UCLA parallel computing cluster (ISIS; see Section ????).
- ***Phase-II (May 2003 - September 2003)***centers on developing full-scale 3-D FEM models of a typical First/Wall Blanket structure to analyze the effects of non-uniform heating, gravity, hydrostatic pressures, and convective cooling on the entire component.
- ***Phase-III (October 2003 - December 2003)***concentrates on developing "damage functions"to analyze the synergistic effects of stress-states and irradiation on the thermostructural response using the models developed in Phase-II of this project. Following completion of VISTA's first three Phase program, the community will need to evaluate and chart a course for further development of integrated integrity and lifetime assessment methods. Success of VISTA will depend to a large extend on the progress and results of the parallel Fusion Materials and Design Database project.

4.5.1 Recent Phase-I Activities

Integrated Multiphysics modeling of full-scale components requires massive computational resources and a multiphysics capable FEM software. The UCLA Beowolf Cluster, ISIS (see Section ???) with 160 Nodes provides such computing powers and the ANSYS Inc. offers a multiphysics FEM code capable of running on Linux-based parallel computing cluster. The parallel computing ANSYS FEM Code V7.0 is the most powerful version that ANSYS Inc. has developed. This code is commercially offered at a price of $100K per year. Because of the high price of this parallel multiphysics FEM code a new educational discount procedure had to be renegotiated between UCLA and ANSYS Inc. The negotiations lasted until January 2003 when ANSYS Inc. agreed to provide UCLA with the parallel version of the mutliphysics code for an anual fee of $2,500 for the first year, with a new price to be determined for subsequent years. In February 2003 the ANSYS Version 7.0 was successfully installed on the Beowolf Cluster. During Phase-I of this project the UCLA team is training four students (Tony Tan, Christopher Williams, Mitchell Styczynsla, and Peter Jeziorek) to use the ANSYS thermal and structural analysis package. Training of these students is to be

completed by the middle of April. In summary, both hardware and software have been secured at UCLA for developing full-scale 3-D FEM analysis of fusion components, such as First Wall and Blanket or Divertor structures.

4.5.2 Phase-II Plans: Three-Dimensional Geometric Features:

The goal of the Phase-II is to develop a 3-D FEM model of an entire representative First Wall/Blanket component. This phase will only model steady state conditions. Effects of transient loadings will be addressed in future phases of this project.

Fusion components are inherently large, and as such prone to non-uniform load distributions, both in the poloidal as well as the radial direction. Load non-uniformities are further exasperated by fluctuations in control parameters, such as start up, shut down, plasma operations, and plasma disruptions. Therefore, focusing on the 3-D geometric features alone introduces a range of issues that require full scale modeling.

Consider the non-uniform heating of FW/Blanket modules: the central part of the module receives the maximum heat loads compared with the upper and lower portions. Superimposed on this heating load is a varying cooling rate. The combination of non-uniform heating and cooling results in temperature gradients, which result in non-uniform thermal stresses both along the poloidal and the radial dimensions of the module. A full scale 3-D FEM model can incorporate these geometric features, which can then be coupled with material properties that are both temperature and stress-state dependent. Thus, a full scale 3-D FEM model is critical for evaluating the reliability and lifetime FW/ blanket structures.

First, it will be approached using full geometry three-dimensional models which would provide a range of boundary conditions for a series of detailed 2D models for local analyses of fracture and plastic flow localization. The following steps ouline the activities planned for this phase:

1. Identify and chose a representative solid First Wall and Blanket component
2. Determine the most likely material combinations to be used in this component
3. Identify the minimal features of the structure, which are necessary to represent:
   - Spatially varying primary coolant pressures and temperatures
   - Spatially dependent surface heat fluxes and volumetric heat deposition
   - Spatially varying irradiation induced damage
4. Identify typical operating parameters
5. Develop a 3-D Solid Model of the First Wall and Blanket component:
   - Test the applicability of ProE and SolidWorks for transporting the model into ANSYS
6. Identify and chose structure-relevant elements from the element tables of ANSYS:
   - Depending on the location within the FW/B structure different areas will require different element, e.g., shell elements, solid elements, beam elements, fluid elements, etc.
7. Establish appropriate boundary conditions to minimize computational time without loss in analysis accuracy:
   bullet Determine where symetry boundary conditions can be applied

8. Determine a set of spatial boundary conditions for:
   - Structural analysis (steady state)
   - Thermal analysis (steady state)
9. Perform structural and thermal analysis using the ISIS cluster
10. Perform a coupled structural/thermal analysis to establish combined primary and secondary stress states inside the stucture

Upon completion of Phase-II of this project the findings will be documented and a report will be distributed to the community for evaluation, comments, and feedback.

4.5.3 Project Plans for Phase-III: Damage Functions

Phase-III will comprise two priamry tasks. First is to carefully analyze and incorporate the feedback from the community to adjust and modify the models and the procedures developed in Phase-II. At the completion of this task the methodology developed will be made readily available to the community at large to model a variety of components, such as divertors. The second task focuses ondeveloping the methodolgy for modeling and incorporating "damage functions"with the FEM models.

Advances in radiation damage modeling and experiments have enabled the fusion materials community to develop complex models for describing damage processes. These models can take into account the effects of the stress state, temperature and irradiation conditions on component performance. Using full scale 3-D component modeling, local stress states and temperatures can be determined by FEM. On the other hand, models of radiation effects on the mechanical properties can then be used to evaluate the interaction between radiation-induced microstructural changes and thermomechanical loads. This approach is tantamount to a feedback system, where thermomechanical loads influence the microstructure, which in turn affects load distributions. This feedback system between material response and loads can be modeled by implementing what are called "damage functions"into advanced FEM software, such as ANSYS. The advent of High Performance Computing (HPC) in the form of parallel computing is making it feasible to use these damage functions in FEM. Development of these damage functions will ultimately result in mapping out potential failure pathways.

To develop the damage functions, VISTA will use hierarchical material damage models that will describe plasticity, visco-plasticity, creep and swelling or other subcategories of constitutive laws. The constitutive laws will be based on a multi-scale integration of materials theory, models, simulations and experiment. The following steps ouline the activities planned for incorporating *Damage Functions*:

1. Map the stress states throughout the FW/B structure.
2. Identify representative models or constitutive equations, which relate microstructural changes to loads.
3. Develop a simplified set of Damage Function
   - Identify most critical damage phenomena inside the structure based on the geometric

location and loads
- Compile representative models of damage phenomena
- Program these damage function models using ANSYS programing tools.

4. Identify areas of maximum synergistic effects between loads and microstructural changes due to irradiation:
   - The midplane cross section is likely to be a location of maximum secondary stresses.
   - Contact areas, such as supports at the bottom and top of the modules could also experience significant loads.
5. Construct 2-D FEM models of identified areas
6. Analyze these representative 2-D FEM models using the damage function
7. Quantify and compare the results based on damage functions with simple FEM analysis

At the conclusion of Phase-III the findings will be published and distributed within the community for feedback and comments.

4.5.4 Future Plans

Virtual Testing of Engineering Performance
The ultimate goal of an integrated modeling effort is to map the response of structures to the effects of irradiation induced material property changes as they are affected by geometric aspects of the 3-D components. Following the multiphysics analysis of the FW/Blanket and the development of damage function, the synergistic effects between component temperature, the stress state, and the effects of irradiation on 3-D structures can be analyzed. Thus, component failure pathways can be evaluated by Virtual Testing of engineering performance of full scale components. **The Fusion Materials Database Network**
The programming efforts of Phases I, II, and III will all be documented maticulously for the purpose of incorporating them into the third branch of Fusion Database Network Web Site: a venue for engineering performance of fusion structures. Following the completion of the third phase of VISTA a concerted effort will be launched between the Database project and the VISTA project to develop an interactive web-based performance knowledge database for the community. The tasks involved for this future phase will depend on the outcome of VISTA project.

4.6 Digital Fusion Materials Database

An ideal and low cost web-site database would be authored, maintained, and up-graded by the users directly without the need of a centralized web-site administration. Such a web-site is being developed by a UCLA/UCSB team of programmers to serve as a community wide Fusion Materials Database Network Site. This site relies on "Automated User-Based Content Management Technology"to provide three cross-linked categories of information:

1. Fusion relevant materials properties,
2. Material property-based constitutive equation models,

3. An engineering performance evaluation venue for fusion structures.

The underlying concept is based on using Relational Database Management Systems (RDBMS)as the core knowledge-managemen structure for the web site. The web-site is thus, in essence a RDBMS which iputs, updates, and pulls data to be presented to the enduser upon his/her request. Recently Internet Technologies are used to program this user-based content management web site for the fusion research community. The development of the Fusion Materials Database Network has been categorized into three Phases.

- ***Phase-I (December 2002 - April 2003)***encompasses setting up the infrastructure of the Relational Database Management System (RDBMS). This Phase involves planning the layout of the web site database structure. Aside from planning, Phase-I also (1) implements the automated conversion of raw data to web-based graphical displays, and (2) establishes a forum to serve as the engine for interactivity between members of the community.
- **Phase-II (May 2003 - September 2003)**centers on (1) finalize programming of core site features, (2) programming up-loadabilty features for users to post their data or to make changes to past postings, and (3) releasing a demonstration web site to select members of the community.
- **Phase-III (October 2003 - December 2003)**will focus on (1) collecting and (2) implenting feedback from the community to the demonstration web-site version. However, the most important aspect to be developed in Phase-III is to establish the protocols and methodology for collaborative content management, e.g., what are the editorial procedures to post/uploaded data or to make modifications to existing data.

The completion of Phase-III will be marked by the release of a fully functional user-based management web site for a fusion materials property database. Following, Phase-III (FY04) the Internet-based RDBMS infrastructure will applied to develop the second and third branches of this Fusion Network: (II) Material property-based constitutive equation models, and (III) Engineering performance evaluation of fusion structures.

4.6.1 Recent Phase-I Activities

Since December 2002, the project has progressed through the first phase of development. A team was assembled between UCLA and UCSB including one RDBMS/Web site programer and several assistants for collecting sample data. The backbone of the Relational Database Management System (RDBMS) for automatic graph generation of raw data was set up. A first version of the community's data reporting aspect is now functional, with completion due at the end of April.

Key Features Already Implemented
- Architecture of the data-table structure of the Relational Database Web Site.
- Automated transformation of raw data into automatically generated graphs.
- Scalable Vector Graphics (SVG) for all graphs and charts
- A multi-featured forum for interaction among database users.

For a complete description of Phase-I activities the reader is referred to Section A-8.

4.6.2 Project Plans for Phase-II (May 2003 - September 2003

The near term activities planned during Phase-II are discussed here. Although, it is difficult to delineate the activities clearly into Phases an attempt has been made to follow a systematic program development path. Most of the activities planned for Phase-II are geared at releasing a featured-rich demonstration version to a select community by the end of Phase-II (September 2003).

4.6.3 Transformation of Raw Data:

Advancements in Dynamic HTML (DHTML) and server-side scripting have led to new aesthetic standards in web design that we aim to uphold with our project. All our database content is prepared for user viewing by PHP, the same "Hypertext Preprocessor"currently being implemented on an enterprise level by Yahoo. Our PHP scripts perform a database query for the raw dataand then apply the rules of the script to fit the data into our visual model. If changes were made to the raw data the graph would be automatically updated the next time the browser screen is refreshed. This feature demonstrates the viability of an automatic up keeping of the materials database without having to invest in exorbitant expenditure to do so.

Proposed Features to be added in Phase-II
Phase-II will add a richer feature set to the users, which include:

1. **Data description:**
   Clicking on the various locations on a data-graph the user can find out who the author was, what sources were used, what type of data it is, and when it was posted and when it was up-dated and by whom.

2. **Direct link to references:**
   From the data-plot the user can determine various references that might have been used by the author to generate a series of curves or data points. If the plot author has posted links to these references, they can then be directly accessed by the end-user.

3. **Illustrations:**
   Often the publisher opts for also displaying relevant micrographs or sketches pertaining to the data. Such illustrations can also be directly vied by the end-user.

4. **Author's email link:**
   The user has the option to interact directly with the author(s) of the figure, curves, or datapoints via an email link to the relevant poeple.

5. **On-site related data links:**
   This is an important feature for cross referencing or researching other related data. The RDBMS backbone of this web site, allows for seamless cross linking to other related data. For example, if thermal conductivity of pure lithium is displayed, the user will have the option to invoke the display of non-pure lithium directly from the current plot/data form (of course the data has to be available).

6. **Related articles:**
   The RDBMS can automatically querry the data-base for related articles that might have been

posted by using the displayed primary keyword identifiers. This feature, however, will only be programmed after a significant data base of relevant articles, descriptions, or summaries have been accumulated.

7. **Comment box:**
   Of great importance for interactivity among the users is the abiblity for a user to post comments regarding the data that has been visited. This feature will also be directly programmed to interact with the forum system (see section on Forums) to inform all of the users that have signed up with relevant news or information groups. As a minimum, the author(s) will be immediately informed of any new postings to be able to respond or interact.

8. **Direct link between data-points on a graph and the raw data:**
   This is one of the more critical features of this web-based database. The ability to direcly display the data points of a curve or plot might fulfill a research need. By clicking on the curve, plot, or data-points, the full list of data points can be displayed and copied.

At this stage of the development we do not have the means to judge the criticallity of each of these features. Following release of the demo and community feedback the list of features will be modified.

4.6.4 Scalable Vector Graphics (SVG)

Scalable Vector Graphics are an essential part of our plan to provide an exceptionally useful research community. We adopted this technology because of the benefits it offers to users and its use of the XML (Extensible Mark-up Language) standard for web documents. During Phase-I Scalable Vector Graphics (SVG) for all graphs and charts has been implemented. We wrote scripts that automatically create graphs from entries in the database, supporting both single and multiple data sources. When a user chooses to display a plot or curve, the data is querried and the figure is plotted "on the fly."With this approach, changes can be made to the data set(s) at any time, which are reflectd next time the screen is refreshed or the data is plotted.

Since SVG are based on vector graphics, they can be scaled without any loss of quality. The resulting image is just as sharp as the original. We feel that users will appreciate these features, even though it requires marginal effort on their part. By selecting a technology that is associated with XML and the World Wide Web Consortium (W3), we are planning to provide additional dynamic features in Phase-II.

Proposed Features to be added in Phase-II
These benefits, however, come at a slight consequence. SVG require a free plug-in from Adobe. During Phase-II user-approved automatic downloading and installation of this plug-in by will be programmed to reduce the level of inconvinience for the user. This plug-in is small (2MB) by today's broadband standards, and does not require a system restart. With an optional, second free software package (Batik, from the Apache Foundation), users will be able to:

1. Download graphs from our site

2. Increase the sizes of the graphs

3. Save graphs as JPEGs

4. Insert graphs into PowerPoint presentations or other software.

These features wouldn't be available with static images like JPEGs and would be too difficult to generate automatically with a product like Macromedia Flash. SVG, however, is an impressive new web standard that can utilize other web technologies like JavaScript, while maintaining simplicity in the coding process. We plan on utilizing the dynamic JavaScript capabilities of SVG to enhance the resources we are offering to researchers. Rather than forcing users to either rely on eye approximation or retrieve raw data from the database, we will offer "mouseovers"on the graphs. Whenever a user places his or her mouse over one of the data points, indicated by symbols, the X and Y values of that point will appear in a nearby window. If a user has a preference for a certain type of chart, there can be a button that automatically switches between bar and pie representation. JavaScript offers a great deal of flexibility, and we will seek to accommodate the suggestions of the community in this area following our demonstration.

4.6.5 Forums To Foster Ease of Interaction

Forums are essential to foster ease of interaction of community members. The forum serves not only to post questions, but it also sends automatic emails to designated users. It allows users to examine the latest comments, uploaded figures, or un-published data. The user can also be automatically informed of new postings in the forum or in the database itself. To facilitate such features, we have implemented as a core feature an open-source forum software package called phpBB. This software functions with PostgreSQL, the same database system used for our Fusion Network database. The user is first welcomed to login in by generating his/her own user-id and password (should he/she forget the system will prompt him to reissue these). With phpBB, we can offer users e-mail notification when their posts are replied to, user groups for interests in various topics, mass-emailing for community announcements, user polls, and above all, constant access to feedback from peers

Proposed Features to be added in Phase-II
Phase-II will aim at incorporating the phpBB forums seamlessly into our web site. Feedback and interesting discussions have made forums very popular elsewhere on the Internet. Some effort will be required during Phase-II to integrate the forum software and the fusion network database. Our philosophy is that no extra effort should be required of users to see what the community is saying about fusion material issues. A region devoted to "Recent Discussions"will be programmed to become a familiar feature throughout our web site. We will create a database table for coordinating forum discussions and subject categories in the database, so that links to related discussions can be added to many areas with automatic updates. The value of keeping the community discussion up to date and accessible cannot be stated enough.

4.6.6 MathML for displaying constitutive equations

MathML (Mathematical Markup Language) is another implementation of XML governed by the W3 Consortium. It prescribes a method for displaying complex mathematical expressions via XML.

The alternative would be storing screen captures of equations from various programs provided by users. Though such an approach does provide a result, it's a makeshift solution at best.

Proposed Features to be added in Phase-II
An image-based equation does not incorporate well into presentations and papers. Therefore, a special effort will be made to utilizing MathML, which will allow users to copy and paste the equation into other applications. Creating an interactive tool to calculate values through the equations is also a possibility and increases the usefulness of our web site. However, this feature will only be implemted if the community response as strong. It's difficult to gauge how far MathML can go when paired with scripting and DHTML. The possibilities for innovation, however, are far fewer without MathML.

4.6.7 Project Plans for Phase-III

Phase-III (October 2003 - December 2003)focuses on (1) collecting and (2) implenting feedback from the community to the demonstration web-site version. Based on the feedback existing ones will be modified and new features may be added. It is premature to plan the details of this aspect of Phase-III. However, during Phase-III commincation with the select test community will intensify in order to establish the protocols and methodology for collaborative content management, which include:

1. Establishment of editorial subgroups
2. Procedures to automate editorial membership
3. Editorial procedures to post and uploaded data
4. Establishment of posting/updating protocols
5. Establishment of security measurements and procedures
6. Determining network access eligibility

More features and collaborative management issues will undoubtedly come to the forefront following release of the first demonstration version. The team is eager to receive the input and to work with the community as diligently as possible to address all concernes and requests. Afer implementing the recommndations from the select community a fully operational version will be ready for release to the greater community at the end of Phase-III (December 2003).

4.6.8 Future Plans

The second and third branch of this fusion database network will utilize the infrastructure, programming experience, codes, and methodolgies developed during development of the first branch, i.e., materials property database. However, some of the features of second branch, Material Property-based Modeling, will already be programmed into the first branch. For example, the user will have the option to click on a data-curve and view data-representative models, if they are provided by the author or other users. These models are stored in databases, which will become part of the

second branch. The third branch, however, will require a completely seperate approach in that the necessary knowledge base for engineering performance evaluation of fusion structures is supposed to be "growing"from the community utilizing the fusion network. In other words, the establishment and fulfillment of a performance evaluation venue should be an outgrowth of an highly interactive community.

4.6.9 Conclusions

We feel that our contributions to the community will be immediate and useful, a solid reflection of the thought and effort poured into this project. The Fusion Network currently consists of over 2,500 lines of code (PHP, Perl, and SQL). When the demonstration is completed, the database will offer extensive data on Vanadium alloys and F82H. More so, however, it will offer an example of what advancements in technology can do to expedite scientific progress via an online fusion materials community.

b

5 Task Time-line and Deliverables

The table below shows a breakdown of the various tasks in this proposal, their proposed timeline, and expected deliverables.

FY03	• KMC simulations of SIA cluster-dislocation decoration & rafting; • Advanced rate theory modeling of helium-vacancy cluster nucleation and growth, • DD simulations of dislocation-defect interaction mechanisms; • Development of coupled DD-FEM model for the DBTT; • Initial development of Web-based fusion materials data-base.
FY04	• KMC simulations of vacancy-helium cluster formation; • Development of rate theory for matrix and grain boundary void/bubble formation; • Continued DD simulations of dislocation-defect interaction mechanisms; • Correlations with radiation hardening experiments on pure metals (Cu & Fe) • Development of self-consistent DD-Grain Boundary-meshfree modeling • DD simulations of flow localization and plastic instabilities in irradiated Cu; • Large-scale, parallel FEM thermoelastic 3-D analysis of FW/Blanket modules; • Generalized plane strain inelastic analysis of critical FW/B sections;
FY05	• KMC modeling of microstructure evolution ; • Micromechanics of grain boundary helium embrittlement & fracture; • Correlations with radiation hardening experiments on Cu and Fe alloys • DD-GBD-meshfree simulations of plastic instabilities; • Elastoplastic FEM analysis of experimental mechanical testing data (Jupiter); • Continued development of 3-D FEM parallel algorithms for VISTA • DBTT experimental data assessment with the coupled DD-FEM model
FY06	• Applications of KMC microstructure evolution modeling to BCC metlas (Fe); • KMC modeling of vacancy-helium cluster formation; • Continued development of the Web-based fusion materials database • Inelastic FEM analysis of critical component lifetime & reliability; • Assessment of 3-D geometric effects on virtual testing (VISTA); • Applied, self-consistent DD-GBD-meshfree simulations of plastic instabilities for radiation-resistent alloy design; • Coupled DD-FEM fracture analysis with coupled DD-FEM
FY07	• Applications of KMC microstructure evolution modeling to FCC metals (Cu) ; • Finalization and deployment of the Web-based fusion materials database; • Determination of the impact of plastic instabilities on component design; • Experimental correlation of DBTT (with FEM-DD) experiments on ODS & NCF steels; • Experimental verification of DBTT modeling of Fe single & bi-crystals; • VISTA component reliability evaluation with damage mechanics & parallel FEM.

6 Facilities and Resources

6.1 The UCLA ISIS Computational Cluster

The ISIS Computational Cluster at the University of California at Los Angeles, under the direction of Professor Nasr Ghoniem of the Mechanical and Aerospace Engineering Department, and managed by Dr. Robert Amodeo, is a "Beowulf Cluster"consisting essentially of 64 computers and a fileserver. The cluster is housed in the Micro and Nano Mechanics Laboratory in the Engineering I Building at UCLA.

The primary purpose of this cluster is to reduce the time it takes to run Monte Carlo, Molecular Dynamic, and Dislocation Dynamic codes which can rely heavily on many body interactive processes. Computations which may be on the O NxN can be reduced significantly, by distributing the process over 64 dual processor computers (128 "effective"nodes, 64 physical nodes).

A secondary purpose of the cluster is to investigate the nature of parallel processing, in conjunction with the associated physics driving micro and nano-mechanical processes. The cluster is "operational"at this time, and is currently running PGI v4.0 Fortran Compilers, on SuSE Linux 8.0 OS. The cluster has passed fundamental benchmarks, and is currently being tested by users at UCLA and Los Alamos National Laboratory.

6.1.1 Hardware

The system consists of one large scale fileserver, which runs the main computational operating system, and serves accounts. Data (source code, input files, output files) are located on this file server. The 64 nodes are used primarily for their processing units, and also have large disks for scratch storage. The visualization workstations have high memory video cards for displaying resulting data, and running structural visualization, animation, and design programs. The webserver is used exclusively to serve up data / information in various formats (database, flash and other animations, pictures, etc.) to the global community.

- Nodes
  - 64 Multiwave Dual AMD MP 1800 processor systems
  - each: Kingston 1.0 GB PC2100 DDR RAM
  - each: IBM 40 GB 7200 RPM Hard drive
- Fileserver
  - 1 Multiwave Dual AMD MP 1900 processor system
  - Kingston 1GB PC2100 DDR RAM
  - 4 IBM 35 GB SCSI Hard Drives in RAID 5
  - 2 IBM Ultra 120 GB IDE 7200 RPM Hard Drives
- Visualization Workstations
  - 2 Multiwave Dual AMD MP 1800 processor systems

  - each: Kingston 1.0 GB PC2100 DDR RAM
  - each: 1 IBM Ultra 120 GB IDE 7200 RPM Hard Drive
  - each: ATI RADEON 7200 64MP AGP Video Card
- Webserver
  - 1 Multiwave Dual AMD MP 1800 processor system
  - Kingston 1.0 GB PC2100 DDR RAM
  - IBM 40 GB 7200 RPM Hard drive
- Switch
  - D-Link DES-6000 128 port 10/100 and Fast Ethernet Switch
  - D-Link DES-6003 16 port modules, 5 total (80 ports)

6.1.2 Software

Summary: Beowulf clusters traditionally use versions of the popular UNIX operating system Linux. In particular, SuSE Linux is a well known, and superior version of Linux which is currently being considered as a world-unified standardized version. The installation, GUI, hardware compatibility, and superior integration with the cluster development software made it the prime choice. The Portland Group software suite provides the versions of Fortran and C++ used in our system, in addition to Cluster Development Kit which combines or cluster debugger, cluster profiler, integrated mpich libraries and PBS (portable batch-queueing system).

- OS (for fileserver, nodes): SuSE Linux 8.0)
  - OS (for visual workstations): Windows 2000
  - OS (for webserver): Windows 2000 Server
- Compilers: Portland Group PGI Fortran 77, Fortran 90, C, and C++
- Portland Group CDK (Cluster Development Kit)
  - PBS (portable batch-queueing system)
  - PBS (portable batch-queueing system)
  - MPI (message passing interface)
  - MPICH libraries

6.1.3 Construction

The 80 tower units are mounted on 5 metal racks, which hold 15 units apiece; 5 units each on 3 plywood shelves (per rack). 4 of the racks hold 59 computers and the D-Link switch, and one rack holds 5 computers, the 2 visualization workstations and monitors, 2 web servers, 1 printer, and 2 scanners. The racks are bolted into the ground, and the units are secured onto the plywood rack shelves. The units are also secured against theft.

6.1.4 Operation

Access to Machines
Machines have limited access; remotely by "host allowed" IP address, and for only a small number of users. Users only access and run jobs from the fileserver; jobs run from the fileserver are distributed over the nodes. The core users consist of UCLA graduate students and researchers. Some of these belong to the UCLA Materials Group directed by Prof. Nasr Ghoniem; and some belong the UCLA Fusion Engineering and Physics Group directed by Prof. Mohamed Abdou. Users outside UCLA will, at the current time, be allowed direct access to the machines; in the future, they will have to run their jobs indirectly through a firewall.

Executing Codes
Individual jobs are run from the user's home directory, which is a mapped share to the RAID 5 drives on the fileserver. The batch processing and message passing occurs (and is distributed over) the 64 nodes (or fraction thereof, depending upon access privileges). The output is designed to be transferred to the larger (non-redundant) drives, and from there will be transferred to the visualization workstations for processing.

Basically, the batch processing (PBS) is used to distribute individual jobs over the different nodes. Message passing (MPI) is used to run portions of code, especially CPU intensive portions, over different nodes. The latter is the prime element for parallel processing, and will be used extensively in the studies undertaken by the UCLA Materials Group.

For using PBS (portable batch-queueing system), jobs submitted are queued according to priority. At the current time, the small number of users does not warrant close monitoring of usage. However, in the future, as more outside agents begin to use the cluster, we will prioritize the usage of the cluster nodes, and delegate portions of it for different classes of users. Cooling

Large Scale A/C Unit
The room is approximately 25 'x50', and is cooled by a large scale Air Conditioning Unit which provides more than adequate 24 hour cooling to the 64 plus machines - it is specifically ducted to pass air over the cluster group (5 racks), and turbulently cool the remainder of the room. The temperature is set to 69 degrees F.

6.1.5 Users / Accounts

- UCLA Materials Group Users
  - Jianming Huang
  - Zeljko Sakota
  - Ming Wen
  - Zhiqiang Wang
  - Qiyang Hu
  - Dr. Silvester Noronha
  - Dr. Shahram Sharafat
  - Dr. Robert Amodeo

- UCLA Fusion Engineering and Physics Users
  - Dr. Neil Morley
- Outside Laboratories
  - Dr. Sriram Swaminarayan (LANL)
  - Prof. Kunugi (Kyoto University)
  - Dr. Satake (Kyoto University)

6.2 Codes / Applications

The types of codes which are ideal for the cluster are the following: Monte Carlo, Molecular Dynamics, and Dislocation Dynamics. At the current time, we are in the testing phases of 2 individual projects on the cluster: Dislocation Dynamics, and Kinetic Monte Carlo. Below is a brief description:

Dislocation Dynamics:

- Researcher: Zhiqiang Wang
- Code type: Dislocation dynamics.
- Programming Language: Fortran 90
- Purpose: To model material plasticicy based on dislocation dynamics.
- Current "1 processor"execution time: 2 days on AMD 1800
- Graphical Output: The code generates data file and then we use other graphical applications, such as TechPlot to view graphical output.

Kinetic Monte Carlo:

- Researcher: Ming Wen
- Code type: Kinetic Monte Carlo - evolution of point defects/clusters
- Programming Language: Fortran 90
- Purpose: to study the effect of elastic interaction on the self interstitial
- atom, cluster rafting, dislocation decoration, cluster pinning, etc, and eventuallyt the nano-micro-structural evolution of defects/defect clusters.
- Current "1 processor"execution time: simulating the motion of 200 SIA clusters with fully considering the interaction between them, takes about 200 hours on a machine with PIV, 1.3GHz, 256MB RAM.
- Graphical Output: The code generates data file and then we use other graphical applications, such as TechPlot to view graphical output

Figure 15: ISIS Computational Cluster Laboatory.

A Appendix A: Biographical Information

A.1 NASR M. GHONIEM, *Principal Investigator*

University of California, Los Angeles (UCLA), 48-121F Engr. IV,
Los Angeles, CA. 90095 - 1597,
Tel. (310) 825-4866, Fax: (310) 206 - 4830, e-mail: ghoniem@ucla.edu

PROFESSIONAL PREPARATION

- B.S. University of Alexandria, Egypt, Dept. of Nuclear Engineering (1971)
- M.Eng. McMaster University, Canada, Dept. of Engineering Physics (1974)
- M.S. University of Wisconsin, USA, Dept. of Nuclear Engineering (1975)
- Ph.D. University of Wisconsin, USA, Dept. of Nuclear Engineering (1977)

APPOINTMENTS

- **Professor,** Materials Science & Engr. Dept. (joint), UCLA (2002-)
- **Professor & Vice Chair,** Mechanical & Aerospace Engr. Dept., UCLA (86-)
- **Associate Professor,** Mechanical & Aerospace Engr. Dept., UCLA (82-86)
- **Assistant Professor,** Mechanical & Aerospace Engr. Dept., UCLA (77-82)

AWARDS

- Royal Society of London Visiting Professorship in Hong Kong, (2000)
- Research fellowship of Japan Society for the Promotion of Science (JSPS) (1999)
- Lifetime Outstanding Achievement Award of ANS (1998)
- Fellow of the American Nuclear Society (1994)
- Who's Who in Frontier Science and Technology (1983)
- Outstanding Young Man of America Award (1978)
- First world patent on Low Activation Ferritic Steels, U.S. Patent No. 4,622,067 (1986)
- Co-founder (w/ Kubin- France) of Dislocation Dynamics for microplasticity . (1987)

SYNERGISTIC ACTIVITIES

- **Member:** The American Nuclear Society (ANS), the American Academy of Mechanics, the Materials Research Society (MRS); The American Society for Mechanical Engineers (ASME), and the American Physical Society (APS).
- **Editorial Boards:**
  1. Associate Editor, Defect and Diffusion Forum, Scitec Publishers.
  2. Associate Editor, Solid State Phenomena, Scitec Publishers.
  3. Journal of Nuclear Materials (JNM)
  4. Journal of Computational Methods in Engineering Science (CMES)
  5. Guest Editor, Journal of Computer Aided Material Design (JCAD)
  6. Guest Editor, Materials Research Society Proceedings (MRS)
  7. Guest Editor, Philosophical Magazine A (Phil Mag)
  8. Guest Editor, Vacuum

PUBLICATIONS {Over 220 articles (165 refereed journal articles) on the mechanics and physics of defects, computational materials science, radiation interaction with materials, instabilities and self-organization in non-equilibrium materials, see: **http://osiris.seas.ucla.edu**}

EDITED BOOKS

1. N.M. Ghoniem, co-editor, "Patterns, Defects and Materials Instabilities,"Kluwer Academic Publishers, The Netherlands, 1990, 393 pages.
2. N.M. Ghoniem, editor, "Plastic and Fracture Instabilities in Materials,"ASME Publications, AMD-**200**/ MD-**57**, 1996, 229 pages.
3. Akira Kobayashi and Nasr M. Ghoniem, co-editors, "Advances in Applied Plasma Science, Vol. I"Proceedings of the First International Symposium on Applied Plasma Science, 22-26 September 1997, UCLA, Los Angeles, CA., USA, 198 pages.
4. Editorial Board, *Diffusion and Defect Data*, Part A: Defect and Diffusion Forum, Part B: Solid State Phenomena, Scitec Publishers.
5. V. Bulatov, T. Diaz de la Rubia, R. Phillips, E. Kaxiras, and N. M. Ghoniem, Co-editors, "Multi-scale Modeling of Materials,"Proceedings of the 1998 MRS Society Symposium, **538**, 1999, 591 pages.
6. Akira Kobayashi and Nasr M. Ghoniem, co-editors, "Advances in Applied Plasma Science, Vol. II"Proceedings of the Second International Symposium on Applied Plasma Science, 20-24 September 1999, Osaka Sun Palace, Osaka, Japan, 453 pages.
7. N.M. Ghoniem, H. Heinisch H. Huang, L. Kubin, Yu, and S. Yip, Guest Editors, Special Issue "Multi-scale Materials Modeling,"*J. Comp.-Aided Mater. Design,* **6, No. 2&3** (1999) 374 pages.

CHAPTERS IN BOOKS

8. N.M. Ghoniem, R. Jones, E. Bloom, Eds., "Fusion Materials and Design,"special issue of *Nuclear Engineering and Design/Fusion*, **2:1**, 1984.

9. N.M. Ghoniem,"Pressure Vessel Technology,"G. Liu and R. Nichols, Pergamon Press, New York, 1989, Book Review in *Nuclear Technology*, 1990.

10. N.M. Ghoniem, R.J. Amodeo, "Computer Simulation of Dislocation Pattern Formation,"in *Non-Linear Phenomena in Materials Science-I*, L. Kubin and G. Martin, Eds., pp. 377-388.

11. N. M. Ghoniem and R. J. Amodeo, "Numerical Simulation of Dislocation Patterns During Plastic Deformation,"in *Patterns, Defects and Materials Instabilities,* D. Walgraef and N. M. Ghoniem, Eds., Applied Sciences, Series E, **183**, NATO ASI Series (Kluwer, The Netherlands, 1990) pp. 303-329.

12. R.J. Amodeo, N.M. Ghoniem, "Rapid Algorithms for Dislocation Dynamics in Micromechanical Calculations,"*Modeling of Deformation of Crystalline Solids,* T. Lowe, T. Rollett, P. Follansbee, and G. Daehn, Eds., TMS Press, 1991, pp. 125-143.

13. N.M. Ghoniem, "Non-Linear Dynamics of Shear Crack Interaction with Dislocations,"*Non-Linear Phenomena in Material Science II,* L. Kubin and G. Martin, Eds., Kluwer Academic Publishers, 1992.

PAPERS IN REFEREED JOURNALS

14. N. M. Ghoniem and G. L. Kulcinski, "A Rate Theory Approach to Time Dependent Microstructural Development During Irradiation,", *Radiat. Eff.*, **39**:47-56, 1978.

15. N. M. Ghoniem and G. L. Kulcinski, "Swelling of Metals During Pulsed Irradiation,"*J. Nucl. Mater.,* **69&70-1&2**:816-820, 1978.

16. J. M. Griesmeyer and Ghoniem, N. M. "The Response of Fission Gas Bubbles to the Dynamic Behavior of Point Defects,"*J. Nucl. Mater.,* **80**:88-101, 1979.

17. N. M. Ghoniem and G. L. Kulcinski,"The Effect of Damage Rate on Void Growth in Metals,"*J. Nucl. Mater.,* **82-2**:392-402, 1979.

18. N. M. Ghoniem and D. D. Cho,"The Simultaneous Clustering of Point Defects During Irradiation,"*Phys. status solidi (a)* **54**:171-178, 1979.

19. N. M. Ghoniem and G. L. Kulcinski,"The Use of the Fully Dynamic Rate Theory to Predict Void Growth in Metals,"*Radiat. Eff.,* **41**:81-89, 1979.

20. N. M. Ghoniem and G. L. Kulcinski,"The Effect of Pulsed Irradiation on the Swelling of 316 Stainless Steel in Fusion Reactors,"*Nucl. Eng. Des.,* **52-1**:111-125, 1979.

21. J. M. Griesmeyer, N. M. Ghoniem, and D. Okrent,"A Dynamic Intragranular Fission Gas Behavior Model,"*Nucl. Eng. Des.,* **55-1**:69-95, 1979.

22. N. M. Ghoniem and G. L. Kulcinski,"Void Growth Characteristics in Laser Fusion First Walls,"*J. Nucl. Mater.,* **85&86,IIA**:547-552, 1979.

23. N. M. Ghoniem, "The Early Stages of Void and Interstitial Loop Evolution in Pulsed Fusion Reactors," *J. Nucl. Mater.,* **89-2&3**:359-371, 1980.

24. N. M. Ghoniem and S. Sharafat, "A Numerical Solution to the Fokker-Planck Equation Describing the Evolution of the Interstitial Loop Microstructure During Irradiation," *J. Nucl. Mater.,* **92-1**:121-135, 1980.

25. H. Gurol and N. M. Ghoniem, "Irradiation Creep by the Climb-Controlled Glide Mechanism in Pulsed Fusion Reactors," *Radiat. Eff.,* **52**:103-126, 1980.

26. H. Gurol, N. M. Ghoniem, and L. K. Mansur, "A Correction to Irradiation Creep by the Climb-Controlled Glide Mechanism in Pulsed Fusion Reactors," *Radiat. Eff. Lett.*, **67(1-2)**:27-30, 1981.

27. N. M. Ghoniem and H. Gurol, "An Analytical Approach to Void Growth in Metals Under Intense Radiation Pulsing," *Radiat. Eff.,* **55**:209-222, 1981.

28. H. Gurol, N. M. Ghoniem, and W. G. Wolfer, "The Role of Dispersed Barriers in the Pulsed Irradiation Creep of Magnetic Fusion Reactor Materials," *J. Nucl. Mater.,* **99**:1-15, 1981.

29. M. E. Sawan, G. L. Kulcinski, and N. M. Ghoniem, "Production and Behavior of Point Defects in Pulsed Inertial Confinement Fusion Reactors," *J. Nucl. Mater.,* **103-104**:109-113, 1981.

30. H. Gurol, N. M. Ghoniem, and W. G. Wolfer, "Enhancement of Irradiation Creep in Pulsed Fusion Reactors," *J. Nucl. Mater.,* **103-104**:1251-1255, 1981.

31. J. Yaung and N. M. Ghoniem, "Modifications of the Fuel Rod Analysis Program FRAP-S3 to Account for the Effects of Fuel Initial Density," *Nucl. Tech., 54-1*:87-91, 1981.

32. R. Schafer and N. M. Ghoniem, "The Interaction of Helium and Displacement Damage in Inertial Confinement Fusion Reactors," *J. Nucl. Mater.,* **104**:1457-1461, 1982.

33. N. M. Ghoniem and M. L. Takata, "A Rate Theory of Swelling Induced by Helium and Displacement Damage in Fusion Reactor Structural Materials," *J. Nucl. Mater.,* **105-2-3**:276-292, 1982.

34. N. M. Ghoniem and R. W. Conn, "Report on the Second American Nuclear Society Topical Meeting on Fusion Reactor Materials," *Nucl. Fusion.,* **22**:977-984, 1982.

35. N. M. Ghoniem and G. L. Kulcinski, "A Critical Assessment of the Effects of Pulsed Irradiation on the Microstructure, Swelling, and Creep of Materials," *Nucl. Technol./Fusion.,* **2-2**:165-198, 1982.

36. R. W. Conn, V. Dhir, N. M. Ghoniem, et al., "Studies of the Physics and Engineering of Deuterium-Deuterium Barrier Tandem Mirror Reactors," *Nucl. Technol./Fusion.,* **2-4**:563-589, 1982.

37. P. S. Chou and N. M. Ghoniem, "Precipitate Dissolution Due to High Energy Collision Cascades," *J. Nucl. Mater.,* **117**:55-63, 1983.

38. N. M. Ghoniem, S. Sharafat, J. Williams, and L. K. Mansur, "The Theory of Helium Transport and Clustering in Materials Under Irradiation," *J. Nucl. Mater.,* **117**:96-105, 1983.

39. N. M. Ghoniem and D. H. Berwald,"Analysis of Blanket-Structure Lifetime for the Tandem Mirror Hybrid Reactor (TMHR)," *Nucl. Technol./Fusion.,* **4(2,2)**:439-444, 1983.

40. N. M. Ghoniem, member TMHR design team (TRW, LLL, Westinghouse, General Atomic, ORNL, ETEC, UCLA)"Fusion Breeder Reactor Design Studies," *Nucl. Technol./Fusion.,* **4(2,2)**:589-598, 1983.

41. R. W. Conn, N. M. Ghoniem, S. P. Grotz, F. Najmabadi, K. Taghavi, and M. Z. Youssef, "Influence of Startup, Shutdown and Staged Power Operation on Tandem Mirror Reactor Design," *Nucl. Technol./Fusion.,* **4(2,2)**:615-622, 1983.

42. N. M. Ghoniem, K. Taghavi, J. Blanchard, and S. P. Grotz,"Limits on Transient Power Variations During Startup and Shutdown of Li-Pb Cooled TMR Blankets," *Nucl. Technol./Fusion.,* **4(2,3)**:769-774, 1983.

43. N. M. Ghoniem, member MARS blanket design team (TRW, General Dynamics, ETEC, UCLA),"MARS High Temperature Blanket," *Nucl. Technol./Fusion.,* **4**:1233-1238, 1983.

44. N. M. Ghoniem and R. W. Conn,"Assessment of Ferritic Steels for Steady-State Fusion Reactors," *Fusion Reactor Design and Tech.*, II IAEA-TC-392/62 (International Atomic Energy Agency, Vienna, 1983) pp. 389-402.

45. R. J. Amodeo and N. M. Ghoniem,"Constitutive Design Equations for Thermal Creep Deformation of HT-9," *J. Nucl. Mater.,* **122&123**:91-95, 1984.

46. J. P. Blanchard and N. M. Ghoniem,"The Influence of Irradiation and Thermal Creep on Stress Redistribution in Fusion Blankets," *J. Nucl. Mater.,* **122&123**:101-105, 1984.

47. E. P. Simonen, N. M. Ghoniem, and N. H. Packan,"Pulsed Flux Effects on Radiation Damage," *J. Nucl. Mater.,* **122&123**:391-401, 1984.

48. S. Sharafat and N. M. Ghoniem,"Stability of Helium-Vacancy Clusters During Irradiation," *J. Nucl. Mater.,* **122&123**:531-536, 1984.

49. N. M. Ghoniem,"Helium Migration and Its Influence on Cavity Formation in Irradiated Materials," *Res Mechanica,* **10**:287-294, 1984.

50. K. Taghavi and N. M. Ghoniem,"Transient Thermal-Hydraulics Considerations of Tandem Mirror Li-Pb Cooled Blankets During Start-Up/Shut-Down Operations," *Nucl. Eng. Des./Fusion.,* **1,4**:369-374, 1984.

51. K. Taghavi and N. M. Ghoniem,"Primary Loop Conditioning and Design Constraints on Li-Pb Cooled Tandem Mirror Reactors During Start-Up/Shut-Down Operations," *Nucl. Eng. Des./Fusion*, **1,4**:375-386, 1984.

52. P. S. Chou and N. M. Ghoniem,"An Approximate Analytical Calculation of Precipitate Dissolution Rate Using a Slowing Down-Diffusion Theory for Charged Particles," *Nucl. Instr. and Meth.,* **B9**:209-217, 1985.

53. J. P. Blanchard and N. M. Ghoniem,"Inelastic Structural Analysis of the MARS Tandem Mirror Fusion Reactor," *Nucl. Eng. Des./Fusion.,* **2**:19-27, 1985.

54. R. S. Amodeo and N. M. Ghoniem,"Development of Design Equations for Ferritic Alloys in Fusion Reactors,"*Nucl. Eng. Des./Fusion.,* **2**:97-110, 1985.

55. R. Bullough and N. M. Ghoniem,"The Effect of Void Surface Motion on the Void Sink Strength for Point Defects,"*J. Nucl. Mater.,* **127**:47-55, 1985.

56. N. M. Ghoniem, J. N. Alhajji, and D. Kalleta,"The Effect of Helium Clustering on Its Transport to Grain Boundaries,"*J. Nucl. Mater.,* **136**:192-206, 1985.

57. P. Chou and N. M. Ghoniem,"On the Stochastic Theory of Point Defect Diffusion During Irradiation: Cascade Size and Shape Effects,"*J. Nucl. Mater.,* **137**:63-72, 1985.

58. J. P. Blanchard and N. M. Ghoniem,"The Influence of Uncertainties in Material Properties, and the Effects of Dimensional Scaling on the Prediction of Fusion Structure Lifetimes,"*Nucl. Eng. Des./Fusion.,* **4**:67-74, 1986.

59. P. S. Chou and N. M. Ghoniem,"Collisional Aspects of Preferential Sputtering Using the Monte Carlo Method,"*J. Nucl. Mater.,* **141-143**:216-220, 1986.

60. R. Martin and N. M. Ghoniem,"Modeling of Tritium Transport in a Fusion Reactor Pin-Type Solid Breeder Blanket Using the DIFFUSE Code,"*J. Nucl. Mater.,* **141-143**:244-248, 1986.

61. J. N. Al-Hajji and N. M. Ghoniem,"Comprehensive Modeling of Creep Fracture by Grain Boundary Cavitation in Irradiated Structural Alloys,"*J. Nucl. Mater.,* **141-143**:536-539, 1986.

62. N. M. Ghoniem, M. A. Firestone, and R. W. Conn,"The Influence of Reactor Operations on the Design and Performance of Tokamaks with Solid Breeder Blankets." Invited Paper Presented at Seventh Top. Mtg. on Technology of Fusion Energy (Reno, NV, June 1986) *Fusion Technol.*, **10**:1133-1145, 1986.

63. G. E. Orient and N. M. Ghoniem,"A Model for the Mechanical Interaction Between Solid Breeder and Cladding Materials,"*Fusion Technol.*, **10**:1617-1622, 1986.

64. J. P. Blanchard and N. M. Ghoniem,"The Bowing of Solid Breeder Rods in a Pin-Type Fusion Reactor,"*Fusion Technol.,* **10**:1623-1627, 1986.

65. P. Levin and N. M. Ghoniem,"Neutronic Optimization of a LiAlO2 Solid Breeder Blanket,"*Fusion Technol.,* **10**:1634-1639, 1986.

66. J. P. Blanchard, N. M. Ghoniem, and S. P. Chou,"An Approximate Solution to the Scattering Integral for General Interatomic Potentials,"*J. Appl. Phys.,* **61**:3120-3123, 1987.

67. J. N. Al-Hajji and N. M. Ghoniem,"Nucleation of Grain Boundary Cavities Under the Combined Influence of Helium and Applied Stress,"*Acta Metall.*, **35**:1067-1075, 1987.

68. P. Chou and N. M. Ghoniem,"Applications of the Monte Carlo Code TRIPOS to Surface and Bulk Ion Transport Problems,"*Nucl. Instr. Meth. Phys. Res.*, **B28**:175-184, 1987.

69. N. M. Ghoniem, member design team,"Updated Reference Design of a Liquid-Metal-Cooled Tandem Mirror Fusion Breeder,"*Fusion Technol.*, **12**:30-70, 1987.

70. R. C. Martin and N. M. Ghoniem,"Monte Carlo Simulation of Coupled Ion-Electron Transport in Semiconductors,"*Phys. status solidi (a)*, **104**:743-754, 1987.

71. R. C. Martin, N. M. Ghoniem, Y. Song, and J. S. Cable,"The Size Effect of Ion Charge Tracks on Single Event Multiple Bit Upset,"IEEE Trans. Nucl. Sci, NS-34(6), Dec. 1987.

72. F. Issacci, N. M. Ghoniem, and I. Catton,"Magnetohydrodynamic Flow in a Curved Pipe,"*Phys. Fluids,* **31**:65-71, 1988.

73. R. J. Amodeo and N. M. Ghoniem,"Dynamical Computer Simulation of the Evolution of a One-Dimensional Dislocation Pileup,"*Int. J. Eng. Sci.,* **26**:653-662, 1988.

74. R. J. Amodeo and N. M. Ghoniem,"A Review of Experimental Observations and Theoretical Models of Dislocation Cells and Subgrains,"*Res Mechanica,* **23**:137-160, 1988.

75. N. M. Ghoniem,"Determination of the Bias Factor by the Moments Solution to to the Fokker-Planck Equation,"*J. Nucl. Mater.,* **155-157**:1123-1127, 1988.

76. N. M. Ghoniem and S. P. Chou,"Binary Collision Monte Carlo Simulations of Cascades in Polyatomic Ceramics,"*J. Nucl. Mater.,* **155-157**:1263-1267, 1988.

77. N. M. Ghoniem and R. Amodeo,"Computer Simulation of Dislocation Pattern Formation,"*Solid State Phenomena*, **3&4**:377-388, 1988.

78. D. Walgraef and N. M. Ghoniem,"Spatial Instabilities and Dislocation Loop Ordering in Irradiated Materials,"*Phys. Rev.* **B39**:8867-8872, 1989.

79. S. P. Chou and N. M. Ghoniem,"On Precipitate Dissolution Using the Cascade Slowing-Down Theory,"*Nucl. Instr. Meth. Phys. Res.* **B42**:145-148, 1989.

80. N. M. Ghoniem,"Stochastic Theory of Diffusional Planar Atomic Clustering and Its Application to Dislocation Loops,"*Phys. Rev.* **B39**:11810-11819, 1989.

81. S. Sharafat, N. M. Ghoniem, and P. I. H. Cooke,"Material Selection for the TITAN Reversed-Field-Pinch Reactor,"*Fusion Eng. and Design,* **8**:305-310, 1989.

82. S. P. Grotz and N. M. Ghoniem,"Overview of the TITAN-I Fusion-Power Core,"*Fusion Eng. and Design,* **9**:367-373, 1989.

83. M. Z. Hasan, J. P. Blanchard, and N. M. Ghoniem,"Thermal-Hydraulic and Structural Design for the Lithium-Cooled TITAN-I Reversed-Field-Pinch Reactor,"*Fusion Eng. and Design,* **9**:431-436, 1989.

84. C. A. Stone and N. M. Ghoniem,"Modeling the Early Stages of Thin Film Formation by Energetic Atom Deposition," *Metall. Trans.*, **20A**:2609-2617, 1989.

85. J. P. Blanchard and N. M. Ghoniem,"Relaxation of Thermal Stress Singularities in Bonded Viscoelastic Quarter Planes,"*J. Appl. Mechanics,* **56**:756-762, 1989.

86. J. P. Blanchard and N. M. Ghoniem,"An Eigenfunction Approach to Singular Thermal Stresses in Bonded Strips,"*J. Thermal Stresses,* **12**:501-527, 1989.

87. F. Issacci, I. Catton, A. Heiss, and N. M. Ghoniem,"Analysis of Heat Pipe Vapor Dynamics," *Chem. Eng. Comm.,* **85**:85-94, 1989.

88. N. M. Ghoniem and J. B. Whitley,"Fusion Neutron Test Facility Requirements for Interactive Effects in Structural and High-Heat-Flux Components," *J. Fusion Energy,* **8**:157-167, 1989.

89. N. M. Ghoniem, J. R. Matthews, and R. J. Amodeo,"A Dislocation Model for Creep in Engineering Materials," *Res Mechanica,* **29**:197-219, 1990.

90. R. J. Amodeo and N. M. Ghoniem,"Dislocation Dynamics: Part I-A Proposed Methodology for Deformation Micromechanics," *Phys. Rev.*, **B41**:6958-6967, 1990.

91. R. J. Amodeo and N. M. Ghoniem,"Dislocation Dynamics: Part II-Applications to the Formation of Persistent Slip Bands, Planar Arrays, and Dislocation Cells," *Phys. Rev.*, **B41**:6968-6976, 1990.

92. S. Sharafat and N. M. Ghoniem,"Non-Equilibrium Agglomeration of Helium-Vacancy Clusters in Irradiated Materials," *Radiat. Eff. and Def.* **113**:331-358, 1990.

93. C. A. Stone and N. M. Ghoniem,"The Effects of Cluster Size-Dependent Aggregation on Thin Film Formation," *Vacuum*, **41**:1111-1113, 1990.

94. J. P. Blanchard and N. M. Ghoniem,"Analysis of Singular Stress Fields in Duplex Fusion Components," *J. Nucl. Mater.,* **174**:54-70, 1990.

95. N. M. Ghoniem,"Nucleation and Growth Theory of Cavity Evolution Under Conditions of Cascade Damage and High Helium Generation," *J. Nucl. Mater.,* **174**:168-177, 1990

96. S. P. Chou and N. M. Ghoniem,"The Effects of Many-Body Interactions on Point-Defect Generation," *J. Nucl. Mater.,* **176**:909-912, 1991.

97. N. M Ghoniem,"Theory of Microstructure Evolution Under Fusion Neutron Irradiation," *J. Nucl. Mater.,* **179**:99-104, 1991.

98. N. M. Ghoniem,"Prospects for Development of Low-Activation Materials," *J. Fusion Energy,* **10(1)**:53-56, 1991.

99. P. Chou and N. M. Ghoniem,"Molecular Dynamics of Collision Cascades with Composite Pair/Many-Body Potentials," *Phys. Rev. B,* **43(4)**:2490-2495, 1991.

100. R. C. Martin and N. M. Ghoniem,"A Hybrid Finite-Element/Particle-Simulation Method for the Analysis of Semiconductor Transients," *Solid- State Electronics,* **36(6)**:573-581, 1991.

101. F. Issacci, I. Catton, and N.M. Ghoniem,"Vapor Dynamics of Heat Pipe Startup," *J. Heat Transfer,* **113**:985-994, 1991.

102. C.A. Stone and N.M. Ghoniem,"The Influence of Low-Energy Particle-Surface Interactions on the Initial Stages of Thin Film Formation," *J. Vac. Sci. Technol.,* **A9(3)**:759-767, 1991.

103. F.J. Perez and N.M. Ghoniem,"Chemical Compatibility of SiC Composite Structures with Fusion Reactor Helium Coolant at High-Temperatures," *Fusion Engineering & Design,* **22**, 1993, pp. 415-426.

104. N.M. Ghoniem,"High-Temperature Mechanical and Material Design for SiC Composites," *J. Nucl.Mater.,* **191-194**:551-519, 1992.

105. H. Huang, N.M. Ghoniem,"Linear Stability Analysis of Helium-Filled Cavities in SiC," *J. Nucl. Mater.,* **191-194**:607-610, 1992.

106. A. El-Azab and N.M. Ghoniem,"Molecular Dynamics Study of the Displacement Threshold Surfaces and the Stability of Frenkel Pairs in Beta-SiC," *J. Nucl. Mater.,* **191-194**:1110-1114, 1992.

107. M. Vicanck and N.M. Ghoniem,"The Effects of Mobility Coalescence on the Evolution of Surface Atomic Clusters,", *Thin Solid Films*, 207, 1992, pp. 90-97.

108. M. Vicanck and N.M. Ghoniem,"Two-Group Approach to the Kinetics of Particle Cluster Aggregation," *J. Computational Phys.,* **100**, 1992, pp. 1-10.

109. C.A. Stone, M. Vicanck, and N.M. Ghoniem,"On the Numerical Accuracy of the Fokker-Planck Approximation to the Hierarchy of Master Equations," *J. Comp. Phys.,* **104**, 1993, pp. 451-456.

110. N.M. Ghoniem and D. Walgraef,"Evolution dynamics of 3-D Periodic Microstructures in Irradiated Materials,", *Modeling in Materials Science and Engineering*, 1, 1993, pp. 569-590.

111. A. Elazab and N.M. Ghoniem,"Green's function for the Elastic Field of an Edge Dislocation in a Finite Anisotropic Medium," *Int. Journ. Fracture Mech.,* **61**, 1993, pp. 17-37.

112. H. Huang and N.M. Ghoniem,"Neutron Displacement Damage Cross-Sections for SiC," *J. Nucl. Mater.,* **199**, 1993, pp. 221-230.

113. M.A. Abdou, A.Y. Ying, M.S. Tillack, N.M. Ghoniem, L.M. Waganar, D.E. Driemeyer, G.L. Linford, and D.J. Drake,"Critical Technical Issues and Evlauation and Comparison Studies for Inertial Confinement Fusion Energy Reactors," *Fusion Engineering & Design,* **23**, 1993, pp. 251-297.

114. F. Najmabadi, P.C. Wong, S. Grotz, R. Schultz, E.T. Chang, P.I.H. Cooke, P.I.H., R.L. Creedon, N.M. Ghoniem, R.A. Krakowski, M. Hassan, R.C. Martin, J.P. Blanchard, S. Sharafat, D. Steiner, D.K. Sze, and W.P. Duggan,"The TITAN-I Reversed-Field-Pinch Fusion Power Core Design," *Fusion Engineering & Design,* **23**, 1993, pp. 81-91.

115. S. Sharafat, N.M. Ghoniem, P.I.H. Cooke, R.C. Martin, F. Najmabadi, K.R. Schultz, and C.P.C. Wong,"Materials Selection Criteria and Performance Analysis for the TITAN-II Reversed-Field-Pinch Fusion Power Core," *Fusion Engineering and Design,* **23**, 1993, pp. 201-218.

116. S.P. Chou and N.M. Ghoniem, "Molecular Dynamics Simulations of Low-Energy Copper Atom Interaction with Copper Surfaces,", *Modeling and Simulation in Materials Science and Engineering*, 1, 1993, pp. 731-740.

117. F. Najmabadi, C.P.C. Wong, S.P. Grotz, K.R. Schultz, E.T. Cheng, P.I.H. Cooke, R.L. Creedon, N.M. Ghoniem, R.A. Grakowski, M.Z. Hasan, R.C. Martin, J.P. Blanchard, S. Sharafat, D. Steiner, D.K. Sze, W.P. Duggan, G.O. Orient, "The TITAN-II Reversed-Field-Pinch Fusion Power Core Design," *Fusion Engineering & Design,* **23**, 1993, pp. 69-80.

118. M.Z. Hasan, N.M. Ghoniem, and J. Blanchard, "Thermal-hydraulic and Structural Design of Titan-I Reversed-Field-Pinch Fusion Power Core," *Fusion Engineering & Design,* **23**, 1993, pp. 115-132.

119. C.P.C. Wong, S.P. Grotz, F. Najmabadi, J.P. Blanchard, E.T. Chang, P.IH. Cooke, R.L. Creedon, N.M. Ghoniem, P.J. Gierszewski, M.Z. Hassan, R.C. Martin, K.R. Schultz, S. Sharafat, D. Steiner, and D.K. Sze, "The TITAN-II Reversed-Field-Pinch Fusion Power Core Design," *Fusion Engineering & Design,* **23**, 1993, pp. 173-200.

120. M.A. Abdou, A.Y. Ying, M.S. Tillack, N.M. Ghoniem, L.M. Waganer, D.E. Driemeyer, G.L. Linford, and D.J.Drake, "Critical Issues and Evaluation and Comparison Studies for Inertial Fusion Energy Reactors," *Fusion Eng. & Design,* **23**: 251-297, 1993.

121. S. Sharafat, N.M. Ghoniem, P.I.H. Cooke, R.C. Martin, F. Najmabadi, K. R. Shultz, and C.Pc¿ Wong, "Materials Analysis for the TITAN-I reversed Field Pinch Fusion Power Core," *Fusion Eng. & Design,* **23, No.2&3**: 99-114, 1993.

122. H. Huang and N.M. Ghoniem, "Molecular Dynamics Calculations of Defect Energetics in Beta-SiC," *Journal of Nuclear Materials,* **212 -215**:148-153, 1994.

123. A. Elazab and N.M. Ghoniem, "Post-Irradiation Fiber Debonding and Pull-out in SiC/SiC Composites," *Journal of Nuclear Materials,* **212-215**: 845-848, 1994.

124. A. Elazab and N.M. Ghoniem, "Molecular Dynamics Simulation of Low Energy Cascades in Beta-SiC," *Radiation Effects and Defects in Solids,* **129**, 1994, pp. 117-126.

125. A. Elazab and N.M. Ghoniem, "Phenomenological Inelastic Constitutive Equations for SiC-SiC Composites Under Irradiation," *Fusion Technology,* **26**:1250-1264, 1994.

126. 26) N.M. Ghoniem and A. Elazab, "Thermo-mechanical Design of the Grazing Incidence Metal Mirror of the Prometheus-IFE Reactor," *Fusion Engineering and Design,* **29**:89-97, 1995.

127. A. Elazab and N.M. Ghoniem, "Mechanical Response and Fatigue Analysis of the First Wall structure of the Prometheus IFE Reactor," *Fusion Engineering and Design,* **27**:536-543, 1995.

128. A. Elazab and N.M. Ghoniem, "Visco-elastic Analysis of Mismatch Stresses in Ceramic Matrix Composites under High-Temperature Neutron Irradiation," *Mechanics of Materials,* **20**:291-303, 1995.

129. H. Hanchen. N.M. Ghoniem, J. Wong, and M. Baskes, "Molecular Dynamics Determination of Defect Energetics in Beta-SiC Using Three Representative Empirical Potentials,", *Mod & Sim in Mat Sci & Eng*, 3: 615-627, 1995.

130. H. Hanchen and N.M. Ghoniem, "Formulation of a Moment Method for n-dimensional Fokker-Planck Equations," *Phys. Rev. E,* **51,6** 5251-5260, 1995.

131. D. Walgraef and N.M. Ghoniem, "Non-linear Dynamics of Self-organized Microstructures Under Irradiation," *Phys. Rev. B,* **52,6** 3951-3962, 1995.

132. A. Elazab and N.M. Ghoniem, "Investigation of Time for sub-critical Crack Propagation in SiC-SiC Composites," *J. Nucl. Mater.,* **219**: 101-109, 1995.

133. A. Elazab and N.M. Ghoniem, "Stability and Evolution of Crack Systems in Dissipative Materials,"ASME, Applied Mechanics Divion (AMD-Vol. 200)/ Materials Division (MD-Vol. 57), 57: 55-73, 1995.

134. A. Elazab and N.M. Ghoniem, "Time-Dependent Micro-mechanics in Damaged High-Temperature Ceramic Composites,"ASME, Applied Mechanics Divion (AMD-Vol. 99)/ Materials Division (MD-Vol. 55), 55:235-38,1995.

135. D. Walgraef, J. Lauzeral, and N.M. Ghoniem, "Theory and Simulations of Defect Ordering in Irradiated Materials,", *Phys. Rev. B*, 53,20: 14782-14794, 1996.

136. H. Huang and Nasr Ghoniem, "A Swelling Model For Stoichiometric SiC At Temperatures Below 1000 °C Under Neutron Irradiation,"*J. Nucl. Mater.,* **250**: 192-199 (1997).

137. D. Walgraef, N.M. Ghoniem, and J. Lauzeral, "Deformation Patterns in Thin Films Under Uniform Laser Irradiation,"*Phys. Rev. B, 56,* **No. 23**: 15361-15377 (1997).

138. Lauzeral, D. Walgraef, and N.M. Ghoniem, "Rose Deformation Patterns in Thin films Irradiated By Focused Laser Beams,"*Phys. Rev. Lett.* **79, No. 14**: 2706-2709 (1997).

139. N.M. Ghoniem, "Atomic Processes During Damage Production and Defect Retention,"*J. Nucl. Mater.,* **258-263**: 113-123 (1997).

140. N.M. Ghoniem, "Clustering Theory of Atomic Defects,"*Radiation Effects and Defects in Solids,* **148**: 269-318 (1999).

141. H. Huang, N.M. Ghoniem, T. Diaz de la Rubia, M. Rhee, H. Zbib and J. Hirth, "Stability Of Dislocation Short-Range Reactions In BCC Crystals,"*J. Eng. Mat. & Tech.,* **121(2)**: 143 (1999).

142. N.M. Ghoniem, "Curved Parametric Segments For The Stress Field Of 3-D Dislocation Loops,"*J. Eng. Mat. & Tech.,* **121(2)**: 136 (1999).

143. N. M. Ghoniem, L. Sun, "Fast Sum Method for the Elastic Field of 3-D Dislocation Ensembles,"*Phys. Rev. B,* **60(1)**: 128-140 (1999).

144. D. Walgraef and N.M. Ghoniem, "Modeling laser-Induced Deformation patterns: Nonlinear Effects and Numerical Analysis,"*J. Comp.-Aided Mat. Design,* **6, No. 2&3**: 323-335 (1999).

145. G. A. Johnson and N.M. Ghoniem,"Hierarchical Modeling of C and Si Nano-cluster Nucleation Utilizing Quantum and Statistical Mechanics,"*J. Comp. -Aided Mat. Design.,* **6, No. 2&3**: 337-347 (1999).

146. L. J. Perkins, B. G. Logan, M.D. Rosen, M.D. Perry, T. Diaz de la Rubia, N.M. Ghoniem, T. Ditmire, S.Wilkes and P.T.Springer, "The Investigation of High-Intensity-Laser Driven Micro Neutron Sources for Fusion Materials Applications at High Fluence,"*Nuclear Fusion.,* **40(1)**:1-19 (2000).

147. N.M. Ghoniem, B. N. Singh, L. Z. Sun, and T. Diaz de la Rubia, "Interaction and Accumulation of Glissile defect Clusters Near Dislocations,"*J. Nucl. Mater,* **276**: 166-177 (2000).

148. N.M. Ghoniem, S.- H. Tong, and L. Z. Sun , "Parametric Dislocation Dynamics: A Thermodynamics-based Approach to Investigations of Mesoscopic Plastic Deformation," *Phys. Rev. B,* **139(1)**: 913-927 (2000).

149. S. Sharafat, A. Kobayashi, V. Odgen, and N. Ghoniem, "Development of composite thermal barrier coatings with anisotropic microstructure," *Vacuum*, **59**:185-193, 2000.

150. S. Sharafat and N.M. Ghoniem, "Comparison of A Microstructure Evolution Model With Experiments On Irradiated Vanadium," *J. Nucl. Mater.,* **283-287**:789-793, 2000.

151. L. Sun, N.M. Ghoniem, and B.N. Singh, "3-D Dislocation Dynamics Study of Plastic Instability In Irradiated Copper," *J. Nucl. Mater.,* **283**:741(2000).

152. S. Sharafat, A. Kobayashi, S. Chen, and N. Ghoniem, "Production of High-Density Ni-Bonded Tungsten Carbide Coatings Using An Axially Fed DC-Plasmatron," *J. Surface and Coatings Technology,* **130**:164-172 (2000).

153. S. Sharafat and N.M. Ghoniem, "Comparison of A Microstructure Evolution Model With Experiments on Irradiated Vanadium", *J. Nucl. Mater.*,**283**:789(2000).

154. S.J. Zinkle and N.M. Ghoniem, "Operating Temperature Windows for Fusion Reactor Structural Materials", *Fusion Engineering and Design*,**51-52**:55(2000).

155. S. Sharafat, M. Demetriou , N. Ghoniem , B. Williams, R. Nygren, "Enhanced surface heat removal using a porous tungsten heat exchanger," *Fus. Tech.* **39(2)**:863-867, Part 2, 2001.

156. L.Z. Sun, N.M. Ghoniem, and Z.Q. Wang, "Analytical and Numerical Determination of the Elastic Interaction Energy between Glissile Dislocations and Stacking Fault Tetrahedra in FCC Metals", *J. Mat. Sci. & Engr.*, **A309-310**:178183 (2001).

157. Nasr M. Ghoniem, "Radiation Damage Correlations For Fusion Conditions", *Encyclopedia of Materials: Science and Technology*, Pergamon Press, Elsevier Science Publication, 3413-3418 (2001), ISBN:0-08-0431526.

158. N.M. Ghoniem, S.H. Tong, B.N. Singh, and L.Z. Sun, "On Dislocation Interaction with Radiation-induced Defect Clusters and Plastic Flow Localization in FCC Metals", *Phil. Mag. A*, **81 (11)**:, 2743-2764 (2001).

159. G.R. Odette, B.D. Wirth, D. J. Bacon and N.M. Ghoniem, "Multi-scale, Multi-physics Modeling of Radiation-damaged Materials: Embrittlement of Pressure Vessel Steels", *MRS Bulletin*, 176-81(2001).

160. N.M. Ghoniem, J.M. Huang, and Z.Q. Wang, "Affine Covariant-contravariant Vector Forms for the Elastic Field of Parametric Dislocations in Isotropic Crystals," *Phil. Mag. Lett.*, **82(2)**: 55-63 (2002).

161. N.M. Ghoniem and J.M. Huang, "Computer Simulations of Mesoscopic Plastic Deformation with Differential Geometric Forms for the Elastic Field of Parametric Dislocations: Review of Recent Progress,"Invited Paper at the 5th Euro-Conference on Mechanics of Materials, Delft, Netherlands, March 6-9, 2001, Also *J. de Physique IV*, **11(5)**:53-60 (2001).

162. D. Walgraef and N.M. Ghoniem, "The Effects of Crystal Anisotropy and Adherence Forces on Laser Induced Deformation Patterns in Thin Films," *Phys. Rev. B*, **65** 1555304-1 to 1555304-10 (2001).

163. N.M. Ghoniem,D. Walgraef and S. J. Zinkle, "Theory and Experiment of Nanostructure Self-organization in Irradiated Materials,"Invited Perspective Article, *J. Comp. Aided Mat. Design*, **8**:1-38 (2002).

164. Jianming Huang and Nasr M. Ghoniem, "The Dynamics of Dislocation Interaction with Sessile Self-Interstitial Atom(SIA) Defect Cluster Atmospheres,", *J. Comp. Mat. Science*,**23**:225234 (2002).

165. R. Martinez and N. M. Ghoniem, "The Infuence of Crystal Surfaces on Dislocation Interactions in Mesoscopic Plasticity: A Combined Dislocation Dynamics- Finite Element Approach,", *J. Comp. Meth. Engr. Science, CMES*, **3(2)**:229-243 (2002).

166. Nasr M. Ghoniem and Kyeongjae Cho, "The Emerging Role of Multiscale Modeling in Nano- and Micro-mechanics of Materials," *J. Comp. Meth. Engr. Science, CMES,* **3(2)**:147-173 (2002).

167. N. M. Ghoniem, S.H. Tong, J. Huang, B.N. Singh, and M. Wen, "Mechanisms of Dislocation-Defect Interactions in Irradiated Metals Investigated by Computer Simulations," *J. Nucl. Mater.*, **307311**: 843851 (2002).

168. B.N. Singh, N.M. Ghoniem and H. Trinkaus, "Experiment-Based Modelling of Hardening and Localized Plasticity in Metals Irradiated Under Cascade Damage Conditions," *J. Nucl. Mater.*, **307311**:159170 (2002).

169. S. Sharafat, Kobayashi A, Chen Y, Ghoniem NM, "Plasma spraying of micro-composite thermal barrier coatings," *Vacuum* **65(3-4)**: 415-425, 2002.

170. Marios D. Demetriou, Nasr M. Ghoniem, Adrienne S. Lavine, "Kinetic Modeling of Phase Selection during Non-Equilibrium Solidification of WC," *Acta Materialia*, **50 (6)**:1421-1432 (2002).

171. Marios D. Demetriou, Adrienne S. Lavine, Nasr M. Ghoniem, "Feasibility of Plasma Spraying in Developing MMC Coatings: Modeling the Heating of Coated Powder Particles," *J. Manufact. Sci. Engr. (JMSE)*, **24**:58-64(2002).

172. Marios D. Demetriou, Nasr M. Ghoniem, Adrienne S. Lavine, "Effects of Nucleation Transience on the Kinetics of Crystallization," *J Chem Phys*, **117**:23 (2002).

173. Marios D. Demetriou, Nasr M. Ghoniem, Adrienne S. Lavine, "Computation of Metastable Phases in Tungsten-Carbon System," *Journal of Phase Equilibria,* **23(4)**:305-309, (2002).

174. Marios D. Demetriou, Nasr M. Ghoniem, Adrienne S. Lavine, "Modeling of Graphitization Kinetics during Peritectic Melting of Tungsten Carbide," *Acta Materialia*, in press, (2002).

175. X. Han, N.M. Ghoniem and Z. Wang, "Parametric Dislocation Dynamics of Anisotropic Crystalline Materials," *Phil. Mag. A.*, in press, (2002).

176. D.Walgraef and N.M.Ghoniem, "The Effects of Glissile Interstitial Clusters on Microstructure Self-organization in Irradiated Materials," *Phys. Rev. B*, in Press, (2002).

177. Nasr M. Ghoniem, Hanchen Huang, Esteban Busso, and Nicolas Kioussis, "Multiscale Modeling of Nano- and Micro-Mechanics: an Overview," *Phil. Mag. A*, in press, (2002).

178. Jianming Huang and Nasr M. Ghoniem, "Accuracy & Convergence of Parametric Dislocation Dynamics (PDD)," *Mod. Sim. Mat. Sci. Engr.,* **10**:1-19 (2002).

179. S. Sharafat, A. Kobayashi, Y. Chen and N.M. Ghoniem, "Plasma Spraying of micro-composite Thermal Barrier Coatings," *Vacuum*, **65(3&4)**:415-25 (2002).

PAPERS IN REFEREED CONFERENCE PROCEEDINGS

180. J. M. Griesmeyer and N. M. Ghoniem, "Intragranular Fission Gas Behavior in Transients,"Proc., Int. Meeting on Fast Reactor Safety Technology (Seattle, WA, 1979).

181. J. M. Griesmeyer, N. M. Ghoniem, and D. Okrent, "A Model for the Dynamic Intragranular Fission Gas Swelling and Release,"Trans., 5th Int. Conf. on Structural Mechanics in Reactor Technology (SMiRT-5) (Berlin, W. Germany, August 1979) p. 8.

182. N. M. Ghoniem and M. Takata, "Modeling Helium Behavior in Fusion Reactor Structural Materials,"Trans., 6th Int. Conf. on Structural Mechanics in Reactor Technology (SMiRT-6)(Paris, France, August 1981) paper no. 315.

183. N. M. Ghoniem, R. W. Conn, V. K. Dhir, S. P. Grotz, and M. Z. Youssef, "Pressure-Vessel Blanket Concepts for D-D Tandem Mirror Fusion Reactors,"Proc., 20th Natl. Heat Transfer Conf. (Milwaukee, WI, August 1981).

184. R. W. Conn, N. M. Ghoniem, et al., "The SATYR Study of d-d Cycle Tandem Mirror Reactors,"Proc., Technical Committee Mtg. and Workshop on Fusion Reactor Design and Technology (IAEA, Tokyo, Oct. 1981).

185. N. M. Ghoniem, S. Sharafat, and L. K. Mansur, "The Kinetics of the Interaction Between Helium and Displacement Damage in Irradiated Materials,"Proc., Yamada V Conf. on Point Defects and Defect Interaction in Metals (Kyoto, Japan, November 1981).

186. N. M. Ghoniem, J. N. Al-Hajji, and F. A. Garner, "Hardening of Irradiated Alloys Due to the Simultaneous Formation of Both Vacancy and Interstitial Loops,"in *Effects of Radiation on Materials*: Proc. 11th Conf., H. R. Brager and J. S. Perrins, eds., ASTM-STP-782 (American Society for Testing and Materials, 1982) pp. 1054-1072.

187. N. M. Ghoniem, A. Shabaik, and M. Z. Youssef, "Development of a 'Low Activation' Vanadium Steel for Fusion Applications,"Proc., Topical Conf. on Ferritic Alloys for Use in Nuclear Energy Technology (Snowbird, Utah, June 1983).

188. N. M. Ghoniem, J. Blink, and N. Hoffman, "Selection of Alloy Steel Type for Fusion Power Plant Applications in the 350-500-C Range,"Proc., Topical Conf. on Ferritic Alloys for Use in Nuclear Energy Technology (Snowbird, Utah, June 1983).

189. J. D. Gordon, J. K. Garner, N. M. Ghoniem, and J. F. Parmer, "Ferritic Steel Applications in the MARS High Temperature Blanket,"Proc., Topical Conf. on Ferritic Alloys for Use in Nuclear Energy Technology (Snowbird, Utah, June 1983).

190. J. P. Blanchard and N. M. Ghoniem, "Global Inelastic Structural Analysis of the MARS Tandem Mirror Blanket Tubes Including Radiation Effects,"Trans., 7th Int. Conf. on Structural Mechanics in Reactor Technology (SMiRT-7)(Chicago, IL, August 1983).

191. J. P. Blanchard and N. M. Ghoniem, "Sensitivity Analysis for Lifetime Prediction of Fusion Structures,"Trans., 8th Int. Conf. on Structural Mechanics in Reactor Technology (SMiRT-8)(Brussels, Belgium, August 1985) N4/5:85-89.

192. S. P. Grotz and N. M. Ghoniem, "Steady-State and Transient Thermal Hydraulics of a Breeder-in-Tube Blanket Design,"86-WAl/HT-5, presented at Winter Ann. Mtg., Amer. Soc. of Mech. Eng. (Anaheim, CA, Dec. 1986).

193. G. Orient, J. P. Blanchard, and N. M. Ghoniem, "Thermostructural Design of the First Wall/Blanket for the TITAN-RFP Fusion Reactor,"in *Structural Mechanics in Reactor Technology* [Trans. 9th Int. Conf. (SMiRT-9) Lausanne, 1987] F. H. Wittmann, ed. (A. A. Balkema, Rotterdam, 1987) p. 169.

194. N. M. Ghoniem and R. J. Amodeo, "Computer Simulation of Dislocation Pattern Formation,"in Proc., Int. Conf. on Nonlinear Phenomena in Materials Science (Aussois, France, Sept. 1987) pp. 1-12.

195. N. M. Ghoniem, member TITAN research group, "The TITAN Reversed-Field-Pinch Fusion Reactor Study,"in *Fusion Engineering* (Proc. 12th Symp., Monterey, 1987) IEEE No. 87CH2507-2, Vol. 1, p. 503.

196. S. P. Grotz, N. M. Ghoniem, and TITAN research group, "The TITAN Reversed-Field-Pinch Lithium-Vanadium Fusion Power Core Design,"in *Fusion Engineering* (Proc. 12th Symp., Monterey, 1987) IEEE No. 87CH2507-2, Vol. 1, p. 776.

197. N. M. Ghoniem, member TITAN research group, "Structure and Insulator Material Choices for the TITAN Reversed-Field-Pinch Reactor Study,"in *Fusion Engineering* (Proc. 12th Symp., Monterey, 1987) IEEE No. 87CH2507-2, Vol. 2, p. 1046.

198. N. M. Ghoniem, member TITAN research group, "Thermal-Hydraulic Design for the Lithium-Cooled TITAN Reversed-Field-Pinch Reactor,"in *Fusion Engineering* (Proc. 12th Symp., Monterey, 1987) IEEE No. 87CH2507-2, Vol. 2, p. 1054.

199. N. M. Ghoniem, member TITAN research group, "The TITAN-II, Reversed-Field-Pinch Aqueous Fusion Power Core Design,"in *Fusion Engineering*, Proc. 12th Symp., Monterey, 1987, IEEE No. 87CH2507-2, Vol. 2, p. 1287.

200. T. D. Naughton, N. M. Ghoniem, and T. H. Lin, "Radiation Effects on the Micromechanical Aspects of Fatigue-Crack Initiation,"in Effects of Radiation on Materials: 13th Int. Symp., pt. II, ASTM-STP-956 (American Society for Testing Materials, 1987) pp. 223-238.

201. N. M. Ghoniem, member ARIES Fusion Reactor Team, "Blanket Concepts for the ARIES Commercial Tokamak Reactor Study,"Trans., 10th Int. Conf. on Structural Mechanics in Reactor Technology (SMIRT-10) (Anaheim, CA, August 1989) Vol. N, p. 13.

202. S. Sharafat, N. M. Ghoniem, S. P. Grotz, L. Y. Yee, and the ARIES Team, "Silicon-Carbide Composite Materials for the ARIES-I Reactor Study,"in *Fusion Engineering,* Proc. 13th Symp., Knoxville, TN, 1989) IEEE No. 89CH2820-9, Vol. 2, p. 1344.

203. N. M. Ghoniem, member ARIES Fusion Reactor Team, "Blanket Design for the ARIES-I Tokamak Reactor,"in *Fusion Engineering* (Proc. 13th Symp., Knoxville, TN, 1989) IEEE No. 89CH2820-9, Vol. 2, p. 1035.

204. N. M. Ghoniem, member ARIES Fusion Reactor Team, "Energy Conversion Options for ARIES-III - A Conceptual D-3He Tokamak Reactor,"in *Fusion Engineering* (Proc. 13th Symp., Knoxville, TN, 1989) IEEE No. 89CH2820-9, Vol. 2, p. 1039.

205. D. Walgraef and N. M. Ghoniem, "Spatial Instabilities and Defect Ordering in Solids,"in Non-Linear Evolution of Spatio-Temporal Structures in Dissipative Continuous Systems (Proc. Conf., Streitberg, Germany, Oct. 1989) F. Busse and L. Kramer, Eds. (Plenum, June 1990).

206. A. J. Sherman, R.H. Tuffias, A.S.B. Chew, and N.M. Ghoniem, "Modeling the Compatibility of Rhenium with Solid Rocket Motor Exhaust,"Proc. Of the 1990 JANAF Propulsion Meeting, CPIA, Vol. 555, 1991, Oct. 2-4, 1990, Anaheim, CA.

207. D.Walgraef and N.M.Ghoniem, "On the Growth and Form of Dislocation Patterns,"in Growth and Form, M.Ben Amar, P.Pelc and P.Tabeling Eds, Plenum Press, New York, 1991, pp. 431-439.

208. Q.B. Jang, R.H. Tuffias, LaFerla and N.M. Ghoniem, "Design,"Analysis and Fabrication of Oxide Coated Iridium/Rhenium Combustion Chambers, JANAF Propulsion Conference, Monterey, CA, 1993.

209. D. Walgraef and N.M. Ghoniem, "An Investigation of Laser-Induced Deformation Instabilities in Thin Films,"Proceedings of Sixth International Workshop on Instabilities and Non-Equilibrium Structures, Dec. 14-19, Valparaiso, Chile.

210. A. Elazab and N.M. Ghoniem, "Stress Fields in Bounded Domains with Multiple Cracks,"Mechanics in design: Canadian Society of Mechanical engineers, CSME Forum, May 7-9, 1996, pp. 869-881.

211. D.Walgraef and N.M.Ghoniem, "An Investigation of Laser-induced Deformational Instabilities in Thin Films,"to appear in the proceedings of the 6th International Workshop on Instabilities and Nonequilibrium Structures, December 14-19, 1995, Valparaiso, Chile.

212. R. Elias, C. Camargo, N.M. Ghoniem, D.C.H. Yang, and S. Sharafat, "Development of a 5-Axis Robotic System for Thermal Spray Applications,"Proceedings of the First International Symposium on Applied Plasma Science, 22-26 September, 1997, UCLA, Los Angeles, CA., USA, page. 53-60.

213. M.D. Demitriou, A. Lavine and N.M. Ghoniem, "Numerical Simulation of Plasma Heating of Powder Particles,"Proceedings of the First International Symposium on Applied Plasma Science, 22-26 September, 1997, UCLA, Los Angeles, CA., USA, pages 75-82.

214. Demetriou, M.D., Lavine, A.S., and Ghoniem, N.M., "Numerical Simulation of Plasma Heating of a Composite Powder Particle,"Proc. of the 5th ASME/JSME Joint Thermal Engineering Conference, Paper No. AJTE99-6158,1999.

215. N.M. Ghoniem, "Computational Methods for Mesoscopic, Inhomogeneous Plastic Deformation,"Proc. of 1st Latin American Summer School on Materials Instabilities, Valparaiso, Chile, Nov. 30- dec. 4, (1998). Kluwer Publishers.

216. N.M. Ghoniem, and B.N. Singh, "Dislocation Dynamics Study of the onset of Plastic Instabilities in Irradiated Materials,"Proc. of 20th RISO International Symposium on Materials Science, Deformation-Induced Microstructures: Analysis and Relationship to Properties, Bilde-Sorensen, et al., Eds., September 6-10, 1999, Roskilde, Denmark, page 41-60.

217. C.P.C. Wong, R.E. Nygren, C.B. Baxi, P. Fogarty, N.M. Ghoniem, H. Khater, K. McCarthy, B. Merril, B. Nelson, E. Reis, S. Sharafat, R. Schleicher, D.K. Sze, M. Ulrickson, S. Williams, M. Youssef, and S. Zinkle, "Helium-cooled Refractory Alloy First Wall and blanket Evaluation,"Proc. of the fifth International Symp. On Fusion Nuclear Technology (ISFNT-5), September 1999, Rome, Italy.

218. S.J. Zinkle and N.M. Ghoniem, "Operating Temperature Windows for Advanced Structural Alloys,"Proc. of the Fifth International Symp. On Fusion Nuclear Technology (ISFNT-5), September 1999, Rome, Italy.

219. L. J. Perkins, B. G. Logan, M.D. Rosen, M.D. Perry, T. Diaz de la Rubia, N.M. Ghoniem, T. Ditmire, P.T. Springer, and S.C. Wilks, "Laser-Driven Micro Neutron Sources for Fusion Materials Testing at High Flux and Fluence,"in Ninth Int. Conf. On Fusion Materials, (ICFRM-9), Colorado Springs, Co., Oct. 11-16, 1999.

220. S. Sharafat, A. Kobayashi, V. Ogden and N.M. Ghoniem, "Development of TBC Coatings Exhibiting Anisotropic Microstructure,"in Advances in Applied Plasma Science, Vol. II, Proceedings of the Second International Symposium on Applied Plasma Science, 20-24 September 1999, Osaka Sun Palace, Osaka, Japan, pages 197-204.

221. M.D. Demetriou, A.S. Lavine, and N.M. Ghoniem, "Modeling Heating of Composite Powder particles in Plasma Spray Processing,"in "Advances in Applied Plasma Science, Vol. II" Proceedings of the Second International Symposium on Applied Plasma Science, 20-24 September 1999, Osaka Sun Palace, Osaka, Japan, page 431-438.

222. S. Sharafat, A. Kobayashi, S. Y. Chen, and N. Ghoniem, "High Density Ni-Bonded Cemented Tungsten Carbide by DC-Plasma Spraying,"Proc. The 6th Annual Meeting of IAPS (Institute of Applied Plasma Science), Saga, Japan, March 1999.

223. Nasr M. Ghoniem, "Computational Methods For Mesoscopic, Inhomogeneous Plastic Deformation", *Proceedings of First Latin American Symposium on Materials Instabilities*, Valpareso, Chile, Kluwer Publication, 2000.

A.2 SHAHRAM SHARAFAT, *Investigator, Principal Development Engineer*

University of California, Los Angeles (UCLA), 48-121F Engr. IV,
Los Angeles, CA. 90095 - 1597,
Tel. (310) 794-5990, Fax: (310) 206 - 4830, e-mail: shahrams@ucla.edu

PROFESSIONAL PREPARATION

- B.S. University of California Los Angeles, Engineering (1978)
- M.S. University of California Los Angeles, Dept. of Ch.& Nucl. Engineering (1980)
- Ph.D. University of California Los Angeles, Dept. of Mech. & Nucl. Engineering (1986)

APPOINTMENTS

• **Director,** The Plasma and Beam Assisted Manufacturing Lab; Mechanical and Aerospace Engr. Dept., UCLA (1995-)
• **Director,** US/Japan Collaborations Thermal Spray; Mechanical and Aerospace Engr. Dept., UCLA/Joining and Welding Research Institute (JWRI), Osaka University, Japan(1995-)
• **Coordinator** IPFR New Research Programs;
Mechanical and Aerospace Engr. Dept., UCLA (1995-1998)
• **Organizer (US),**First, Second, and Third International Meeting of Applied Plasma Science (UCLA/OSAKA; Mechanical and Aerospace Engr. Dept., UCLA/JWRI, Japan (1995-)
• **Member,** Fusion Energy Advisory-Committee (Feac) - Panel-6 (1994)
• **Management,**Principal Development Engr, UCLA (1993-)
• **Team Leader,** Material Response and Design Integration, The ICF Study, UCLA (1991-1992)
• **Group Leader,** Principal Design Integration, The ARIES/PULSAR Study UCLA (1988-1994)
• **Principal Coordinator,** Material Choices and Issues, The TITAN Study (1986-1988)

SYNERGISTIC ACTIVITIES

- Instructor: Mechanical Engineering Courses (UCLA)
- Investigator: $20K Grant, TRW's Microelectronic Division (IPFR/UCLA)
- Initiator: IPFR New Research Programs (UCLA)
- Co-Founder: The Plasma and Beam Assisted Manufacturing Lab, (IPFR/UCLA)
- Advisor: Numerous Graduate Students (UCLA)
- Introduction of and site license agreements for various parametric 3-D CAD/FEM Software (UCLA)

PUBLICATIONS {Over 102 articles (69 refereed journal articles) on defects, radiation interaction with materials, fusion materials, and design concepts.}

PAPERS IN REFEREED JOURNALS

1. S. Sharafat, Kobayashi A, Chen Y, Ghoniem NM, "Plasma spraying of micro-composite thermal barrier coatings,"Vacuum **65(3-4)**:415-425, 2002.

2. S. Sharafat, M. Demetriou , N. Ghoniem , B. Williams, R. Nygren, "Enhanced surface heat removal using a porous tungsten heat exchanger,"Fus. Tech. **39 (2)**:863-867, 2001.

3. S. Sharafat, A. Kobayashi, V. Odgen, and N. Ghoniem, "Development of composite thermal barrier coatings with anisotropic microstructure,"Vacuum, **59**:185-193, 2000.

4. S. Sharafat, A. Kobayashi, S. Chen, and N. Ghoniem, "Production of high-density Ni-bonded tungsten carbide coatings using an axially fed dc-plasmatron,"Surf. Coat. Technol., **130**:164-172, 2000.

5. S. Sharafat, N. M. Ghoniem, "Comparison of a microstructure evolution model with experiments on irradiated vanadium,"J. Nucl. Mater., **283-287**:789-793, 2000.

6. S. Sharafat, R. H. Jones, A. Kohyama, P. Fenici, "Status and Prospects for SiC/SiC Composite Materials Development for Fusion Applications,"Fus. Eng. Des. **29**:411-420, 1995.

7. S. Sharafat, N.M. Ghoniem, P.I.H. Cooke, R. Martin, F. Najmabadi, K. Schultz, C.P.C. Wong, and the TITAN Team, "Materials analysis of the TITAN-I reversed-field-pinch fusion power core,"Fus. Eng. Des. **23**:99-113, 1993

8. S. Sharafat, N.M. Ghoniem, P.I.H. Cooke, R. Martin, F. Najmabadi, K. Schultz, C.P.C. Wong, and the TITAN Team, "Materials selection criteria and performance analysis for the TITAN-II reversed-field-pinch fusion power core,"Fus. Eng. Des. **23**:201, 1993.

9. S. Sharafat, F. Najmabadi, C.P.C. Wong, and the ARIES Team, "ARIES-I Fusion-Power-Core Engineering,"Fus. Eng. Des. **18**:215, 1991.

10. S. Sharafat and N. M. Ghoniem, "Non-Equilibrium Agglomeration of Helium-Vacancy Cluster in Irradiated Materials,"Radiation Effects and Defects in Solids, **113** (1990) 331; Vacuum, Volume 42, Issues 10-11, 1991, Page 681

11. S. Sharafat, N. M. Ghoniem, P. I. H. Cooke, and the TITAN Research Group, "Material Selection for the TITAN Reversed-Field-Pinch Reactor,"Fus. Eng. Des., **8**:305, 1989.

12. S. Sharafat and N. M. Ghoniem, "Stability of Helium-Vacancy Clustering During Irradiation,"J. Nucl. Mat., **122** [**1-3**] (1984) 531.

13. S. Sharafat, Ghoniem NM, "Helium Migration And Clustering Under Irradiation Pulsing,"T. Am. Nucl. Soc. **43**:354-355, 1982.

14. S. Sharafat, Ghoniem NM, "Helium Diffusion In Materials Under Irradiation,"T. Am. Nucl. Soc. **41**:249-250, 1982.

15. Wong CPC, Nygren RE, Baxi CB, Fogarty P, Ghoniem N, Khater H, McCarthy K, Merrill B, Nelson B, Reis EE, Sharafat S, Schleicher R, Sze DK, Ulrickson M, Willms S, Youssef M, Zinkle S, "Helium-cooled refractory alloys first wall and blanket evaluation,"Fusion Engineering and Design **49**:709-717, 2000.

16. Wong CPC, et al., "Evaluation of the tungsten alloy vaporizing lithium first wall and blanket concept,"Fus. Tech. **39 (2)**:815-822, 2001.

17. M. A. Abdou, Ying A, Morley N, Gulec K, Smolentsev S, Kotschenreuther M, Malang S, Zinkle S, Rognlien T, Fogarty P, Nelson B, Nygren R, McCarthy K, Youssef MZ, Ghoniem N, Sze D, Wong C, Sawan M, Khater H, Woolley R, Mattas R, Moir R, Sharafat S, Brooks J, Hassanein A, Petti D, Tillack M, Ulrickson M, Uchimoto T., "On the exploration of innovative concepts for fusion chamber technology,"Fusion Engineering and Design, **54**:181-247, 2001.

18. C. P. C. Wong, Nygren RE, Baxi CB, Fogarty P, Ghoniem N, Khater H, McCarthy K, Merrill B, Nelson B, Reis EE, Sharafat S, Schleicher R, Sze DK, Ulrickson M, Willms S, Youssef M, Zinkle S., "Helium-cooled refractory alloys first wall and blanket evaluation,"Fusion Engineering and Design, **49-50**:709-717, 2000.

19. M. Abdou, S. E. Berk, A. Ying, M. Y. Peng, S. Sharafat, et al., "Results of An International Study On A High-Volume Plasma-Based Neutron Source For Fusion Blanket Development,"Fus. Tech. **29**:1-57, 1996.

20. G. T. Sager, et al., "Using the shield for thermal energy storage in pulsar,"Fus. Eng. Des. **29**:43-50, 1995.

21. M. Okamoto, T. Nakano, M Aida, M. Nomura, Y. Fujii and S. Sharafat, "Interaction of Hydrogen Plasma with SiC/SiC Composite,"Fus. Eng. Des. **28**:227, 1995

22. K., Berkner K, Siemon R, Batchelor K, Bloom E, Davis J, Davis J, Dean So, Garnier J, Goldston R, Haas G, Jones R, Kulcinski G, Piet Sj, Reardon P, Sharafat S, Smith D, Stringer J, Wilson K, Wong C, "Fusion Energy Advisory-Committee (Feac) - Panel-6 Report On The Neutron-Interactive Materials (NIM) Program,"J. Fusion Energy, **13(2-3)**:185-231, 1994

23. M. Z. Hasan, R. W. Conn, F. Najmabadi, S. Sharafat, and the ARIES Team, "First Wall/Blanket/Shield Design and Power Conversion for the ARIES-IV Tokamak Fusion Reactor,"ISFNT-3, July 1994.

24. "Engineering Design of the ARIES-IV Gaseous Divertor,"M. Z. Hasan, T. Kunugi, F. Najmabadi, S. Sharafat, and the ARIES Team,ISFNT-3, July 1994.

25. M. Tillack, S. Sharafat, M. Youssef, S. Herring, S. Malang, D.K. Sze, "Fusion nuclear technology and materials: status and R&D needs,"Fus. Eng. Des., **25**:21, 1994.

26. Najmabadi F, Conn RW, Krakowski RA, et al., "Introduction And Synopsis Of The TITAN Reversed-Field-Pinch Fusion-Reactor Study,"Fusion Eng Des **23(2-3)**:69-80, 1992.

27. Najmabadi F, Wong CPC, Grotz SP, et al. "The TITAN -I Reversed-Field-Pinch Fusion-Power-Core Design,"Fusion Eng Des **23(2-3)**:81-98, 1993.

28. Hasan MZ, Ghoniem NM, Blanchard JP, et al., "Thermal-Hydraulic And Structural Design Of The TITAN -I Reversed-Field-Pinch Fusion Power Core," Fusion Eng Des **23(2-3)**:115-132, 1993.

29. Wong CPC, Grotz SP, Blanchard JP, et al., "Safety Design And Radioactive-Waste-Disposal Analysis For The TITAN -I Reversed-Field-Pinch Reactor Design," Fusion Eng Des **23(2-3)**:133-156, 1993.

30. Najmabadi F, Wong CPC, Grotz SP, et al., "The TITAN-II Reversed-Field-Pinch Fusion-Power-Core Design," Fusion Eng Des **23(2-3)**:172-200, 1993

31. Najmabadi F, Conn RW, Bathke CG, et al., "The ARIES-II and ARIES-IV 2nd Stability Tokamak Reactors," FUSION TECHNOL **21(3)**:1721-1728, 1992.

32. Najmabadi F, Conn RW, Bathke CG, et al., "The ARIES-II And ARIES-IV 2nd-Stability Tokamak Reactors," Fusion Technol**21(3)**:1721-1728, 1992.

33. Sze DK, Sviatoslavsky I, Sawan M, et al., "Organic Coolant For Aries-III," Fusion Eng Des **18**:435-441, 1991.

34. C. P. C. Wong, S. Sharafat, et al., "Safety design and radioactive-waste-disposal analysis for the TITAN-II reversed-field-pinch reactor design," Fus. Eng. Des., **23**:233, 1993

35. R. W. Conn, J. P. Holdren, S. Sharafat, et al., "Economic, Safety and Environmental Prospects of Fusion Reactors," Nuclear Fusion, **30(9)**:1919, 1990.

36. Cooke PIH, Grotz SP, Hasan MZ, et al., "Properties Of Concentrated Aqueous Lithium-Nitrate Solutions And Applications To Fusion-Reactor Design," Fusion Eng Des **8**:379-385, 1989.

37. Grotz SP, Ghoniem NM, Bartlit JR, et al., "Overview Of The Titan-I Fusion-Power Core," Fusion Eng Des **9**:367-373, 1989.

38. Cooke PIH, Bathke CG, Blanchard JP, et al., "Engineering Design Of The Titan-II Divertor," Fusion Eng Des **9**:417-423, 1989.

39. Wong CPC, Grotz SP, Blanchard J, et al., "The Safety Designs For The Titan Reversed-Field Pinch Reactor Study," Fusion Eng Des **10**:447-453, 1989.

40. N. M. Ghoniem, S. Sharafat, J. M. Williams, and L. K. Mansur, "The Theory of Helium Transport and Clustering in Materials Under Irradiation," J. Nucl. Mater., **117**:96-105, 1983.

41. Wong CPC, Creedon RI, Cheng ET, Grotz SP, Sharafat S, Cooke PIH, "Overview Of The Titan-Ii Reversed-Field Pinch Aqueous Fusion Power Core Design," Fusion Engineering and Design **8**:127-132, 1989.

42. N. M. Ghoniem, S. Sharafat, and L. K. Mansur, "The Kinetics of the Interaction between Helium and Displacement Damage in Irradiated Materials," in Point Defects and Defect Interactions in Metals, Editor Jin-Ichi Takamura, University of Tokyo Press, 1982, pp. 865.

43. N. M. Ghoniem and S. Sharafat, "A Numerical Solution to the Fokker-Planck Equation Describing the Evolution of the Interstitial Loop Microstructure During Irradiation," J. Nucl. Mater., **92**[**1**]:121, 1980.

44. Ghoniem NM, S. Sharafat, "Numerical-Solution Of The Fokker-Planck Equation For Loop Evolution,"T. Am. Nucl. Soc **33**:261-262, 1979.

PAPERS IN REFEREED CONFERENCE PROCEEDINGS

45. S. Sharafat, A. Kobayashi, Y.J. Chen, V. Ogden, J. Eastman, M. Demetriou, and N. Ghoniem, "Micro-Composite Plasma Sprayed Coatings for High Functionally Graded Coatings,"Proc. The 7th Annual Meeting of IAPS, Gakushikai-bunkan, Tokyo, March 17-18, 2000.

46. S. Sharafat, A. Kobayashi, V. Odgen, and N. Ghoniem, "Development of Composite TBC Coatings Exhibiting Anistropic Microstructure,"Proc. The Second International Symposium on Applied Plasma Science, Osaka, Japan, Sept. 21-24, 1999; Advances in Applied Plasma Science, **2**107, 1999.

47. S. Sharafat, A. Kobayashi, S. Y. Chen, and N. Ghoniem, "High Density Ni-Bonded Cemented Tungsten Carbide by DC-Plasma Spraying,"Proc. The 6th Annual Meeting of IAPS (Institute of Applied Plasma Science), Saga, Japan, March 1999, pp. 9.

48. John M Dawson and S. Sharafat, "Plasma Physics Basic Science and Technology,"Proc. The First International Symposium on Applied Plasma Science, UCLA, Sept. 22-26, 1997, pp. 1.

49. S. Sharafat, R. Junge, F. Najmabadi, I. Sviatoslavsky, C.P.C. Wong, and the ARIES Team, "Design Layout and Maintenance of The ARIES-IV Tokamak Fusion Power Plant,"Proc. 15th IEEE/NPSS Symp. on Fusion Engineering, Hyannis, MA, Oct., 11-15, 1993, pp. 417.

50. S. Sharafat, F. Najmabadi, "Advanced Composites for Nuclear Applications,"in Embedded Topical Meeting on National Critical Technologies-Advanced Technology Applications, American Nuclear Society, 1993 Annual Meeting San Diego, CA, June 20-24, 1993, Transaction, **68**, Part B, TANSAO 68 (PART B) 1-40 (1993) pp.13.

51. S. Sharafat, F. Najmabadi, and the ARIES Team, "Design Layout and Maintenance of The ARIES-III Tokamak Reactor,"Proc. 14th IEEE/NPSS Symp. on Fusion Engineering, San Diego, CA, Oct. 3, 1991, pp. 1039-1042.

52. S. Sharafat, F. Najmabadi, C. P. C. Wong, and the ARIES Team, "ARIES-I Fusion-Power-Core Engineering,"Proceedings of the 2nd International Symposium on Fusion Nuclear Technology, Karlsruhe, Germany, June 2-7, 1991, Ed. D. Vollath, Part C, Northholland Amsterdam, pp. 215.

53. S. Sharafat, C. P. C. Wong, E. E. Reis , and the ARIES Team, "SiC-Composite First-Wall Design for the ARIES-I Reactor,"Proceedings of ANS 9th Topical Meeting on Technology of Fusion Energy, Oakbrook, Illinois (1990) p. 901.

54. S. Sharafat, M. Z. Hasan, T. K. Kunugi, C. P. C. Wong, E. E. Reis , and the ARIES Team, "Divertor Engineering For The ARIES-I Reactor,"Proceedings of ANS 9th Topical Meeting on Technology of Fusion Energy, Oakbrook, Illinois (1990).

55. C. P. C. Wong, et al., "ARIES-I SiC Composite Blanket Design,"Proceedings of ANS 9th Topical Meeting on Technology of Fusion Energy, Oakbrook, Illinois (1990) p. 938.

56. S. Sharafat, N. M. Ghoniem, L. Y. Lee, and the ARIES Team, in Fusion Engineering. "Silicon-Carbide Composite Materials for the ARIES-I Reactor Study,"Proceedings of IEEE 13th Symp. Knoxville, TN, October 2-6, 1989, IEEE NO. 89CH2820.9, **2**:1344, 1989.

57. C. P. C. Wong, et al., "Blanket Design for the ARIES-I Reactor," Proceedings of IEEE 13th Symposium on Fusion Engineering, Knoxville, Tennessee (1989) 1035.

58. S. Sharafat, N. M. Ghoniem, S. P. Grotz, L. Y. Lee, and the ARIES Team, "SiC-Composite Materials for the ARIES-I Reactor,"in Transactions of the 10th Int. Conf. on Structural Mechanics in Reactor Technology, SMIRT, Anaheim, CA, August 14-18, 1989, pp. 125.

59. S. Sharafat, N. M. Ghoniem, E. Cheng, P. I. H. Cooke, R. Martin, and the TITAN Team, "Structure and Insulator Material Choices for the TITAN Reversed-Field-Pinch Reactor Study,"Proceedings of IEEE 12th Symposium on Fusion Engineering, Monterey, CA (1987) 1046.

60. A. Kobayashi, S. Sharafat, Y. Chen, and N. Ghoniem, "Heat Transfer Modeling of High Hardness Zirconia Composite Coatings by Gas Tunnel Type Plasma Spraying,"Progress Report of Joint Research , Joining and Welding Research Institute, Osaka University, **5**. March 2002, pp 27-34.

61. A. Kobayashi, S. Sharafat, and N. Ghoniem, "Formation of High Functionally Graded Materials by High Energy Plasma Process,"Progress Report of Joint Research , Joining and Welding Research Institute, Osaka University, **5**:41-45, 2002.

62. C. P. C. Wong, et al., "ARIES-IV Nested Shell Blanket Design,"Proceedings of IEEE 15th Symposium on Fusion Engineering, Hyannis, MA, Oct., 11-15, 1993 (1993) 254.

63. D. K. Sze, et al., "Organic coolant for ARIES-III,"Proceedings of the 2nd International Symposium on Fusion Nuclear Technology, Karlsruhe, Germany, June 2-7, 1991, Ed. D. Vollath, Part C, Northholland Amsterdam, pp. 435.

64. S. P. Grotz, et al., "The TITAN Reversed-Field Pinch Lithium-Vanadium Fusion Power Core Design," Proceedings of IEEE 12th Symposium on Fusion Engineering, Monterey, California (1987) 776.

65. P. I. H. Cooke, et al., "Divertor Design for the TITAN Reversed-Field Pinch Reactor,"Proceedings of IEEE 12th Symposium on Fusion Engineering, Monterey, California (1987) 1050.

66. M. Z. Hasan, et al., "Thermal-Hydraulic Design for the Lithium-Cooled TITAN Reversed-Field Pinch Reactor,"Proceedings of IEEE 12th Symposium on Fusion Engineering, Monterey, California (1987) 1054.

67. C. P. C. Wong, et al., "The TITAN-II, Reversed-Field Pinch Aqueous Fusion Power Core Design,"Proceedings of IEEE 12th Symposium on Fusion Engineering, Monterey, California (1987) 1057.

68. C. P. C. Wong, et al., "Safety Design of the TITAN RFP Lithium Self-Cooled Reactor Design,"Proceedings of IEEE 12th Symposium on Fusion Engineering, Monterey, California (1987) 720.

TECHNICAL PAPERS and REPORTS

69. S. Sharafat, m. Demetriou and N. M. Ghoniem, "Modeling Heat Removal of a Tungsten-Foam Filled Tungsten Tube", University of California Report, UCMEP-00-01, May 2000.

70. S. Sharafat, N. Ghoniem, and A. Chen, "Cyclic Inertial Load Testing of SiC-Foam Disks for In-Cylinder Thermal Regenerators,"UCLA-MBR-98-03, March 1998.

71. S. Sharafat, N. Ghoniem, I. Catton, S. Jones, "Development of Ceramic Foam-Based Regenerators for Regenerated Diesel Engines,"UCLA-MatPRO-98-05, Feb. 1998.

72. S. Sharafat, S. Chen, and N. Ghoniem, "Plasma-Assisted Manufacturing Using Composite Hollow Micro-Spheres,"UCLA-MatPRO-98-07, September 1998.

73. S. Sharafat, N. Ghoniem, and A. Chen, "Mechanical Fatigue of Ceramic Foams,"UCLA-MatMOD-97-03, Dec. 1997.

74. S. Sharafat and N. M. Ghoniem, "Numerical Solution to the Time-Dependent 2-D Fokker-Planck Equation Representing Stochastic Atomic Clustering in Solids,"University of California report, UCLA-ENG-8630, PPG-896, June 1986.

75. S. Sharafat and N. M. Ghoniem, "The Theory of Helium Transport, Clustering and Cavity Evolution in Structural Materials Under Irradiation,"University of California Los Angeles report, UCLA-ENG-8604, PPG-930, February 1986.

76. S. Sharafat, R. Amadeo, and N. M. Ghoniem, "Materials Data Base and Design Equations for the UCLA Solid Breeder Blanket,"University of California Los Angeles report, UCLA-ENG-8611, PPG-937, February 1986.

77. S. Sharafat and N. M. Ghoniem, "Helium Diffusion in Materials Under Irradiation,"University of California Los Angeles report, PPG-112, June 1982.

78. S. Sharafat and N. M. Ghoniem, "Microstructure Evolution in Metals During Irradiation Using a Unified Rate Theory Continuum Approach,"University of California Los Angeles report, UCLA-ENG-8041, June 1980.

79. S.J. Zinkle, S. Majumdar, N.M. Ghoniem, S. Sharafat, "Materials Consideration and Data Base,"University of California Los Angles, APEX Interim Report November, 1999, pp. 13.1-13.29.

80. N. M. Ghoniem and S. Sharafat, "A Preliminary Assessment of Structural Materials Requirements for the Compact Fusion Power Systems,"University of California Los Angeles report, UCLA-ENG-8629, PPG-974, November 1985.

81. N. M. Ghoniem, S. Sharafat, and L. K. Mansur, "The Kinetics of the Interaction Between Helium Displacement Damage in Irradiated Materials,"University of California Los Angeles report, PPT-602, December 1981.

82. N. M. Ghoniem and S. Sharafat, "A Numerical Solution to the Fokker-Planck Equation Describing Microstructure Evolution,"University of California Los Angeles report, UCLA-ENG-7962, September 1979.

83. M. Abdou, S. Sharafat et al., "Phase-1 Report of the IEA Study on High Volume Plasma-Based Neutron Source (HVPNS)," University of California Los Angeles report, UCLA-ENG-95-111, Dec. 1994.

84. S. Sharafat, in US Contribution to ITER Test Program Tasks D2 and D3, "A Helium-Cooled Solid Breeder Silicon-Carbide Composite Blanket ITER Test Module," University of California Los Angeles report, UCLA-ENG-94-38, UCLA-FNT-88, Dec. 1994.

85. G. T. Sager, S. Sharafat et al., "Using the Shield for Thermal Energy Storage in Pulsar," General Atomics report, GA-A21671, April 1994.

86. R. W. Conn, F. Najmabadi, S. Sharafat, K. Schultz, R. A. Krakowski, "The Requirements of a Demonstration Fusion Reactor and the STARLITE Study," University of California Los Angeles Report,UCLA-PPG-1394, Feb. 1992.

87. R. W. Conn, F. Najmabadi, S. Sharafat, K. Schultz, and the ARIES/STARLITE Team, "The STARLITE/DEMO Study: Its Implications for the Development of the National Fusion Program," University of California Los Angeles Report, 1993.

88. L. M. Waganer, S. Sharafat et al., "Inertial Fusion Energy, Reactor Design Studies: Prometheus-L; Prometheus-H, Final Report," McDonnell Douglas Aerospace report, DOE/ER-54101, MDC 92E0008, March , 1992.

89. S. Sharafat, A. El-Azab, and F. Najmabadi, "Comments Regarding Silicon-Carbide Design Limits for Fusion Applications," University of California Los Angeles report, UCLA-PPG-1471, NOV. 1992.

90. S. Sharafat and F. Najmabadi, in The collection of papers presented at The IEEE 14th Symposium on Fusion Engineering, San Diego, California, Oct. 1-3, 1991, "Design Layout and Maintenance of The ARIES-III Tokamak Reactor," University of California Los Angeles report, UCLA-PPG-1386, Dec. 1991.

91. F. Najmabadi, et al., in The collection of papers presented at The IEEE 14th Symposium on Fusion Engineering, San Diego, California, Oct. 1-3, 1991, "The ARIES-III D-3He Tokamak Reactor-Study," University of California Los Angeles report, UCLA-PPG-1386, Dec. 1991.

92. L. Bromberg, et al., in The collection of papers presented at The IEEE 14th Symposium on Fusion Engineering, San Diego, California, Oct. 1-3, 1991, "Magnet Design for The ARIES-III D-3He Reactor," University of California Los Angeles report, UCLA-PPG-1386, Dec. 1991.

93. C. P. C. Wong, et al., in The collection of papers presented at The IEEE 14th Symposium on Fusion Engineering, San Diego, California, Oct. 1-3, 1991, "ARIES-III Divertor Engineering Design," University of California Los Angeles report, UCLA-PPG-1386, Dec. 1991.

94. M. Z. Hasan, et al., in The collection of papers presented at The IEEE 14th Symposium on Fusion Engineering, San Diego, California, Oct. 1-3, 1991, "Thermo-Structural Design of the ARIES-III Divertor with Organic Coolant in Subcooled Flow Boiling," University of California Los Angeles report, UCLA-PPG-1386, Dec. 1991.

95. F. Najmabadi, et al., University of California Los Angeles report, "The ARIES-I Tokamak Reactor Study: Final Report," UCLA-PPG-1323, 1991.

96. M. S. Tillack, et al., "Initial Design of the PROMETHEUS Wetted Wall IFE Reactor Cavity,"University of California Los Angeles report, UCLA-FNT-51, Oct. 1991.

97. F. Najmabadi, et al., "The TITAN Reversed-Field Pinch Fusion Reactor Study: Final Report,"University of California Los Angeles report, UCLA-PPG-1200, 1990.

98. F. Najmabadi, et al., in The collection of papers presented at The 9th Topical Meeting on Technology of Fusion Energy, Oak Brook Illinois, October 7-11, 1990, "The ARIES-I Tokamak Reactor Study,"University of California Los Angeles report, UCLA-PPG-1339, Dec. 1990.

99. F. Najmabadi, et al., in The collection of papers presented at The First International Symposium on Fusion Nuclear Technology, Tokyo, Japan, April 10-19, 1988, "The TITAN Reversed-Field Pinch Fusion Reactor Study,"University of California Los Angeles report, UCLA-PPG-1135, March, 1988.

100. R. W. Conn, et al., Joint Report of UCLA, LANL, GAT, and RPI, "The TITAN Reversed-Field Pinch Reactor Study-The Scoping Phase Report,"UCLA-PPG-1100 (1987).

101. R. W. Conn, et al., "TOKOPS: TOKamak Reactor OPerations Study: The Influence of Reactor Operations on the Design and Performance of Tokamaks with Solid Breeder Blankets, Final Report,"University of California Los Angeles report, UCLA-ENG-86-38, UCLA-PPG-1009, Sep. 1986.

A.3 SILVESTER J. NORONHA, *Investigator, Post-doctoral Fellow*

University of California, Los Angeles (UCLA)
Los Angeles, CA. 90095 - 1597,
Tel. (310) 825-8917, Fax: (310) 206 - 4830, e-mail: noronha@seas.ucla.edu

PROFESSIONAL PREPARATION

• B.Sc.	University of Kerala, Kerala, India,	Chemistry, Math & Physics	(1989)
• M.Sc.	Mahatma Gandhi University, India,	Chemistry	(1991)
• Ph.D.	Indian Institute of Science, India,	Materials Research Centre	(1998)

Postdoctoral Experience

• **Postdoctoral Researcher**	Mechanical & Aerospace Engr. Dept., UCLA	(2002-)
• **Postdoctoral Researcher**	Materials Science & Engr. Dept., Virginia Tech, VA	(2001-2002)
• **Postdoctoral Researcher**	Department of Materials, University of Oxford, UK	(1999-2001)

Professional recognitions

• Invited speaker, at the Research Workshop on "Statistical mechanics of plastic deformation", ICTP, Trieste, Italy , (April, 2002)
• Invited speaker, at the International conference on Nonlinear Dynamics: Chaos and Integrability, Centre for nonlinear dynamics, Bharathidasan University, Trichy, India (Feb. 1998).
• Also given invited seminars at several institutes including Los Alamos National Lab, Argonne National Lab and National Institute of Standards and Technology, MD.
bullet Oral presentations at MRS meeting and other scientific conferences.

SYNERGISTIC ACTIVITIES

- **Member:** Materials Research Society (MRS) and The Minerals, Metals and Materials Society (TMS).
- Reviewer, for Acta Materilia (2002), Pramana - Journal of Physics (1999) and several conference proceedings.

PUBLICATIONS

PAPERS IN REFEREED JOURNALS

1. G. Ananthakrishna and S.J. Noronha, "Monomer Aggregation model for DLA Dendrite crossover,", *Physica A*, **224**, 412-421, 1996.
2. S. J. Noronha, G. Ananthakrishna, L. Quaouire, and C. Fressengeas, "Chaos in Jerky Flow - Experimental Verification of a Theoretical Prediction," *Pramana - J. Phys.*, **48** 705-715, 1997.

3. S. J. Noronha, G. Ananthakrishna, L. Quaouire, C. Fressengeas and L.P. Kubin, "Chaos in Portevin-Le Chatelier effect, "*Int. Jl. of Bifurcation and Chaos*, **7**, 2577-2586, 1997.

4. G. Ananthakrishna, S. J. Noronha, C. Fressengeas and L. P. Kubin, "Crossover from chaotic to self-organized critical dynamics in jerky flow of single crystals,"*Phys. Rev. E.* **60**, 5455-5462, 1999.

5. G. Ananthakrishna, S. J. Noronha, C. Fressengeas and L. P. Kubin, "Crossover in the dynamics of Portevin-Le Chatelier effect from Chaos to SOC, "*Mat. Sci. Eng. A*, **309**, 316-319 (2001).

6. S. G. Roberts, S.J. Noronha, A. J. Wilkinson and P. B. Hirsch, "Modelling the initiation of cleavage fracture of ferritic steels,"*Acta. Mater.* **50** 1229-1244, 2002.

7. S. J. Noronha and D. Farkas, "Effects of dislocation pinning on fracture behaviour: atomistic and dislocation simulation, "*Phys. Rev. B*, **66** 132103 2002.

8. S. J. Noronha and D. Farkas, "Effect of dislocation blocking on fracture behavior of Al and α-Fe: a multiscale study, "*Mat. Sci. Eng. A*, (in press) 2003.

9. S.J. Noronha, G.Ananthakrishna and C. Fressengeas, "Improved Estimation of Lyapunov exponents from Time Series, "*Int. Jl. of Bifurcation and Chaos*, (in press), 2003.

PAPERS IN REFEREED CONFERENCE PROCEEDINGS

10. G. Ananthakrishna and S. J. Noronha , "Chaos in Jerky Flow: Theory and Experiment,", *Solid State Phenomena*, **42-43** 287-296, 1995.

11. S. J. Noronha, S. G. Roberts and A. J. Wilkinson, "Multiple slip plane model for crack-tip plasticity, MRS Proceedings 578, "Multiscale phenomena in Materials - experiments & modeling ", eds. I.M. Robertson et al., (Materials Research Society, Warrendale, PA, USA, 2000), 309-314.

12. S. J. Noronha , G. Ananthakrishna, Lyapunov Exponent as a Discriminating Statistic in Surrogate Data Analysis,"Nonlinear dynamics, Integrability and Chaos", edited by M. Daniel et al., (Narosa, New Delhi, India, 2000), 235.

B Appendix B: Current and Pending Support

B.1 Nasr M. Ghoniem, P.I.

Ghoniem, Principal Investigator

CURRENT:

Source of Support: National Science Foundation
Title of Project/Proposal: Computational Design of Semiconductor Thin Film Systems
Total Award Amount: $284,595 **Total Award Period:** 09/01/01 - 8/31/04
Location of Project: UCLA
Person-Months Per Year Committed to Project; 0.5 summer; 0.5 AY

Source of Support: U.S. Department of Energy
Title of Project/Proposal: Laser Effects on Surface Deformation and Roughening of Optics
Total Award Amount: $390,000.00 **Total Award Period:** 08/15/00 - 08/14/03
Location of Project: UCLA
Person-Months Per Year Committed to Project; 0.5 summer, 0.5 AY

Source of Support: U.S. Department of Energy
Title of Project/Proposal: Mechanisms of Plastic and Fracture Instabilities for Alloy development of Fusion Materials.
Total Award Amount: $810,000.00 **Total Award Period:** 07/15/98 - 07/14/03
Location of Project: UCLA
Person-Months Per Year Committed to Project; 0.5 summer, 0.5 AY

Source of Support: ORNL
Title of Project/Proposal: Parallel Computing Cluster for Fusion Materials Fusion Energy Sources
Total Award Amount: $84,602 **Total Award Period:** 01/03/03 - 03/30/06
Location of Project: UCLA
Person-Months Per Year Committed to Project; 0 summer, 0.2 AY

Source of Support: AFOSR
Title of Project/Proposal: Modeling the Deformation of Nano-Layered Structures by Computer Simulation
Total Award Amount: $359,999 **Total Award Period:** 01/03/03 - 03/30/06
Location of Project: UCLA
Person-Months Per Year Committed to Project; 0.5 summer, 0.2 AY

Source of Support: LANL
Title of Project/Proposal: Development of a Parallel, Experimentally Verifiable Computer Simulation Methodology for Studies of Micro-scale Plasticity
Total Award Amount: $224,999 **Total Award Period:** 01/01/02 - 10/31/05
Location of Project: UCLA

Person-Months Per Year Committed to Project; 0.25 summer, 0.15 AY

PENDING:
Source of Support: Naval Research Laboratory
Title of Project/Proposal: Micro-engineered Surfaces for High Average Power Laser (HAPL) Chambers for High Average Power Laser Chambers
Total Award Amount: $465,000 **Total Award Period:** 03/01/03 - 02/30/06
Location of Project: UCLA
Person-Months Per Year Committed to Project; 0.5 summer; 0.2 AY

B.2 Shahram Sharafat, Investigator

No current or pending support

B.3 Silvester Noronha, Post Doctoral Fellow

No current or pending support

C Appendix C: Final Project report for DOE Grant DE-FG03-98ER54500

C.1 Introduction and Background

During the period: July 1998 through July 2003, our research on fusion materials was supported by the DOE Grant DE-FG03-98ER54500. The main objective of this research was to develop new computational tools for the simulation and analysis of plasticity and fracture mechanisms of fusion materials, and to assist in planning and assessment of corresponding radiation experiments. In the following, we give a brief summary of the salient achievements of research supported by this grant, as evidenced by the extensive publication list during this period.

C.2 Development of Dislocation Dynamics (DD)

The method of PDD is described in sufficient details in references (Ghoniem, 1999)(Ghoniem and Sun, 1999),(Ghoniem et al., 2000a), (**?**), and we will attempt here to give only a brief description. The first step is to calculate the stress field of curved parametric segments. Let the Cartesian orthonormal basis set be denoted by $\mathbf{1} \equiv \{\mathbf{1}_x, \mathbf{1}_y, \mathbf{1}_z\}$, $\mathbf{I} = \mathbf{1} \otimes \mathbf{1}$ as the second order unit tensor, and $\otimes$ denotes out tensor product. Now define the three vectors ($\mathbf{g}_1 = \mathbf{e},\ \mathbf{g}_2 = \mathbf{t},\ \mathbf{g}_3 = \mathbf{b}/|\mathbf{b}|$) as a covariant basis set for the curvilinear segment, and their contravariant reciprocals as(Holzapfel, 2000): $\mathbf{g}^i \cdot \mathbf{g}_j = \delta^i_j$, where δ^i_j is the mixed Kronecker delta and $V = (\mathbf{g}_1 \times \mathbf{g}_2) \cdot \mathbf{g}_3$ the volume spanned by the vector basis, as shown in FIG. 18 . The parametric representation of a general curved dislocation line segment, shown in the figure, can be described by a parameter ω that varies from 0 to 1 at end nodes. The segment is fully determined as an affine mapping on the scalar interval $\{\omega \in [0,1]\}$, if we introduce the tangent vector $\mathbf{T}$, the unit tangent vector $\mathbf{t}$, and the unit radius vector $\mathbf{e}$ as follows:

$$\mathbf{T} = \frac{\mathbf{dl}}{d\omega},\ \mathbf{t} = \frac{\mathbf{T}}{|\mathbf{T}|},\ \mathbf{e} = \frac{\mathbf{R}}{R}$$

Ghoniem, Huang and Wang (Ghoniem et al., 2002) have shown that the elastic field of such a parametric segment can be obtained as an affine mapping transformation of the scalar parameter ω, and that the stress field differential $d\sigma$ introduced by a parametric differential $d\omega$ are related as:

$$\frac{d\sigma}{d\omega} = \frac{\mu V|\mathbf{T}|}{4\pi(1-\nu)R^2}\left\{\left(\mathbf{g}^1 \otimes \mathbf{g}_1 + \mathbf{g}_1 \otimes \mathbf{g}^1\right) + (1-\nu)\left(\mathbf{g}^2 \otimes \mathbf{g}_2 + \mathbf{g}_2 \otimes \mathbf{g}^2\right) - (3\mathbf{g}_1 \otimes \mathbf{g}_1 + \mathbf{I})\right\} \quad (19)$$

The affine map described by EQN. 19 can also be given by the covariant, contravariant and mixed vector and tensor functions (Ghoniem et al., 2002):

$$\mathbf{S} = sym[tr(A^i_{\cdot j}\mathbf{g}_i \otimes \mathbf{g}^j)] + A^{11}(3\mathbf{g}_1 \otimes \mathbf{g}_1 - \mathbf{1} \otimes \mathbf{1}) \quad (20)$$

The scalar metric coefficients $A^i_{\cdot j}, A^{11}, B^{11}$ are obtained by direct reduction of EQN.19 into EQN.20. Once the parametric curve for the dislocation segment is mapped onto the scalar interval $\{\omega \in [0,1]\}$, the stress field everywhere is obtained as a fast numerical quadrature sum from EQN. 19 (Ghoniem and Sun, 1999). The self-force is obtained from knowledge of the local curvature at the point of interest.

To simplify the problem, let us define the following dimensionless parameters:

$$r^* = \frac{r}{a}, \qquad \mathbf{f}^* = \frac{\mathbf{F}}{\mu a}, \qquad t^* = \frac{\mu t}{B}$$

Here, a is lattice constant, μ the shear modulus, and t is time. Substitute these to the variational formula of the governing equation of motion of a single dislocation loop (Ghoniem et al., 2000a), we get the dimensionless matrix form as:

$$\int_{\Gamma^*} \delta \mathbf{r}^{*\top} \left(\mathbf{f}^* - \frac{\mathbf{dr}^*}{dt^*} \right) |d\mathbf{s}^*| = 0 \tag{21}$$

Here, $\mathbf{f}^* = [f_1^*, f_2^*, f_3^*]^\top$, and $\mathbf{r}^* = [r_1^*, r_2^*, r_3^*]^\top$, which are all dependent on the dimensionless time t^*. Following reference (Ghoniem et al., 2000a), a closed dislocation loop can be divided into N_s segments. In each segment j, we can choose a set of generalized coordinates q_m at the two ends, thus allowing parameterization of the form:

$$\mathbf{r}^* = \mathbf{CQ} \tag{22}$$

Here, $\mathbf{C} = [\mathbf{C}_1(\omega), \mathbf{C}_2(\omega), ..., \mathbf{C}_m(\omega)]$, $\mathbf{C}_i(\omega), (i = 1, 2, ...m)$ are shape functions dependent on the parameter $(0 < \omega < 1)$, and $\mathbf{Q} = [q_1, q_2, ..., q_m]^\top$, q_i are a set of generalized coordinates. Now substitute EQN.22 into EQN.21, we obtain:

$$\sum_{j=1}^{N_s} \int_{\Gamma_j} \delta \mathbf{Q}^\top \left(\mathbf{C}^\top \mathbf{f}^* - \mathbf{C}^\top \mathbf{C} \frac{d\mathbf{Q}}{dt^*} \right) |d\mathbf{s}| = 0 \tag{23}$$

Let,

$$\mathbf{f}_j = \int_{\Gamma_j} \mathbf{C}^\top \mathbf{f}^* \, |d\mathbf{s}| \,, \qquad \mathbf{k}_j = \int_{\Gamma_j} \mathbf{C}^\top \mathbf{C} \, |ds|$$

Following a similar procedure to the FEM, we assemble the EOM for all contiguous segments in global matrices and vectors, as:

$$\mathbf{F} = \sum_{j=1}^{N_s} \mathbf{f}_j, \qquad \mathbf{K} = \sum_{j=1}^{N_s} \mathbf{k}_j$$

then, from EQN 23 we get,

$$\mathbf{K} \frac{d\mathbf{Q}}{dt^*} = \mathbf{F} \tag{24}$$

EQN. 24 represents a set of ordinary differential equations, which describe the motion of an ensemble of dislocation loops as an evolutionary dynamical system. Given the initial condition and boundary conditions, solving EQN. 24, the position and configuration of each dislocation is set, and hence at each time step, the total stress field can be known, and based on this, we can check the material reliability. But as can be seen from previous discussion, the crucial point is how to solve the motion problem of dislocation. In the following part, we will fully discussed the so call Parametric Dislocation Dynamics(PDD) we developed in recent years, its convergence, accuracy in time and space domain, its success in simulation on the PSBs and so on.

In the following applications, we specifically use cubic splines as shape functions, and confine dislocation motion to be on its glide plane, the climb effect is ignored. Thus, we end up with only 8 DOF for each segment with each node associated with 4 independent DOF. These cubic spline shape functions are given by:

$$\mathbf{C} = [2\omega^3 - 3\omega^2 + 1, \omega^3 - 2\omega^2 + \omega, -2\omega^3 + 3\omega^2, \omega^3 - \omega^2]$$

$$\mathbf{Q} = [\mathbf{P}_1, \mathbf{T}_1, \mathbf{P}_2, \mathbf{T}_2]^\top$$

Here, $\mathbf{P}_i$ and $\mathbf{T}_i$ $(i = 1, 2)$ correspond to the position and tangent vectors, respectively.

C.2.1 Spatial and Temporal Resolution of Dislocation Mechanisms

As shown in the previous section, after the initial conditions are set, the major problem is to solve EQN. 24. Two kinds of integration methods, implicit and explicit, are utilized. For the explicit integration, simple one step Euler forward method are used. Modified Gear's implicit integration for stiffness equation (Gear, 1971) developed by LLNL are used for implicit time integration. The comparisons between implicit and explicit integrations with different time steps are shown in FIG. 19, and error estimations at Table 1.

In the explicit scheme, it is noted that when the time step is larger than ≈ 3000, there will be a numerical shape instability. For the parameters chosen here, this corresponds to a physical time step of ≈ 6 ps. The shape tends to diverge more along near screw segments of the F-R source. For a time step on the order of 1000 (i.e. $\Delta t \approx 2$ps), the F-R shape is numerically stable, but not accurate. Finally, when the explicit time step is lowered to less than 500 (i.e. $\Delta t \approx 1$ ps), PDD tends to give a stable and accurate F-R source shape. Such small limit on the time step for high mobility crystals (e.g. FCC metals) can result in severe restrictions on the ability of current simulation for large scale plastic deformation. With the method designed by Gear for the numerical integration of ordinary differential stiff equations, a variable time step can be automatically determined based on the variation of any of the DOF. A level of relative accuracy of 10^{-6} is selected as a convergence constraint. Since the time step is automatically adjusted to capture the specified level of accuracy, the overall scheme is stable and convergent. It is shown in Table 1 that the overall running time in explicit integration is much less than that with explicit integration scheme at small time step. That is due to the ability of adjusting time step during implicit integration according to the stiffness of the equation, while explicit Euler method can't, and only with very small time step can we get the same level of accuracy and convergence.

For large-scale computer simulations, there is an obvious need to reduce the computational burden without sacrificing the quality of the physical results. The smallest number of spline segments with the largest time step increment for integration is a desirable goal. However, one must clearly identify the limits of this approach. We study here the influence of the nodal density on the dislocation line, and the time integration scheme on the ability to satisfactorily resolve the shape of a dynamic F-R source.

FIG.20 shows a stable(with applied $\sigma_{11} = 80\ MPa$, $\tau/\mu = 0.064\%$) and an unstable ($\sigma_{11} = 200\ MPa$, $\tau/\mu = 0.16\%$) F-R source configuration. The dislocation loop is divided into different number of segments, and its motion is gained by different numerical integrations. It is shown that one can achieve very high precision in describing the stable F-R shape with very small number of segments. The corresponding error is shown in Table 2. For comparisons, we choose here the result

Table 1: Error Estimation for Different Integration Scheme. The implicit scheme is chosen as the reference configuration for error estimation.

Integration Scheme	Absolute Error ϵ_a	Relative Error ϵ_r	Runtime(sec)
Explicit Int.($\Delta t^* = 3000$)	168.4	6.11%	0.92
Explicit Int. ($\Delta t^* = 1500$)	141.5	5.40%	1.82
Explicit Int. ($\Delta t^* = 1000$)	56.90	2.34%	2.76
Explicit Int. ($\Delta t^* = 500$)	0.06	0.003%	5.68
Implicit Integration	0	0	1.52

Table 2: Error Estimation for Stable State Frank-Read Source

No. of Segments	Absolute Error ϵ_a	Relative Error ϵ_r	Runtime(sec)
2	6.06	0.17%	0.12
6	6.01	0.15%	0.42
15	1.32	0.018%	1.53
30	0	0	5.77

with 30 segments as the reference configuration(thus the relative and absolute error is set to zero). It is found that with the increasing number of segments, both the relative and absolute error are decreased sharply, but the running time is increased significantly. It is interesting to note here that with only 2 segments, one can achieve almost the same resolution as that with 30 segments, with the relative error less than 0.2%, 2% of the CPU time used in 30 segments. However, when the F-R source becomes unstable, the variation of curvature is considerable between its middle section and the sections close to the pinning points, 2 segments is not enough. FIG.20-b and Table 3 show the configuration and corresponding absolute, relative error and running time respectively in the unstable case. The reference configuration is chosen as that with 40 segments. It is found that only 2 segments is unable to achieve high accuracy, although it still converges. It is due to the complicate configuration compared to that at stable case. The curvature is much higher at the zone near the fixed point. Only 2 segments is not enough to capture such a high curvature, the error is mainly from these two zones. In Table 3, it is shown that with the increasing number of segments, the accuracy increased greatly with the compensation of increasing CPU time.

Table 3: Error Estimation for Unstable Frank-Read Source at $t^* = 5 \times 10^6$.

No. of Segments	Absolute Error ϵ_a	Relative Error ϵ_r	Runtime(sec)
2	1408.8	20.15%	0.02
6	191.1	5.04%	0.20
15	133.8	3.24%	2.53
30	142.0	2.93%	24.14
40	0	0	27.57

Table 4: Error Estimation for different nodal distribution of dipole formation. The configuration with 20 segments each dislocation is chosen as the reference configuration.

No. of Segments	Absolute Error ϵ_a	Relative Error ϵ_r	Runtime(sec)
2	26.5	3.16%	12.7
4	18.6	2.37%	43.3
5	7.8	1.13%	84.9
10	3.6	0.36%	438.2
20	0	0	1503.1

Table 5: Error Estimation for different nodal distribution of junction formation. The configuration with 12 segments each dislocation is chosen as the reference configuration.

No. of Segments	Absolute Error ϵ_a	Relative Error ϵ_r	Runtime(sec)
3	27.8	20.05%	406.2
4	19.7	14.25%	841.1
6	16.0	8.75%	2932.6
8	4.97	1.00%	4902.4
12	0	0	8320.2

C.2.2 Simulation of Complex Dislocation Reactions

Finite-Size Dipoles

FIG. 21 shows a 2-D projection on the (111)-plane of the dynamic process finite-size dipole formation. Two initially straight dislocation segments with the same Burgers vector $\frac{1}{2}[\bar{1}01]$, but of opposite line directions are allowed to glide on nearby parallel {111}-planes without the applying an external stress. The two lines attract one another, thus causing the two loop segments to move and finally reach an equilibrium state of a finite-size dipole. The two parallel dislocations are pined at both ends, the upper loop glides on the "upper" plane, while the "lower" one glides on the "lower" one as shown in the figure. The mutual attraction between the two dislocations becomes significant enough to simultaneously reconfigure both of them only during the latter stages of the process. Because the two dislocations start with a mixed character, a straight and tilted middle section of the dipole forms. The length of this middle section, which we may simply ascribe as the dipole length, is only determined by the balance between the attractive forces on the middle straight section, and the self-forces on the two end sections close to the pinning points. The separation of the two planes is $25\sqrt{3}$, which is approximately 60 $|\mathbf{b}|$.

The error estimation of different nodal distribution of same dipole formation is shown in Table 4. It is shown that with only 2 segments in each dislocation, high accuracy can be obtained, the relative error is less than 5%.

Dislocation Junctions

FIG.22 shows the dynamics of an attractive junction formation without any externally applied stress. Two initially straight dislocations $1/2[01\bar{1}](111)$ and $1/2[101](11\bar{1})$ are pinned at their ends,

and allowed to move on the two intersected gliding plane respectively, approaching each other until they are locked at equilibrium. The length of the straight section (junction) that forms at the intersection of the two glide planes is approximately 200. FIG. 22-a shows a 2-D projection view of the successive motion of $\frac{1}{2}[01\bar{1}](111)$, while the 3-D view of the junction structure is shown in FIG. 22-b. In order to calculate the error generated by different nodal distribution, the configuration with 12 nodes each dislocation is set as the reference one. The error estimation is shown in Table 5. It is shown that one can get good shape junction with less than 8 segments in each dislocation loop.

C.2.3 Interaction with SIA clusters

FIG.23 considers the interaction of F-R source with a row of 15 SIA clusters. During the F-R source expanding process under the external stress, it will subject to the elastic stress field of these clusters. Each segment of the dislocation line will subject to the attractive or repulsive force, together with its own self-force, external applied stress, the combined effect of all these forces will determine the dynamic process of the motion of the dislocation. As shown in the figure, the 15 SIA clusters each with diameter of 40 is located above the gliding plane at the distance of 50 with the same inter-cluster distance of 100 and normal direction [011]. The external stress σ_{11}/μ or CRSS(τ/μ) is added gradually from 0 with an interval of $\Delta\tau/\mu = 0.008\%$. At each stage, it reaches a stable state as shown in FIG.23a. The clusters generate a repulsive stress field, and hence at low stress, the F-R source cannot go through the row of clusters, the dislocation line generated an unsymmetrical configuration. When CRSS is increased to 0.0984%, it starts to break away from one side, and once one side break through the effect of the cluster, due to the repulsive effect of the cluster, it will help other parts to break away quickly, it is a speed up process, and the whole breaking time is about a few ns as shown in FIG.23-b.

It is shown in FIG.23 that, when the dislocation approaches the cluster, the dislocation generated a wavy configuration, especially the part near the effect field of the cluster. The details are shown in FIG. 24. In FIG. 24a,b,c, the whole dislocation line is initially equally divided to 6, 18, 30 segments respectively. During the unlocking process, as shown in the figure, with more segments, the length of the segment is less than the inter-cluster distance, thus, the dislocation line can adjust itself more easily, and hence the dislocation is more flexible, configuration is more wavy. When the segment number is decreased to 6, the segments are much longer than the inter-cluster distance, thus it can not sense the variation of the stress field of the clusters, and consequently, no local wavy configuration is generated, the precision is decreased. Compare all the previous results, it is interested to note that, for complicated shape(i.e. unstable F-R source, interaction with clusters, and so on), although less segment can also get convergence shape, their overall accuracy may not acceptable, more nodes are needed.

C.3 Radiation Hardening and Plastic Instabilities

C.3.1 Introduction.

Metal deformation in response to external forces is well-established to be a result of dislocation generation and motion. While the onset of plastic yield is correlated with the *initiation* of dislocation motion, subsequent hardening or softening are clearly controlled by the *continuation* of

such motion. Plastic yield and subsequent hardening (or softening) are primarily determined by the mechanisms that control dislocation motion. In unirradiated metals, dislocation-dislocation interactions play a very significant role in determining the characteristics of plastic deformation, where the impedance of dislocation motion is associated with the formation of sessile junctions or dipoles. In Body Centered Crystals (BCC), however, the flow stress and the presence of an upper yield point can be drastically changed by small additions of impurities. Also, in some alloyed FCC metals (e.g. copper crystals containing zinc), the upper yield point has also been observed. To explain this effect, Cottrell (Cottrell, 1948) showed that the flow stress at the upper yield point is a consequence of dislocation detrapping from impurity *clouds*, which are attracted to dislocations because of their elastic interaction with dislocations. It has thus long been recognized that interactions between dislocations and impurities, extrinsic and intrinsic lattice defects play a significant role in determining the mechanical properties of materials. In an irradiation environment, however, neutron collisions with lattice atoms produce copious densities of intrinsic defects, thus reducing or inhibiting dislocation motion in response to external forces. The initiation of plastic yield in irradiated metals is therefore almost entirely controlled by dislocation interaction with intrinsic defects. This situation is to be contrasted with the deformation characteristics of un-irradiated materials, where the flow stress and subsequent plastic work hardening are mainly determined by dislocation-dislocation interaction mechanisms.

The general features of the stress-strain curve of irradiated pure FCC metals are similar to those of unirradiated BCC metals containing impurities. At some critical irradiation dose (e.g. $\sim$ 0.1 dpa in Cu), an upper yield point emerges, followed by a drop in the yield strength. Most dislocations are observed to be heavily *decorated* by small, sessile interstitial clusters (Singh et al., 1997). To explain the experimentally observed yield drop, and to understand the relationship between dislocation decoration and the yield behavior of irradiated materials, the *Cascade Induced Source Hardening* (CISH) model has been proposed (see references (Singh et al., 1997; Trinkaus et al., 1997a; Trinkaus, Singh and Foreman, 1997b)). In this concept, Self Interstitial Atom (SIA) defect cluster mobility and trapping in the stress field of grown-in dislocations are assumed to be the main reason behind experimental observations of dislocation decoration, and the corresponding presence of an upper yield point in irradiated FCC metals and alloys. Decorations of dislocations in irradiated FCC metals indicate the presence of sessile interstitial dislocation loops produced by coalescence of mobile SIA clusters outside a *stand-off* distance from the dislocation core. Mobile SIA clusters that approach the dislocation at closer distances are absorbed into the dislocation core (Trinkaus et al., 1997a; Ghoniem, Singh, Sun and Diaz de la Rubia, 2000b). On the basis of this picture, the CISH model was used to estimate the flow stress of irradiated metals as the stress necessary to *unlock* dislocations from immobile SIA coagulated clusters. In this model, however, as in Kropua's analysis of similar hardening problems (Kroupa, 1960), dislocations are assumed to be rigid during their interaction with defects.

Once dislocations are released from localized SIA clusters, they will undoubtedly move very fast under the same applied stress that unlocked them, and unless their motion is further hindered, strain softening may occur. In irradiated FCC metals, dislocation motion past the initial yield point is determined by *additional* interactions with lattice defects in the form of sessile Stacking Fault Tetrahedra (SFTs) or Frank vacancy loops. On the other hand, it is found that a high density of microvoids in BCC metals control the post-yield hardening or softening behavior in irradiated BCC metals (Singh, Ghoniem and Trinkaus, 2002). The overriding theme here is that the phenomena of yield initiation, emergence of an upper yield point in FCC metals, the magnitude

of radiation hardening (i.e. increase in CRSS), the subsequent hardening or softening, the formation of micro slip bands (i.e. dislocation channels), and eventual fracture of irradiated materials are all dictated by the details of dislocation-defect interactions. In companion overview articles (Singh et al., 2002; Osetsky, Bacon, Singh and Wirth, 2002) address the relationships between dislocation-defect interaction and experimental observations on radiation hardening, yield drop, and post-yield plasticity of irradiated BCC and FCC metals. The main objective of the present work, however, is to focus on the computational and mechanistic aspects of dislocation-defect interactions in irradiated materials. The two papers are therefore complementary, and are aimed at providing a comprehensive account of the major phenomena involved in determining plasticity and fracture of irradiated metals and alloys.

The specific goal of the present work is to utilize large-scale computational simulations to explore the mechanisms by which dislocation motion is impeded in irradiated materials. First, we discuss how dislocations are decorated, trapped and detrapped by SIA defect clusters. We then determine the mechanisms of dislocation-defect interactions during subsequent deformation in irradiated materials. The computational and modeling aspects of the Parametric Dislocation Dynamics and Kinetic Monte Carlo (KMC) technique are briefly described in subsections (**??**) and (4.1), respectively. Results for the kinetics of dislocation decoration with SIA cluster atmospheres in irradiated Cu are then shown in subsection (C.6.3). Computer simulations for the process of dislocation unlocking from coalesced and immobilized SIA clusters are presented in subsection (C.3.2). Scaling laws for the dependence of the CRSS on SIA cluster density and stand-off distance will be developed. The post-yield dynamics of dislocation interaction with SFTs and sessile Frank loops in irradiated Cu are explored in subsection (C.3.4). To understand the formation of micro shear bands (dislocation channels) in irradiated materials, a full simulation for the dynamics of dislocation motion and interactions *within* dislocation channels in both FCC (e.g. Cu) and BCC (e.g. Fe) will be presented. Also, the effects of microvoids on dislocation channel formation in irradiated Fe are presented in subsection (C.3.5). Finally, conclusions and future directions are given in section (C.3.6).

C.3.2 Dislocation Unlocking from Cluster Atmospheres

We present here results for the unlocking of dislocations from the collective elastic field of immobilized SIA cluster atmospheres, following the work of Ghoniem and Huang (n.d.). In FIG.(25), a total of 15 SIA prismatic clusters, each with the same $\mathbf{b} = \frac{1}{2}[011]$, $d = 40$, $l = 100$, and $y = 80$, are shown to interact with an advancing dislocation on its glide plane. The external shear stress σ_{11}/μ or τ/μ is gradually increased from 0 at intervals of $\Delta\tau/\mu = 0.008\%$. At each stage, the dislocation reaches a new stable configuration, as shown in FIG. (25-a). The dislocation line becomes asymmetric, as interacts with the row of SIAs. When the normalized applied stress is increased to 0.112%, the dislocation breaks away from one side of the cluster atmosphere. Once this process of *unzipping* begins, it is further accelerated by the change in local curvature, as can be seen in FIG. (25-b).

The scaling of the CRSS with the inverse stand-off distance is shown In FIG. (26). The analytical results of Trinkaus et al. (1997a) are also compared with the current numerical simulations. In FIG. (26), 15 equally-spaced clusters interact with a glide edge dislocation with two pinned ends, $d = 40$, and $\mathbf{b} = \frac{1}{2}[\bar{1}10]$ for both dislocation and clusters. The CRSS decreases with the increase in the stand-off distance, consistent with analytical estimates. Because of the short distance in between

clusters, the dislocation breaks away in a rigid manner from its middle section. It is interesting to note that computer simulations show two distinct regimes: regime A ($l < 2d$), and regime B ($l \geq 2d$). In regime A, cluster fields overlap, and the force distribution on the segment does not vary significantly to allow dislocation *buckling*. Thus, the resistance to dislocation motion is controlled by the collective field of all clusters. In regime B, however, once the inter-cluster separation is larger than twice its diameter, the force variation of clusters over the segment is large, and the dislocation prefers to *buckle* in between them. The radius of curvature of this bulge is on the order of $\frac{1}{2}$ the inter-cluster distance. Thus, the resistance to dislocation motion becomes more local, where its radius of curvature determines the CRSS. A sudden jump is clearly observed when we cross from regime A to B (FIG. 26).

C.3.3 Dislocation Interaction with Sessile Defect Clusters

A comprehensive computational algorithm has been developed to simulate dislocation interactions with dispersed barriers, which interact with dislocations with localized force fields that can be approximated as point forces. Nano-scale precipitates, Stacking Fault Tetrahedra (SFTs) and small voids are all sessile in irradiated materials, and one can assume that their force field is localized at a point on the glide plane. Because of the large density and the numerous interactions of such obstacles to dislocation motion, dislocation loops are parametrically represented as small circular arcs inscribed in between obstacle points on the glide plane. The general calculational algorithm works as described below.

The total number of obstacles (e.g. precipitates, vacancy clusters and SFTs) are calculated from their experimentally measured densities and the simulation cube size. The percentage of destructible obstacles (e.g. SFTs or vacancy clusters) is also specified. Each loop segment is represented by a circular arc, and its curvature is determined by the applied stress, sum of all interaction forces, and Burgers vector. When a loop segment encounters the nearest obstacle, it splits into two segments and each segment continues to move until it reaches its equilibrium curvature, or when the angle between the two tangents at the obstacle reaches a critical value, Φ_c. A Kinetic Monte Carlo (KMC) procedure is implemented to determine the probability of obstacle destruction (for SFTs and microvoids), or the dislocation cutting through the obstacle (for precipitates). The probability of cutting/ destruction is calculated from the height of the energy barrier, the work done by the local forces at tangent points, and the lattice temperature. Once an event has been determined, the *waiting time* t_w is calculated by the KMC method described in the previous section, and the obstacle is either destroyed or cut-through. After annihilation, these two segments merge into one and the unified segment is advanced till it meets the next obstacle on the plane, and the corresponding free flight time t_f is also recorded. The total advance time between obstacles is the sum of these two, i.e. $t_a = t_w + t_f$. The procedure is repeated for all segments, and a general time clock records the corresponding time for the evolution of the dislocation loop shape.

When a vacancy cluster or microvoid is destroyed, the vacancy contents are assumed to be absorbed immediately into the dislocation core in between two obstacles, and a climb distance is obtained from the number of vacancies contained in the obstacle divided by the segment length. An expanding dislocation loop will then have segments on different, parallel glide planes. When the segment climbs and jumps to another parallel plane, the intersections between obstacles and the new plane are calculated and used for finding new interactions on that plane. The properties of every obstacle in 3D are tracked by array variables, which store integer numbers representing

different properties. Once an obstacle (SFT or microvoid) is destroyed, it is immediately detected by tracking the corresponding array variable.

Periodic boundary conditions are implemented for the expansion of loops emanating from Frank-Read sources. The distance between each segment and the nearest boundary is calculated with every time step. Once a segment is detected to be out of the simulation boundaries, a different integer is assigned to the array variables, and the segment motion is continued from the boundary at the opposite side, and the segment is placed on a parallel glide plane. The distance between any two segments from the same dislocation loop (FR-source) is calculated to determine if it is less than a prescribed length (about the half of average segment length). The two closest segments are then determined, and annihilation is implemented. The old loop will then be split at these two segments and re-connected to the segment on the other side. This process involves the generation of a new open loop with two pinned ends (F-R source), and the majority of the old loop becomes an expanding closed loop. All properties from the old loop are also assigned to the new open loop in order that it can continue its motion. The interaction forces between segments are calculated every time step because they are used to determine the segment curvature. The free flight time t_f for a segment is measured from an initial straight segment in between two obstacles to the curved configuration, where the segment touches the nearest obstacle. Therefore, the free flight time is determined by the curvature and segment length. The waiting time is measured from the time an obstacle is contacted till its cutting or annihilation.

C.3.4 Interaction with Stacking Fault Tetrahedra (SFTs) in FCC Metals

Once dislocations are freed from their locking defect cluster atmospheres, they will move on their glide planes till they encounter other obstacles to their motion. The yield drop at this moment is associated with a sudden increase in the plastic strain originating from released dislocations, thus requiring a drop in the applied stress to maintain a constant rate of total strain. The post yield behavior of irradiated FCC specimens is determined by dislocation interaction with sessile vacancy clusters, which can be either SFT type, or vacancy loop type. Here, we consider the case of irradiated annealed copper at room temperature. The experimentally-measured values of SFT density and size are given in Table (6) below.

Table 6: Experimentally-measured SFT density, size and hardening ($\Delta\sigma_{exp}$) in annealed Cu, and calculated results for different critical angles
(Singh, Edwards and Toft, 2001)

Case	Dose	$\Delta\sigma_{exp}$	SFT Density	SFT Size	Calculated $\Delta\sigma$		
		(MPa)	($\times 10^{-23}$ M^{-3})	(nm)	$\Phi_c = 160^\circ$	$\Phi_c = 165^\circ$	$\Phi_c = 170^\circ$
1	0.01	38	0.45	3.0	71	39	31
2	0.1	105	1.4	4.5	120	105	80
3	0.2	115	1.7	4.5	145	115	100
4	0.3	120	2.5	4.0	155	125	110

FIG. (27) shows the results of computer simulations for the expansion of dislocation loops generated from Frank-Read sources on [111]-glide planes in Cu under incrementally increasing

applied stress. The resistance of SFTs to the expansion of dislocations from F-R sources requires an increase in the applied stress to maintain a constant rate of strain. Thus, on active glide planes, a *local* stress-strain diagram can be obtained, as seen in FIG. (27), where the results are shown for four different irradiation doses. The macroscopic stress-strain curve, however, cannot be precisely determined unless one knows the fraction of active slip volumes within the tested sample; a task beyond the capabilities of current simulations. Following the yield drop, the lower yield point can be predicted by computer simulations for the interaction between released dislocations and SFTs that intersect glide planes. FIG. (28) shows a direct comparison between experimentally-measured values for the increase in the yield strength and those calculated by computer simulations as a function of the irradiation dose. The only adjustable parameter in these calculations is the critical angle for destruction of a single SFT, which is found to be $\Phi_c = 165^\circ$ for optimum correspondence between experiment and computer simulations. Table (6) shows the sensitivity of the results of computer simulations to variations in the value of the critical angle, Φ_c.

C.3.5 Interaction with Microvoids in BCC Metals

In irradiated BCC metals, vacancies generated by collision cascades form small voids, while interstitials are carried away from cascade centers in SIA clusters. Therefore, dislocations that are released from SIA cluster atmospheres will interact with dispersed voids in the matrix in a similar fashion to the situation in FCC metals, where dislocations interact with SFTs or vacancy loops. Under the action of an applied stress, dislocations impinge on nano-size voids and may destroy them if the work done by local forces exerted by dislocations on microvoids exceeds a critical value determined by the elastic interaction energy. In the present computer simulations, we *assume* that the small nano-size void is destroyed by the dislocation, once the angle between the arms of the dislocation that surround the void exceeds a critical value, Φ_c. Thus, Φ_c is viewed as the only adjustable parameter here, and its value can be precisely calculated through Molecular Dynamics (MD) computer simulations (Osetsky et al., 2002). It is important, however, to determine the *energy* of dislocation cutting through voids rather than Φ_c in MD simulations, and then convert that energy into the corresponding Φ_c by the elastic point force model.

FIG. (29) shows the results of computer simulations for the stages of dislocation channel evolution in irradiated Fe. The model parameters are given in Table(7) below. Initially, dislocations in a local area of stress concentration or statistically-low SIA cluster atmosphere density are activated when the local shear stress reaches a critical value. In FIG. (29-a), one such F-R source is activated at a stress level of 30 MPa. When the applied stress is increased to 65 MPa (FIG. (29-b)), several F-R sources are shown to have their dislocations bowing out in response to the applied stress and mutual interaction forces. However, only a few have expanded significantly to reach the edge of the simulation cube. Also shown in the same figure is the pre-annihilation stage of one of the F-R source dislocations, where two segments are about to annihilate, thus creating a full loop and restoring the initial pinned dislocation segment of the source. In FIG. (29-c), further activation of dormant F-R sources is achieved, when the local microvoid density is effectively reduced by the passage of nearby dislocations. A *domino* effect is thus created, where the destruction of microvoids in a local region by one source activates other nearby sources. It is to be noted that the dislocation loop structure is not planar, because of the continuous climb process associated with each dislocation glide event. At a stress level of 70 MPa, dislocation loops start to impinge on the simulation box boundary, and at that point, periodic boundary conditions are implemented to inject those loop segments

that emerge from one side of the boundary to the other side, as can be seen in FIG.(29-d&e). The evolution process is terminated when the leading-edge loop reaches the grain boundary or surface (which is assumed here to be $10\mu m$), and successive dislocation loops interact with one another to form a non-planar pileup of loops that would exert sufficient back stress on all sources to shut them off. The structure of the evolving non-planar pileup of loops is shown from the side view (the $< 0\bar{1}0 >$-direction is towards the viewer) in FIG. (29-f)).

Table 7: Input parameters for the computer simulations of FIG.(29) for irradiated Fe.

Dose (dpa)	σ_{exp} (MPa)	Void Density ($\times 10^{-23}$ M^{-3})	Void Size (nm)	Simulation Cube Size (μm)	Number of F-R sources	Grain Size (μm)
0.01	65	0.5	0.6	2.6	10	10

C.3.6 Conclusions and Future Outlook

The main theme of the present overview is to delineate how large-scale computer simulations of dislocation-defect interactions in irradiated materials can reveal physical insights that can be used to construct either simpler analytical models, or help in experimental design. The ultimate objective of computer simulations is to be useful in designing radiation-resistant alloys, once the basic mechanisms are clearly determined. This task is not complete, however, unless the results of computer simulations are compared to specific experiments that are designed to test the validity of the mechanisms themselves. In this article, we've shown that large-scale computer simulations provide insight that cannot be gained from analytical theory or experiments alone, but once all aspects are considered, one is more certain of the nature of investigated mechanisms. In a companion article ((Singh et al., 2002)), the emphasis is shifted towards the question of how one can use experimental observations to drive more realistic computer models. We conclude here that the current methods of computer simulations of dislocation defect interactions, namely, the DD and KMC techniques used separately and in combination, have resulted in defining a clearer picture of how SIA clusters attract to dislocations to decorate and lock them in place, how they form rafts and how they pin themselves and not move around at vast speeds. It also resulted in understanding the fundamental mechanism of dislocation unlocking from defect cluster atmospheres, where dislocations pull themselves out of such atmospheres by reconfiguration and shape instabilities. Finally, the basic mechanisms of radiation hardening beyond the upper yield point, and the ensuing nucleation and propagation of *dislocation channels* have been demonstrated by large-scale computer simulations. The agreement with experimental observations of radiation hardening has been demonstrated with only one adjustable parameter. In addition, correspondence between TEM observations on dislocation decoration, raft formation and dimensions of dislocation channels has been shown, and is fully discussed in reference ((Singh et al., 2002)).

Future efforts are expected to address a number of yet un-resolved issues in the area of radiation embrittlement and plastic instabilities. These are:

1. Computer simulations of entire grains, coupling DD with the more macroscopic crystal plasticity models, where lattice rotations, load transfer, and dislocation interaction with boundaries

may determine the spacings observed in between dislocation channels;

2. An emphasis on *materials design* aspects, where one would integrate computer models of alloyed materials with experimental design to understand how plastic flow can be managed over larger volumes to delay or retard dislocation channel formation and fracture;

3. Utilization of computer simulations to design new experiments, which would reveal the synergistic effects of applied stress and irradiation on material deformation.

C.4 Non-equilibrium Phase Transitions

C.4.1 Overview of Achievements

The Principal investigator supervised the thesis of Marios Demetriou, which had the objective of developing kinetic models for the non-equilibrium formation of tugsten carbides during rapid heating and solidification. The work resulted in the publication of a number of papers, and the establishment of a kinetic methodology for determination of the phase fraction of non-equilibrium carbides. This work can be readily extended to the irradiation conditions to treat the formation of carbides, nitrides and oxides. In the following, we outline some of the model highlights.

A dynamic computational model developed within the context of the classical theory of phase evolution has been developed and applied to the W-C system to simulate the kinetics of graphite nucleation during non-equilibrium peritectic melting of WC. The kinetic variables used in the model are obtained directly from the free energy formulations that characterize the stable and metastable equilibria between WC, liquid, and graphite. The isothermal kinetic analysis suggests that transformation time decreases monotonically with increasing superheat such that the minimum transformation time occurs at the metastable congruent melting point of WC ($\sim$ 3107 K). To crystallize 1-ppm of graphite, the minimum transformation time is computed to be$\sim$2 ns. The non-isothermal kinetic analysis suggests that under moderate to high heating rates ($10^4 - 10^6$ K/s) graphitization is completed at superheats of 40-50 K, while under ultra-high heating rates ($\sim 10^8$ K/s) graphitization remains incomplete giving rise to metastable congruent melting of WC.

In this study, a computational model is developed to simulate the kinetics of graphite nucleation upon WC superheating. The aim is to assess the importance of nucleation kinetics in limiting the rate of peritectic melting reaction. This study constitutes the first attempt to model nucleation kinetics in peritectic melting. The present model, which was developed in the context of classical nucleation theory, simulates the stochastic process of crystal nucleation by modeling the dynamics of cluster evolution. The model also accounts for size-dependent growth of finite size nuclei. The kinetic variables used in the model were obtained directly from the free energy formulations that characterize the stable and metastable equilibria between WC, liquid, and graphite. The empirical relations that govern kinetic properties under conditions of supercooling are adopted in the present model and are extrapolated above equilibrium to approximate properties under superheating conditions. Furthermore de-carburization was neglected and fixed composition at 50%-C was assumed throughout the process. The model was applied to investigate the kinetics of graphite nucleation via the stable peritectic reaction $WC \rightarrow liq + gra$ upon annealing or continuous heating, and to examine the possibility of complete kinetic bypassing of the graphite phase.

C.4.2 Publications on Phase Evolution

The following publications resulted form the thesis of Marios Demetriou on non-equilibrium phase transformations:

1. Marios D. Demetriou, Nasr M. Ghoniem, Adrienne S. Lavine, "Kinetic Modeling of Phase Selection during Non-Equilibrium Solidification of WC," *Acta Materialia*, **50 (6)**:1421-1432 (2002).

2. Marios D. Demetriou, Nasr M. Ghoniem, Adrienne S. Lavine, "Effects of Nucleation Transience on the Kinetics of Crystallization," *J Chem Phys*, **117**:23 (2002).

3. Marios D. Demetriou, Nasr M. Ghoniem, Adrienne S. Lavine, "Computation of Metastable Phases in Tungsten-Carbon System," *Journal of Phase Equilibria,* **23(4)**:305-309, (2002).

4. Marios D. Demetriou, Nasr M. Ghoniem, Adrienne S. Lavine, "Modeling of Graphitization Kinetics during Peritectic Melting of Tungsten Carbide," *Acta Materialia*, in press, (2002).

C.5 Irradiation-induced Self-organization

C.5.1 Overview

Irradiation of materials by energetic particles (e.g. electrons, ions and neutrons) is associated with very high internal power dissipation, which can drive the underlying nano- and microstructure far from normal equilibrium conditions. One of the most unusual responses in this connection is the ability of the material's nano- and microstructure to self-assemble in well-organized, two- and three-dimensional periodic arrangements. We reviewed and assessed experimental evidence and theoretical models pertaining to the physical understanding of nano- and microstructure self-organization under irradiation conditions. Experimental observations on the formation of self-organized defect clusters, dislocation loops, voids and bubbles were presented and critically assessed. Implantation of metals with energetic helium results in remarkable self-assembled bubble super-lattices with wavelengths (super-lattice parameters) in the range of 5-8 nm. Ion and neutron irradiation produce a wide variety of self-assembled 3-D defect walls and void lattices, with wavelengths that can be tailored in the range of 10's to 100's of nanometers. Theoretical models aimed at explaining these observations were introduced, and a consistent description of many features is outlined. The primary focus of the most recent modeling efforts, which are based on stability theory and concepts of non-linear dynamics, was to determine criteria for the evolution and spatial symmetry of self-organized microstructures. The correspondence between this theoretical framework and experimental observations was also examined, highlighting areas of agreement and pointing out unresolved questions.

C.5.2 Background

The phenomena of pattern formation and self-organization have been viewed as natural responses of complex systems to strong external stimulation. The collective interaction between system components under external driving forces that drive the system far from equilibrium results in the

self-organization of its constituents (e.g. (Nicolis, Dewel and Turner, 1981), (Cross and Hohenberg, 1993)). Some of the salient successes of this viewpoint can be found in the behavior of chemical (e.g. (Borckmans, Dewel, De Wit and Walgraef, 1994), (Baras and Walgraef, 1992)), liquid crystal nematics (e.g. (Bodenschatz and Kramer, 1988), (Rehberg, Winkler, de la Torre Juarez, Rasenat and Schopf, 1989)), and fluid systems (e.g. (Busse, 1978), (Busse and Riahi, 1980)). It has also been recognized that condensed matter systems show a rich variety of patterns and self-assembled microstructures under conditions as diverse as solidification (Sivashinsky, 1983), electro-chemical deposition (López-Salvans, Sagués and Claret, 2000), plastic deformation (e.g. (Neuhauser, 1990), (Kratochvil, 1988)), surface modifications (Kossowsky, 1984), rapid laser heating (Bauerle, 1996), irradiation by energetic particles (Evans, 1971), magnetic domains (Seul and Wolfe, 1992), and more recently, atom deposition into self-assembled mono-layers (*Nanotechnology Research Directions: IWGN Workshop Report Vision for Nanotechnology Research and Development in the Next decade*, 1999), (Suo and Lu, 2000). The particular situation of energetic particle irradiation is quite interesting , and we plan to focus our attention in this article on reviewing the current understanding of the underlying physical mechanisms. The existence of an extensive experimental database in this area, and the concurrent evolution of contemporary theoretical frameworks allow us to present a broad perspective on the physical nature of self-organization in irradiated materials.

During the last three decades, numerous experimental observations on irradiated materials have systematically demonstrated the existence of fully or partially ordered nano- and microstructure in materials under energetic particle irradiation. The phenomenon appears to be of a general nature, and not confined to one type of microstructure. Voids, precipitates, vacancy clusters, Stacking Fault Tetrahedra (SFT's), gas bubbles and Self-Interstitial-Atom (SIA) clusters have all been observed to be spatially arranged in nano-scale, self-assembled patterns of typical dimensions 2-3 orders of magnitude greater than the atomic spacing. Striking observations have shown that in some cases, complete spatial isomorphism exists between the periodic structure of defect distributions and that of the fundamental atomic lattice. These experimental observations are particularly true for the spatial ordering of bubble and void microstructures in irradiated materials (Sass and Eyre, 1973), (Wiffen, 1972). Singh and Evans (Singh and Evans, 1995) have recently reviewed the experimental results obtained on defect production and accumulation in irradiated materials, and emphasized the systematic differences between void and defect clusters in FCC and BCC metals and alloys. An important characteristic of void and bubble lattices is their spatial orientation along crystallographic directions, at least for the three main metal structures (FCC, BCC, and HCP). Jäger and Trinkaus reviewed the experimental observations of ordered defect structures in irradiated materials, and concluded that the isomorphy of the ordered defect structures with the host lattice is due to elastic interactions in the case of defect walls and anisotropic defect transport in the case of bubble and void superlattices (Jäger and Trinkaus, 1993).

The implications of understanding the physical nature of nano- and microstructure self-organization are quite clear from a technological perspective. The relationships between the material's microstructure and its mechanical and physical characteristics are established by a combination of experimental, empirical and theoretical methods. It is expected, therefore, that a physical understanding of the nano- and microstructure and its dependence on irradiation and material conditions would lead to better approaches to the design of radiation-resistant materials in nuclear technologies (e.g. fission and fusion energy). At the same time, ion, plasma and electron beam processing are becoming valuable tools in the manufacturing of electronic, photonic and microelectromechanical (MEMS) devices. While the impact of a physical understanding of nano- and microstructure

self-organization phenomena on the variety of technologies discussed here is difficult to assess, the intrinsic scientific value is quite valuable. The collective behavior of constituents in hydrodynamic, chemical and liquid crystal systems has been systematically shown to result in pattern formation driven by dynamical instabilities. In the solid state, however, few examples exist, where the link between dynamical instabilities and the evolution of a self-organized nano- and microstructure has been clearly established. For example, while self-organized dislocation microstructure has been widely observed under cyclic and monotonic deformation conditions (e.g. Persistent Slip Bands, dislocation arrays, cells and subgrains), the reasons for its emergence have not yet been established (Amodeo and Ghoniem, 1988).

Concepts on the behavior of dynamical systems have been successfully applied to the problem of microstructure evolution in irradiated materials. Self-organization of irradiated microstructures can thus be viewed as one of the few examples in the solid state, where patterning can be directly linked to the collective dynamical behavior of constituent defects. The aim of this work was to review current models of self-organized microstructure in irradiated materials, and compare the theoretical findings with experimental observations.

C.5.3 Summary and Conclusions

One may conclude that a comprehensive theoretical framework for the analysis of spatial instabilities in the nano- and microstructure of irradiated materials has now been obtained. This framework, which was initiated over two decades ago, results from the succession of works based on a well-established rate theory of microstructure evolution under irradiation. The theory has been pursued both qualitatively and numerically to ascertain the main processes leading to nano-structure pattern selection in irradiated materials. Throughout this review, we emphasized theoretical conditions, which are consistent with experimental observations, for the development of spatially organized (or self-assembled) nano-structures. Some areas which still lack clear understanding include the effects of void density on the magnitude of the selected wavelength, the smaller wavelength of bubble lattices as compared to void lattices, and the unique conditions that lead to loop patterning in Cu.

The rate theory kinetic models described here incorporate basic elements of defect generation, interactions and mobility. They also allow an explicit determination of the instability threshold and its dependence on material and irradiation parameters. Determination of selected nano-structure and its subsequent evolution requires post-bifurcation analysis. Such analysis may be performed analytically and numerically (Walgraef and Ghoniem, 1996). In the weakly non-linear regime, the analysis is based on a derivation of density perturbations for the Fourier components of immobile defects, by invoking a quasi-static approximation. With this approximation, Ginzburg-Landau type amplitude equations for the nano-structure may be derived, with slowly varying time-(or dose-) dependent coefficients. Generic conclusions of pattern selection theory are then recovered, showing non equilibrium phase transitions leading to the eventual formation of wall defect structures, with a wavelength that decreases with the irradiation dose. Furthermore, the nano-structure is expected to be extremely sensitive to even small anisotropies. In particular it should have parallel orientations with the directions of high interstitial mobility, as is experimentally observed for vacancy cluster walls, and for void and bubble super-lattices as well.

The results of the theory are in general agreement with the majority of experimental observations. Most of the qualitative features of self-assembled nano-structures can be explained on the

basis of the present level of theoretical development. Theory predictions for the gradual transition from spatially random to self-assembled nano-structure, the insensitivity of the selected wavelength to temperature and its weak dependence on dose rate, the isomorphism between the nano-structure super-lattice and the underlying crystal, the decrease of observed wavelength with dose and the zig-zag patterns of vacancy clusters are all in qualitative agreement with experimental observations. Surprisingly good quantitative agreement between theory and experiment is obtained for the phase boundaries between ordered and random nano-structures, and for the magnitude of the selected pattern wavelength. On the other hand, the apparent experimental difficulty in verifying the exact mechanism responsible for pattern formation in irradiated copper is somewhat unresolved. While Jäger clearly showed well-defined self-assembled vacancy clusters in copper, the majority of other experimental results did not show pattern formation. To resolve the fundamental differences that lead to such unusual on/off condition within the framework of the current theory require additional specifically planned experiments.

In summary, the necessary ingredients for the kinetic rate theory model to be consistent with experimental observations are three. These are :

1. An excess bias of dislocations towards interstitial atom absorption ;
2. A fraction of vacancies to be produced directly in clusters, as a result of collision cascades;
3. A small degree of interstitial diffusional anisotropy.

The production asymmetry (so called production bias) appears not to be essential to triggering microstructure instabilities (i.e. $\varepsilon_i = 0$), as long as a small fraction of vacancies is produced in clustered sessile configurations. However, if sessile SIA clusters are also produced in collision cascades (i.e. $\varepsilon_i \neq 0$), their presence combines to accelerate the onset of spatial instabilities. Comparison between theory predictions and experimental data is shown in Figure (30). The data include Ni+ ion (Kulcinski and J.L., 1973; Brimhall, 1974; Westmoreland, J.A., F.A. and P.R., 1975)-(Whitley, 1978), fission neutron (Stiegler and Farrell, 1974; Zinkle and Snead, 1995), and proton (Jäger and et. al, 1987; Jäger and Schilling, 1988) irradiations. The filled symbols denote conditions where defect cluster wall formation was observed.

C.6 KMC & Rate Theory Modeling of Microstructure Evolution

C.6.1 KMC Simulations of Decoration and Raft Formation

The Monte Carlo (MC) method refers to any stochastic techniques, which investigate problems by sampling from random numbers and using probability statistics. It is generally believed that the widespread use of Monte Carlo concept began with the Metropolis algorithm in the calculation for a rigid-sphere system (Metropolis et al., 1953). The Metropolis algorithm (Metropolis et al., 1953) for generating a thermal equilibrium ensemble of configuration states, at a specified temperature, for an array of atoms can be illustrated as follows. Assume that we know the energy states for any given configurations of the array. The algorithm proceeds as a series of repetition of the following process: (1) Select an initial configuration of the array at random; (2) Compute the energy state E_1 for this configuration; (3) Change the configuration somehow, for example, exchange the positions of two atoms; (4) Compute the energy state E_2 for the new configuration; (5) Determine

$\Delta E = E_2 - E_1$; (6) If ΔE is negative, retain the new configuration given by the change; (7) If ΔE is positive, computer $p = \exp(-\Delta E/k_B T)$ where k_B is Boltzmann's constant and T is the absolute temperature; (8) Select a random number ξ from the unit interval $[0, 1]$; (9) If ξ is less than p, accept the new configuration given by the change; otherwise reject the new configuration. This process generates an ensemble of configuration status, the ensemble average energy provides an estimate of the average energy for the system at temperature T. This technique can be readily used to study equilibrium properties of a system of atoms.

In Metropolis MC methods we decide whether to accept a move by considering the energy difference between the states. In or near the equilibrium state, the standard MC scheme using a Boltzmann kinetic factor, $exp(-\Delta E/k_B T)$, becomes very inefficient since the Boltzmann factor is usually very small in comparison with a random number over the interval $[0, 1]$ (Bortz et al., 1975). Because of this, the n-fold way (the predecessor of KMC) was designed to replace the standard MC algorithm in generating new configurations in simulating Ising spin systems in 1975 (Bortz et al., 1975; Lu, Petroff and Metiu, 1990; , n.d.). This technique chooses a spin site from the entire ensemble based upon its probability of flipping. Once a site was selected, the flipping was guaranteed and could be immediately performed. The n-fold way also provided a new simulation time concept. At each flip, the time was incremented by a stochastic variable, Δt, whose expectation value is proportional to Q^{-1} (where Q is the number of spins times the average probability that an attempt will produce a flip for a given configuration). Mathematically, $\Delta t = -(\tau/Q) \ln \xi$, where ξ is a random fraction and τ a system dependent time. This choice reflects properly the distribution of time intervals between flips for a reasonable physical model. The cumulative time thus summed is approximately proportional to real time. The n-fold way reduced computation time by an order of magnitude or more for many applications (Bortz et al., 1975). A similar concept was used in Voter's 1987 transition state theory (Voter and Doll, 1985). Based on the n-fold way algorithm, Horia Metiu, Yan-Ten Lu and Zhenyu Zhang in a 1992 Science paper titled "Epitaxial Growth and the Art of Computer Simulations" proposed the so-called "Kinetic Monte Carlo" (KMC) method (Metiu, Lu and Zhang, 1992). The paper first pointed out the demands on atomic level control of modern electronic and photonic devices and the importance of *in situ* STM observations of small atomic "clusters" to a theorist who wants to understand growth and segregation; it then elaborated on the usefulness of KMC simulations in reproducing these experimental observations. The basic feature of their model was to move atoms site-to-site on a square lattice terrace. They postulated rates for all of the elementary processes involved, such as the site-to-site jumps, the jumps to leave or join a step or an existing adsorbate cluster, and so forth. The atoms were deposited on the surface and moved from site to site with a frequency proportional to the rate of the respective move: if the rate constant of the i-th kinetic process was r_i, the largest rate was chosen as a reference and denoted r_r. The probability $P_i = r_i/r_r$ was then used in a Monte Carlo program as the probability that the atom performed a jump i. The work used Voter's transition state theory (Voter and Doll, 1985) to monitor the simulation time.

Kinetic Monte Carlo (KMC) for Defect Motion in Stress Fields

The first step in KMC simulations is to tabulate the rate at which an event (i) will take place anywhere in the system, r_i. The probability of selecting an event is simply the ratio of the rate at which the event occurs relative to the sum of all possible event rates. Once an event is chosen, the system is changed appropriately, and the list of events that can occur at the next KMC step is updated. Therefore, at each KMC step, one event denoted by m is randomly selected from all possible M events, as follows:

$$\frac{\sum_{i=0}^{m-1} r_i}{\sum_{i=0}^{M} r_i} < \xi < \frac{\sum_{i=0}^{m} r_i}{\sum_{i=0}^{M} r_i}$$

where ξ is a random number uniformly distributed in the range [$\in (0,1)$]. After an event is selected and carried out, the total number of possible events, M, and the sequence in which the events are labeled, are updated. In conventional KMC simulations, a fixed time increment is chosen such that at most one event happens during each time step. However, this approach is inefficient since in many time steps, no events will happen. An alternative technique, introduced by Bortz et al. (1975) ensures that one event occurs somewhere in the system, and the time increment itself can be determined at each step. In this approach, since one event occurs at each simulation step and different events occur at different rates, the time increment, dt, corresponding with each step is dynamic and stochastic: $dt = -\ln(\xi)/\sum_{i=1}^{M} r_i$. This method is particularly useful in simulations of radiation-induced defect motion, where the events occur at vastly different time scales.

So far, all KMC computer simulations for microstructure evolution under irradiation have not considered the influence of the internal and applied stress fields on defect motion. We present here computer simulations, where the elastic interactions between SIA clusters themselves, and between SIA clusters and dislocations are explicitly accounted for. SIA clusters are directly produced on the periphery of neutron collision cascades, and they may contain from a few atoms up to tens of atoms in the near vicinity of the cascade (Yu. N. Osetsky and Priego, 1998). Such clusters are extremely mobile, and migrate predominantly along highly-packed crystallographic directions, with migration energies of less than 0.1 eV (Yu. N. Osetsky and Priego, 1998; Soneda and Diaz de la Rubia, 1998). Small SIA clusters may also spontaneously change their Burgers vector, and thus have the flexibility to translate along various crystallographic directions if their motion is not obstructed by internal strain fields. In this work, we represent SIA clusters as small prismatic, rigid and circular dislocation loops.

The temperature dependence of the jump frequency of SIA cluster diffusion can be written as follows: $\omega = \omega_0 \exp(-\frac{E_m}{kT})$, where ω is the cluster jump frequency, ω_0 the pre-exponential factor, E_m the migration energy in a perfect crystal structure, T the temperature of the crystal and k the Boltzmann constant. In our KMC simulations, the elastic interaction is considered. The influence of other defects and the external stress on one SIA cluster is given by the stress field σ_{ij}. The work necessary to form the loop characterized by normal $\mathbf{n}$, Burgers vector $\mathbf{b}$ and area δA in the stress field σ_{ij} is SIA cluster interaction energy E_{int}, and is given by (Kroupa, 1960): $E_{\text{int}} = n_i b_j \sigma_{ij} \delta A = \mathbf{n} \cdot \sigma \cdot \mathbf{b}$
The total cluster migration energy is then given by: $\tilde{E}_m = E_m + \Delta E_{\text{int}}$
where ΔE_{int} is the change in the interaction energy of an SIA cluster placed at two neighboring equivalent points in the crystal. This includes the effects of forces and moments on the virtual loop motion. It has been shown that small SIA clusters can form perfect loops and perform one-dimensional (1D) random motion in the slip direction (Yu. N. Osetsky and Priego, 1998; Yu. N. Osetsky and Serra, 1999). There is a total of eight equivalent $< 111 >$ slip directions for SIA clusters in BCC Fe. Thus, there are eight equivalent choices for each cluster at each KMC step. However, the restriction of diffusion to 1-D motion implies that the possibility of reorientation for an SIA cluster is rather small, and the migration energy of a preferred $< 111 >$ direction is much lower than that of all other seven equivalent directions. We use the frequency of a loop jumping along a $< 111 >$ orientation, ω, as the rate at which an event occurs in our KMC model. Therefore, there is a total of $8N$ possible events for the N SIA clusters at each KMC step.

C.6.2 Dislocation Interaction with Glissile Defect Clusters

During irradiation, mobile SIA clusters migrate very quickly, interact with other features of the microstructure or amongst themselves, and they become immobilized as a consequence of such interactions. If they end up near the core of grown-in dislocations, they form what is known as a cluster atmosphere, similar to the well-known Cottrell impurity atmosphere around dislocations in unirradiated BCC metals. The yield behavior of the material is thus expected to be heavily dependent on the local cluster density near the dislocation core, and on how dislocations interact with such clusters. First, we present a study of cluster motion under the influence of the internal stress field created by grown-in dislocations as well as the clusters themselves. In post-irradiation tensile tests, dislocation unlocking from immobilized clusters controls the magnitude of the initial plastic yield (i.e. the upper yield stress), and thus, we will present computer simulations for the unlocking process also in this section.

C.6.3 Dislocation Decoration

To study how glissile SIA clusters migrate and interact amongst themselves, and with internal stress fields generated by dislocations and applied mechanical loads, a computational box of $400a \times 400a \times 400a$ (a: lattice constant of BCC Fe) is used with periodic boundary conditions. A uniaxial tensile stress of 121 MPa is applied along the $< 100 >$ direction. In order to study dislocation-cluster interaction, a dislocation loop lying on the $< 0\bar{1}1 >$ plane, with Burgers vector $\frac{1}{2} < \bar{1}11 >$ is introduced into the simulation box. The loop is generated by using the parametric method described above. The dislocation loop consists of two curved segments and two straight junction segments that are normal to the loop's Burgers vector. An initial number of SIA clusters with the same size (1.7 nm diameter) are first randomly distributed in the simulation cell, and their initial jump directions are also randomly specified. The SIA cluster density is varied in the range $5 \times 10^{22} - 2 \times 10^{23}$ M^{-3}. The orientation of each cluster's Burgers vector is kept the same as the jump direction, because clusters are represented as small prismatic dislocation loops. When a cluster approaches the dislocation loop at distances closer than the *standoff* distance (taken as 1.5 nm), the cluster is stopped, and all the events related to it are removed from the event table. The code allows cluster coalescence when two clusters overlap with one another. The input variables summarized in Table (8) below are used in the present KMC simulations.

Computer simulations of cluster-cluster-dislocation interactions reveal a number of interesting features. First, the migration of SIA clusters is very fast, and within a few nano-seconds at room temperature, clusters migrate along highly-packed crystallographic directions over microstructurally-significant distances. Previous MD simulations of motion of isolated SIA clusters indicated that their migration along {111} in BCC metals is extremely fast, as a result of their very low migration energies (∼0.02 eV) (Osetsky, Bacon, Serra, Singh and Golubov, 2000). However, our KMC simulations reveal that their mutual elastic interactions reduces such mobility very drastically. Their mutual interaction fields, aided by the focusing effects of internal dislocation fields, renders these clusters virtually immobile just after a few nano-seconds, as can be seen in FIG. (31). In effect, these clusters re-orient themselves by rotation of their Burgers vector to respond to the elastic field of internal dislocations. Thus, their migration is *focused* towards internal stress fields, and not random, as implied by MD simulations. Moreover, because of their close proximity, which is induced by the tendency to crowd space in the vicinity of dislocations, their mutual interaction becomes

very strong. Clusters that are oriented along non-parallel crystallographic orientations will either coalesce forming larger ones, or just pin one another at a short distance and become immobile. Another interesting feature of this problem is that when clusters are within a distance of several nanometers from each other, and have their Burgers vectors in parallel directions, will trap one another and tend to move in a self-organized group or *raft*. This feature has been experimentally observed for some time (Singh et al., 2002).

Table 8: Migration Energy E_m, lattice constant a, initial cluster radius R, Temperature T, pre-exponential factor ω_0, ratio of migration energy of 1D motion relative to reorientation energy f, shear modulus μ, and Poisson's ratio ν for BCC Fe.

E_m(eV)	$a(\mathring{A})$	$R(a)$	$T(K)$	$\omega_0(s^{-1})$	f	μ(GPa)	ν
0.02	2.8665	3.0	300.0	2.5×10^{13}	7.0	81.8	0.29

C.6.4 Evolution of Void/Bubble Microstructure in Vanadium

A kinetic rate theory model, which includes the formation of cascade-induced clusters (CIIC), was developed by Sharafat and Ghoniem (2000). Comparison of the model to ion irradiation data on vanadium reveals the effects of helium generation and cascade-induced interstitial and vacancy clusters on microstructure evolution. The model is based on a simplification of hierarchical rate equations for the clustering of helium bubbles, immobile vacancy clusters, glissile interstitial clusters, sessile dislocation loops, as well as precipitates and grain boundaries. The model shows that the transport of helium to dislocations, bubbles and grain boundaries is strongly transient because of coupling between the nucleation and growth modes of bubble evolution. Helium agglomeration in vacancy clusters is shown to reduce the excess vacancy flux to grow matrix and precipitate bubbles. The direct formation of vacancy and interstitial clusters in cascades reduces the growth rate of bubbles, and leads to enhanced nucleation of matrix bubbles. In addition to the dislocation and production bias mechanisms, a new mechanism of 'helium nucleation bias' is shown to exist under high helium generation rates.

C.7 Integrated Materials-Structural Modeling

C.7.1 VISTA: Virtual International Structural Test Assembly Facility

In April 2002 an IEA Workshop on "Advanced Ferritic Steel-Blanket Designs, Materials and Technologies"was held in San Diego, USA. Discussions made clear that despite significant progress in modelling material behaviour of fusion materials, a lack of an integrated material property-structural loading performance map is stifling design efforts. As a result, the need to develop a methodology to relate research on material properties and structural integrity modelling effort was identified. The concept of a Virtual International Structural Test Assembly (VISTA) was proposed. The primary goal of VISTA is to facilitate the development and implementation of advanced and fully integrated integrity and lifetime assessment methods.

An initial VISTA team was formed consisting of both US and EU members:

- **US**

R. Odette	UCSB	*odette@engineering.ucsb.edu*
N. Ghoniem	UCLA	*ghoniem@ucla.edu*
R. Mattas	ANL	*mattas@anl.gov*
Y. Takuya	UCSB	*yamataku@engineering.ucsb.edu*
S. Sharafat	UCLA	*shahrams@ucla.edu*

- **EU**

Diegele	FZK	*diegele@imf.fzk.de*

The team members met two times during the the US Fusion Materials Sciences Program Strategic Planning Meeting held at the University of California at Santa Barbara, August 26-30, 2002. During those meetings a roadmap for achieving VISTA's goals was developed. It was concluded that in essence VISTA is to provide a *methodology and physical basis to evaluate relations between research on material properties, failure paths and structural integrity assessment methods* as they relate to:

- Various Material Properties
- Geometric Realization
- Interaction of different sources of loading and damage
- Performance and lifetime limits of fusion structures
- Facilitating the development and implementation of advanced and fully integrated integrity and lifetime assessment methods.

The main focus of the program is to enhance the interaction between the materials and the component design communities. The need for an effective material-design interface has been widely overlooked in the past, but will become very important for the guidance of future work.

C.7.2 The VISTA Project Roadmap

VISTA is a modelling tool in a very broad sense. The aim goes well beyond establishing new models, new codes or analyzing a particular blanket concept. Rather the objective is to combine wide range of models including constitutive and damage laws, Finite Element models, geometrical configurations and loading conditions, to perform "virtual experiments"over a wide range of conditions, to carry out sensitivity studies and to evaluate a range of potential interactions and failure paths. In the near term, researchers must rely upon computer modelling tools to study integrated behaviour of blanket components, since the fusion environment cannot be completely simulated prior to operation of a fusion power device. The VISTA project can be divided into three phases:

1. **Phase-I: Geometric Realization of 3-D FEM**
   First, VISTA will develop full-scale geometry three-dimensional FEM models which would provide a range of boundary conditions for a series of detailed 2-D models for local analyses of fracture and plastic flow localization.

2. **Phase-II: Damage Functions**
   Second, VISTA will develop material models that will describe plasticity, visco-plasticity, creep and swelling or other subcategories of constitutive laws. The constitutive laws themselves will be hierarchical and based on a multi-scale integration of materials theory, models, simulations and experiment.

3. **Phase-III: Loading Performance Maps and Virtual Testing**
   Third, VISTA will develop a hierarchy of integrated material property-structural loading performance maps by integrating the Damage Functions with the series of 2-D detailed FEM models to guide advanced component design efforts.

During the three phases of the VISTA project a series of benchmark models and methodolies will be established. The benchmarks should be as simple as possible in a FE modeling sense but must have a set of attributes that make them useful. For example, a simple pressurized tube model is useful for examining FE methods and constitutive-plasticity laws but would not serve the main function of this effort. The attributes must provide surrogates for the consequences of:

• High and spatially dependent surface heat fluxes and volumetric heat deposition;
• High and spatially varying primary coolant pressure;
• Geometry involving 3-D aspects of duct runs with corners, turns and both local and component scale gradients (in all things) as well as displacement constraints and compliance;
• Time-history dependent relaxation and inelastic deformation processes that redistribute stresses and allow the accumulation of strains;
• Postulated transient loading associated with rapid shut-down, start-up and infrequent unplanned events;
• Other details (like cracks).

The FE benchmarks must be able to incorporate material models for elastic-plastic-viscoplastic deformation and fracture, including the effects of temperature, stress, irradiation and other sources of in-service damage and their synergisms. Ideally the subset of bechmarks can be simplified to the point of providing a basis for extensive sensitivity-probablistic studies. Also they can be incorporated into advanced neural network and other approaches to assessing the dynamics of complex systems responding to sets of large combinations of input variables or driving forces.

C.7.3 Phase-I: Geometric Realization of 3-D FEM

Advances in computer hardware and software for structural analysis have enabled easy creation of computer models for the analysis of complex structures. Despite these technological advances most fusion component design efforts focus on modeling simplified 2-D surrogates. Such analyses do not take into account the full-scale 3-D geometry effects, and they tend to omit the multi-physics aspects of a number of loading conditions, such as fluid, thermal, and electromagnetic.

The first phase of the VISTA project invovles development of full geometry 3-D FE models.

Ideally, a number of simple benchmark 3-D models will be developed for analysis. These simple benchmark FE models will include enough detail to allow evaluation of spatial and temporal loading conditions as well as the geometric aspects associated with large components. Furthermore, load-history dependent relaxation and inelastic deformation processes redistribute stresses that result in accumulation of strains. Modeling of lifetime or long-term performance of fusion components will have to include such temperature and load histories.

C.7.4 Hardware/Software Set up at UCLA

FEM of analysis of 3-D full geometry models requires massive computational resources plus multiphysics capable FEM software. The UCLA Beowolf Cluster, ISIS with 160 Nodes provides such computing powers and ANSYS Inc. offers a multiphysics FEM code capable of running on Linux-based parallel computing cluster.

In September 2002 ANSYS Inc. offered a daylong seminar to introduce the latest capabilities and features of the latest ANSYS code V7.0. S. Sharafat attended the seminar and initiated negotiations to for the acquisition of the multiphysics parallel processing ANSYS code. The parallel V7.0 code is the most powerful version that ANSYS Inc. has developed and it is commercially available at a price of $100K per year. Because of the high price of this code new educational discount procedures had to be renegotiated between UCLA and ANSYS Inc. The negotiations started in October and lasted until January 2003, when ANSYS Inc. agreed to provide UCLA with the parallel version of the mutliphysics FEM code for only $2,500 for the first year, with a new price to be determined for subsequent years. In February 2003 the ANSYS Version 7.0 was successfully installed on the Beowolf Cluster. In parallel with the acquisition of the software, the UCLA team is training four students (Tony Tan, Christopher Williams, Mitchell Styczynsla, and Peter Jeziorek) to use the ANSYS thermal and structural analysis package. Training of these students is to be completed by the middle of April. In summary, at the present time, both the hardware and software requirements to perform full geometry 3-D FEM analysis have been met at UCLA's Mechanical and Aerospace Engineering Department.

C.7.5 3-Dimensional Geometric Features

Fusion components are inherently large and as such are subject to non-uniform load distributions, both in the poloidal as well as toroidal and radial directions. The load non-uniformities are further exasperated by fluctuations in control parameters, such as start up, shut down, plasma operations, and disruptions. As part of VISTA the stress states throughout the component need to be mapped before a series of detailed 2-D models for local fracture and plastic flow localization2-D can be analyzed. To this end a detailed 3-D model of a component must be developed, which captures the primary effects of full geometry aspects. The following are some of the main aspects, which have been shown to impact the stress states of components. A simple multiprocessor COSMOS FEM code was used to perform these simple analyses. These results are very preliminary and serve only to show the limitations of using multiprocessors. Complete and full geometry 3-D models will be developed as part of Phase-I of Vista using the parallel version of the ANSYS V7.0 code.

Gravity Effects

A several meter high blanket module will be subject to gravity induced non-uniform loads along

the length of a First Wall/Blanket module. Each of the sixteen FliBe cooled outboard FW/Blanket sectors of a typical APEX fusion reactor would have to hold about 40 tons of FliBe (see Fig.**??**). Figure **??** shows a typical 8-m tall modules, nine of which comprise one FW/Blanket sector. From a neutron economy point of view the structural material of FW/Blanket modules needs to be minimized, which results in very thin-walled structures (3 - 5 mm). Effects of gravity alone on the stress states inside the structural material of a FW/Blanket can thus be substantial and must be estimated.

Non-Uniform Heating Effects

Consider the non-uniform heating of the FW/Blanket module. The central part of the module receives the maximum heat loads compared with the upper and lower portions. Superimposed on this heating load is the cooling rate. The combination of non-uniform heating and cooling results in temperature gradients, which result in non-uniform thermal stresses both along the poloidal and the radial dimensions of the module. A full scale 3-D FEM model can incorporate these geometric features, which can then be coupled with material properties that are both temperature and stress-state dependent. Figure **??** and 32 show samples of the 3-D variations in structure temperature soley due to geometric aspects of the components.

Fluid-Flow Effects

Variations in heat transfer coefficients caused by variations in coolant temperature distributions may affect the structure temperature distribution in poloidal, toroidal, and radial directions. Inclusion of these fluid effects is critical to map the stress states inside the component. Figure **??** show an example of how these fluid induced variations can manifest themselves in both temperature and pressure variations throughout the component.

C.7.6 Phase-II: Damage Functions

Advances in radiation damage modeling and experiments have enabled the fusion materials community to develop complex models for describing damage processes. These models can take into account the effects of stress states and temperature. During Phase-II of the VISTA project material models that will describe plasticity, visco-plasticity, creep and swelling or other subcategories of constitutive laws will be developed. The constitutive laws themselves will be hierarchical and based on a multi-scale integration of materials theory, models, simulations and experiment. These damage functions will then be programmed into the ANSYS V7.0 code.

C.7.7 Phase-III: Loading Performance Maps and Virtual Testing

In Phase-III the VISTA Project will concentrate on developing a hierarchy of integrated material property-structural loading performance maps by integrating the Damage Functions into the FEM analysis. The full geometry 3-D FE models developed during Phase-I will provide a range of boundary conditions for a series of detailed 2-D models for local analysis of fracture and plastic flow localization. The Damage Functions developed during Phase-II will be used to analyze the effects of radiation induced material property changes in these 2-D models. Effects of temperature, stress, irradiation and other sources of in-service damage and their synergisms can thus be analyzed. By selecting a series of critical locations for the 2-D models integrated material property-structural loading performance maps of the component can be developed. In essence, component failure

paths can thus be evaluated by **Virtual Testing of Engineering Performance** of full scale components.

C.7.8 Ancillary Benefits of VISTA's Integrated Modeling

The combination of (1) 3-D geometric feature modeling, (2) damage-function based evaluation of failure paths, and (3) virtual engineering performance testing for the first time will integrate research on materials properties, failure paths and structural integrity assessment methods. Furthermore, VISTA's integrated modeling facilitates:

• The development and implementation of advanced and fully integrated integrity and lifetime assessment methods;
• Provide guidance to both the experimental and modeling efforts of fusion material development;
• Provide the basis to identify composite materials component systems, shapes and configurations that optimize multifunctional performance;
• Provide the basis to design semi-scale benchmark experiments including the possible use of surrogate materials;
• Provide the basis to develop a hierarchy of integrated material property-structural loading performance maps to enlighten and guide advanced design efforts;
• Development of a functional library, archiving a growing knowledge base (subject of the next section).

Ideally during the course of VISTA a subset of bechmarks can be simplified to the point of providing a basis for extensive sensitivity-probablistic studies. Also they can be incorporated into advanced neural network and other approaches to assess the dynamics of complex systems responding to sets of large combinations of input variables or driving forces.

C.8 List of Publications

1. N.M. Ghoniem, H. Heinisch H. Huang, L. Kubin, Yu, and S. Yip, Guest Editors, Special Issue "Multi-scale Materials Modeling," *J. Comp.-Aided Mater. Design,* **6, No. 2&3** (1999) 374 pages.

2. N.M. Ghoniem, "Clustering Theory of Atomic Defects," *Radiation Effects and Defects in Solids,* **148**: 269-318 (1999).

3. H. Huang, N.M. Ghoniem, T. Diaz de la Rubia, M. Rhee, H. Zbib and J. Hirth, "Stability Of Dislocation Short-Range Reactions In BCC Crystals," *J. Eng. Mat. & Tech.,* **121(2)**: 143 (1999).

4. N.M. Ghoniem, "Curved Parametric Segments For The Stress Field Of 3-D Dislocation Loops," *J. Eng. Mat. & Tech.,* **121(2)**: 136 (1999).

5. N. M. Ghoniem, L. Sun, "Fast Sum Method for the Elastic Field of 3-D Dislocation Ensembles," *Phys. Rev. B,* **60(1)**: 128-140 (1999).

6. L. J. Perkins, B. G. Logan, M.D. Rosen, M.D. Perry, T. Diaz de la Rubia, N.M. Ghoniem, T. Ditmire, S.Wilkes and P.T.Springer, "The Investigation of High-Intensity-Laser Driven Micro Neutron Sources for Fusion Materials Applications at High Fluence," *Nuclear Fusion.,* **40(1)**:1-19 (2000).

7. N.M. Ghoniem, B. N. Singh, L. Z. Sun, and T. Diaz de la Rubia, "Interaction and Accumulation of Glissile defect Clusters Near Dislocations," *J. Nucl. Mater,* **276**: 166-177 (2000).

8. N.M. Ghoniem, S.- H. Tong, and L. Z. Sun , "Parametric Dislocation Dynamics: A Thermodynamics-based Approach to Investigations of Mesoscopic Plastic Deformation," *Phys. Rev. B,* **139(1)**: 913-927 (2000).

9. L. Sun, N.M. Ghoniem, and B.N. Singh, "3-D Dislocation Dynamics Study of Plastic Instability In Irradiated Copper," *J. Nucl. Mater.,* **283**:741(2000).

10. S. Sharafat and N.M. Ghoniem, "Comparison of A Microstructure Evolution Model With Experiments on Irradiated Vanadium", *J. Nucl. Mater.*,**283**:789(2000).

11. S.J. Zinkle and N.M. Ghoniem, "Operating Temperature Windows for Fusion Reactor Structural Materials", *Fusion Engineering and Design*,**51-52**:55(2000).

12. S. Sharafat, M. Demetriou , N. Ghoniem , B. Williams, R. Nygren, "Enhanced surface heat removal using a porous tungsten heat exchanger," *Fus. Tech.* **39(2)**:863-867, Part 2, 2001.

13. L.Z. Sun, N.M. Ghoniem, and Z.Q. Wang, "Analytical and Numerical Determination of the Elastic Interaction Energy between Glissile Dislocations and Stacking Fault Tetrahedra in FCC Metals", *J. Mat. Sci. & Engr.*, **A309-310**:178183 (2001).

14. Nasr M. Ghoniem, "Radiation Damage Correlations For Fusion Conditions", *Encyclopedia of Materials: Science and Technology*, Pergamon Press, Elsevier Science Publication, 3413-3418 (2001), ISBN:0-08-0431526.

15. N.M. Ghoniem, S.H. Tong, B.N. Singh, and L.Z. Sun, "On Dislocation Interaction with Radiation-induced Defect Clusters and Plastic Flow Localization in FCC Metals", *Phil. Mag. A*, **81 (11)**:, 2743-2764 (2001).

16. G.R. Odette, B.D. Wirth, D. J. Bacon and N.M. Ghoniem, "Multi-scale, Multi-physics Modeling of Radiation-damaged Materials: Embrittlement of Pressure Vessel Steels", *MRS Bulletin*, 176-81(2001).

17. N.M. Ghoniem, J.M. Huang, and Z.Q. Wang, "Affine Covariant-contravariant Vector Forms for the Elastic Field of Parametric Dislocations in Isotropic Crystals," *Phil. Mag. Lett.*, **82(2)**: 55-63 (2002).

18. N.M. Ghoniem and J.M. Huang, "Computer Simulations of Mesoscopic Plastic Deformation with Differential Geometric Forms for the Elastic Field of Parametric Dislocations: Review of Recent Progress,"Invited Paper at the 5th Euro-Conference on Mechanics of Materials, Delft, Netherlands, March 6-9, 2001, Also *J. de Physique IV*, **11(5)**:53-60 (2001).

19. N.M. Ghoniem,D. Walgraef and S. J. Zinkle, "Theory and Experiment of Nanostructure Self-organization in Irradiated Materials,"Invited Perspective Article, *J. Comp. Aided Mat. Design*, **8**:1-38 (2002).

20. Jianming Huang and Nasr M. Ghoniem, "The Dynamics of Dislocation Interaction with Sessile Self-Interstitial Atom(SIA) Defect Cluster Atmospheres,", *J. Comp. Mat. Science*,**23**:225234 (2002).

21. R. Martinez and N. M. Ghoniem, "The Infuence of Crystal Surfaces on Dislocation Interactions in Mesoscopic Plasticity: A Combined Dislocation Dynamics- Finite Element Approach,", *J. Comp. Meth. Engr. Science, CMES*, **3(2)**:229-243 (2002).

22. Nasr M. Ghoniem and Kyeongjae Cho, "The Emerging Role of Multiscale Modeling in Nano- and Micro-mechanics of Materials," *J. Comp. Meth. Engr. Science, CMES,* **3(2)**:147-173 (2002).

23. N. M. Ghoniem, S.H. Tong, J. Huang, B.N. Singh, and M. Wen, "Mechanisms of Dislocation-Defect Interactions in Irradiated Metals Investigated by Computer Simulations," *J. Nucl. Mater.*, **307311**: 843851 (2002).

24. B.N. Singh, N.M. Ghoniem and H. Trinkaus, "Experiment-Based Modelling of Hardening and Localized Plasticity in Metals Irradiated Under Cascade Damage Conditions,"*J. Nucl. Mater.*, **307311**:159170 (2002).

25. Marios D. Demetriou, Nasr M. Ghoniem, Adrienne S. Lavine, "Kinetic Modeling of Phase Selection during Non-Equilibrium Solidification of WC," *Acta Materialia*, **50 (6)**:1421-1432 (2002).

26. Marios D. Demetriou, Nasr M. Ghoniem, Adrienne S. Lavine, "Effects of Nucleation Transience on the Kinetics of Crystallization," *J Chem Phys*, **117**:23 (2002).

27. Marios D. Demetriou, Nasr M. Ghoniem, Adrienne S. Lavine, "Computation of Metastable Phases in Tungsten-Carbon System,"*Journal of Phase Equilibria,* **23(4)**:305-309, (2002).

28. Marios D. Demetriou, Nasr M. Ghoniem, Adrienne S. Lavine, "Modeling of Graphitization Kinetics during Peritectic Melting of Tungsten Carbide,"*Acta Materialia*, in press, (2002).

29. X. Han, N.M. Ghoniem and Z. Wang, "Parametric Dislocation Dynamics of Anisotropic Crystalline Materials," *Phil. Mag. A*., in press, (2002).

30. D.Walgraef and N.M.Ghoniem, "The Effects of Glissile Interstitial Clusters on Microstructure Self-organization in Irradiated Materials," *Phys. Rev. B*, in Press, (2002).

31. Nasr M. Ghoniem, Hanchen Huang, Esteban Busso, and Nicolas Kioussis, "Multiscale Modeling of Nano- and Micro-Mechanics: an Overview,"*Phil. Mag. A*, in press, (2002).

32. Jianming Huang and Nasr M. Ghoniem, "Accuracy & Convergence of Parametric Dislocation Dynamics (PDD)," *Mod. Sim. Mat. Sci. Engr.,* **10**:1-19 (2002).

33. N.M. Ghoniem, and B.N. Singh, "Dislocation Dynamics Study of the onset of Plastic Instabilities in Irradiated Materials,"Proc. of 20th RISO International Symposium on Materials Science, Deformation-Induced Microstructures: Analysis and Relationship to Properties, Bilde-Sorensen, et al., Eds., September 6-10, 1999, Roskilde, Denmark, page 41-60.

34. C.P.C. Wong, R.E. Nygren, C.B. Baxi, P. Fogarty, N.M. Ghoniem, H. Khater, K. McCarthy, B. Merril, B. Nelson, E. Reis, S. Sharafat, R. Schleicher, D.K. Sze, M. Ulrickson, S. Williams, M. Youssef, and S. Zinkle, "Helium-cooled Refractory Alloy First Wall and blanket Evaluation,"Proc. of the fifth International Symp. On Fusion Nuclear Technology (ISFNT-5), September 1999, Rome, Italy.

35. Nasr M. Ghoniem, "Computational Methods For Mesoscopic, Inhomogeneous Plastic Deformation", *Proceedings of First Latin American Symposium on Materials Instabilities*, Valpareso, Chile, Kluwer Publication, 2000.

References

(n.d.).

Abaqus V6.2 (2001). Hibbit, Karlsson and Sorenson, Inc., Providence, RI.

Alexander, D., Zinkle, S. and Rowcliffe, A. (1999). Fracture toughness of copper-base alloys for fusion energy applications, *J. Nucl. Mater.* **271&272**: 429.

Amodeo, R. and Ghoniem, N. M. (1988). A review of experimental observations and theoretical models of dislocation cells, *Res Mech.* **23**: 137.

Ashby, M. (1972). A first report on deformation-mechanism maps, *Acta Metall.* **20**: 887.

ASTM, E. .-. (2002). Standard test method for determination of reference temperature, t_0, for ferritic steels in the transiton range, *2002 Annual Book of ASTM Standards* **V03.01**: 1139.

Bacon, D. and Diaz de la Rubia, T. (1994). Molecular dynamics computer simulations of displacement cascades in metals, *J. Nucl. Mater.* **216**: 275.

Bacon, D., Gao, F. and Osetsky, Y. (2000). The primary damage state in fcc, bcc and hcp metals as seen in molecular dynamics simulations, *J. Nucl. Mater.* **276**: 1.

Baras, F. and Walgraef, D. (1992). *Physica*.

Battaile, C. and Srolovitz, D. (1997). A kinetic monte carlo method for the atomic-scale simulation of chemical vapor deposition: application to diamond, *J. Appl. Phys.* **82**(12): 6293.

Bauerle, D. (1996). *Laser Processing and Chemistry*, Springer-Verlag, New York.

Bodenschatz, E., Z. W. and Kramer, L. (1988). *J.Phys.*

Borckmans, Dewel, G., De Wit, A. and Walgraef, D. (1994). Turing bifurcations and pattern selection, *Chemical Waves and Patterns, Kapral R., and Showalter K. (Eds.)* **Kluwer, Dordrecht**: 323.

Bortz, A., Kalos, M. H. and Lebowitz, J. L. (1975). A new algorithm for monte carlo simulation of ising spin systems, *J. Comput. Phys.* **17**(1): 10.

Brimhall, J. (1974). Battelle pacific northwest laboratory report, *Technical Report BNWL-1839*.

Busse, F. H. (1978). *Rep. Prog. Phys.* **41**: 1929.

Busse, F. H. and Riahi, N. (1980). *J. Fluid Mech.* **96**: 243.

Caturla, M., Soneda, N., Alonso, E., Wirth, B., Diaz de la Rubia, T. and Perlado, J. (2000). Comparative study of radiation damage accumulation in cu and fe, *J. Nucl. Mater.* **276**: 13.

Conway, J. (1984). Mechanical and physical properties of refractory metals and alloys, *Proc. Symp. on Refractory Alloy Technology for Space Nuclear Power Applications, CONF-8308130, Oak Ridge National Lab* p. 252.

Cottrell, A. (1948). Report of conference on the strength of solids(university of bristol), england, physical society, london, **30**: 30.

Cox, B. and Wiffen, F. (1973). The ductility in bending of molybdenum alloys irradiated between 425 and 1000 c, *J. Nucl. Mater* **85&86**: 901.

Cross, M. C. and Hohenberg, P. C. (1993). *Rev. Mod. Phys.* **65**: 851.

Crowin, W. R. and et al (1993). Small specimen test techniques applied to nuclear reactor vessel thermal annealing and plant life extension, *ASTM STP* p. 1204.

Demetriou, M., Ghoniem, N. M. and Lavine, A. (2002a). Computation of metastable phases in tungsten-carbon system, *Journal of Phase Equilibria* **23(4)**: 305–309.

Demetriou, M., Ghoniem, N. M. and Lavine, A. (2002b). Effects of nucleation transience on the kinetics of crystallization, *J Chem Phys* **117**: 23.

Demetriou, M., Ghoniem, N. M. and Lavine, A. (2002c). Kinetic modeling of phase selection during non-equilibrium solidification of wc, *Acta Materialia* **50(6)**: 1421–1432.

Dudarev, S. (2000). Inhomogeneous nucleartion and growth of cavities in irradiated materials, *Phys. Rev. B* **62**(14): 9325.

Evans, J. (1971). *Nature* **29**: 403.

G. R. Odette, M. He, D. G. D. K. and Lucas, G. E. (2002). ome recent innovations in small specimen testing, *J. Nucl. Mater.* **307-311**: 1643–1648.

Gear, C. (1971). *Numerical Initial Value Problems in Ordinary Differential Equations*, Prentice-Hall, Englewood Cliffs.

Gelles, D. (1996). icrostructural examination of commercial ferritic alloys at 200 dpa, *J. Nucl. Mater.* **233-237**: 293.

Ghoniem, N. (1999). Curved parametric segments for the stress field of 3-d dislocation loops, *J. Eng. Mater. Tech.* **121**(2): 136.

Ghoniem, N. and Huang, J. (n.d.).

Ghoniem, N. and Sun, L. (1999). Fast-sum method for the elastic field of three-dimensional dislocation ensembles, *Phys. Rev. B* **60**(1): 128.

Ghoniem, N. M., Huang, J. M. and Wang, Z. Q. (2002). Affine covariant-contravariant vector forms for the elastic field of parametric dislocations in isotropic crystals, *Phil. Mag. Lett.* **82(2)**: 55–63.

Ghoniem, N., Singh, B., Sun, L. and Diaz de la Rubia, T. (2000a). Interaction and accumulation of glissile defect clusters near dislocations, *J. Nucl. Mater.* **276**: 166.

Ghoniem, N., Singh, B., Sun, L. and Diaz de la Rubia, T. (2000b). Interaction and accumulation of glissile defect clusters near dislocations, *J. Nucl. Mater.* **276**: 166.

Goldberg, D. (1969). Nonferrous alloys, *Aerospace Structural Metals Handbook, Metals and Ceramics Information Center, Battelle Columbus Laboratories, USA, 1969.* p. 68.

Gorynin, I. and et al. (1992). Effects of neutron irradiation on properties of refractory metals, *J. Nucl. Mater.* **191-194**: 421.

Gruber, E., Galvin, T. and Chopra, O. (1998). Effects of irradiation to 4 dpa at 390 c on the fracture toughness of vanadium alloys, *in Fusion Materials Semiann. Prog. Report for period ending June 30 1998, DOE:ER-0313:24, Oak Ridge National Lab* p. 28.

Gustafson, P. (1986). *Mater Sci Tech* **2**: 653.

Hartranft, R. and Sih, G. (1969). The use of eigenfuntion expansions in the general solution of three-dimensional crack problems, *Journal of Mechanics and Mathematics* **19**: 123–138.

Hartranft, R. and Sih, G. (1977). Stress singularity for a crack with an arbitrarily curved front, *Engineering Fracture Mechanics* **9**: 705–718.

Heinisch, H. (1990). Computer simulation of high energy displacement cascades, *Radiat. Eff. Def. Solids* **113**: 53.

Heinisch, H. (1995). Simulating the production of free defects in irradiated metals, *Nucl. Instrum. & Meth. in Phys. Res. B* **102**: 47.

Heinisch, H. and Singh, B. (1996). Stochastic annealing simulation of differential defect production in high energy cascades, *J. Nucl. Mater.* **232**: 206.

Heinisch, H. and Singh, B. (1997). Stochastic annealing simulation of intracascade defect interactions, *J. Nucl. Mater.* **251**: 77.

Hirsch, P. B. and Roberts, S. G. (1991). The brittle-ductile transition in silicon, *Phil. Mag. A* **A64**: 85.

Hirsch, P. B. and Roberts, S. G. (1997). Modelling crack tip plastic zones and the brittle-ductile transition, *Phil. Trans. R. Soc. Lond.* **A355**: 1991.

Hirsch, P. B., Roberts, S. G. and Samuels, J. (1989). The brittle-ductile transiton in silicon. ii. interpretation, *Proc. R. Soc. Lond. A* **421**: 25.

Hishinuma, A., Kohyama, A., Klueh, R., Gelles, D., Dietz, W. and Ehrlich, K. (1998). Current status and future r&d for reduced-activation ferritic:martensitic steels, *J. Nucl. Mater.* **258-263**: 193.

Holzapfel, G. (2000). *Nonlinear Solid Mechanics*, Wiley, West Sussex, England, p. 36.

Huang, J. and Ghoniem, N. M. (2002). The dynamics of dislocation interaction with sessile self-interstitial atom(sia) defect cluster atmospheres, *Computational Material Science* **23**: 225–234.

Hutchinson, J. (1968). Singular behaviour at the end of a tensile crack in a hardening material, *J. Mech. and Phys. of Solids* **16**: 13.

Jäger, W. and et. al (1987). *Mater. Sci. Forum* **15-18**: 887.

Jäger, W. and Trinkaus, H. (1993). *J. Nucl. Mater.* **205**: 394.

Jäger, W., E. P. and Schilling, W. (1988). *Solid State Phenomena* **3-4**: 297.

Jaraiz, M., Gilmer, G., Poate, J. and de la Rubia, T. (1997). Atomistic calculations of ion implantation in si: Point defect and transient enhanced diffusion phenomena, *Appl. Phys. Lett.* **68**(3): 409.

Jr., R. M. (2000). *The influence of crystal surface on dislocation behavior in mesoscopic plasticity: A combined dislocation dynamics - finite element menthod*, Master's thesis, University of California, Los Angeles.

Kassir, M. and Sih, G. (1966). Three-dimensional stress distribution around an elliptical crack under arbitrary loading, *Journal of applied mechanics, Trans. ASME* **33**: 601–611.

Klueh, R. and Alexander, D. (1995). Embrittlement of cr mo steels after low fluence irradiation in hfir, *J. Nucl. Mater.* **218**: 151.

Knott, J. (2000). The micro-mechanicsms of fracture in steels used for high-integrity structural components, *Fracture, Plastic Flow and Structural Integrity* **IOM Communications Ltd.**(London): 21.

Kossowsky, R., S. S. (1984). *Surface Engineering, Surface Modification of Materials*, Dordrecht.

Kratochvil, J. (1988). *Rev.Phys.Appliquée* **23**: 419.

Krautwasser, P. and Derz, H.and Kny, E. (1976). Influence of fast neutron fluence on the dbtt of tungsten, w 10re and w 3.4ni 1.6fe, *High Temperatures-High Pressures* **22**: 25.

Kroupa, F. (1960). *Czech. J. Phys.* **B10**: 284.

Kroupa, F. (1966). Theory of crystal defects, *Academia Publishing Prague* p. 275.

Kulcinski, G. and J.L., B. (1973). *Effects of radiation on substructure and mechanical properties of metals and alloys*, ASTM STP 529, American Society for Testing and Materials, Philadelphia.

Lardner, R. (1974). *Mathematical theory of dislocations and fracture*, University of Toronto Press.

Lin, K., Lin, H., Chen, K. and Chang, H. (1997). Elastic interaction between screw dislocation and a circular surface crack, *Materials Science and Engineering* **A224**: 216–220.

lin Pan, K. (1995). Effect of shape of crack tip on dislocation image force, *Mechanics Research Communications* **22**(2): 123–128.

Loomis, B. and Smith, D. (1992). Vanadium alloys for structural applications in fusion systems: a review of vanadium alloy mechanical and physical properties, *J. Nucl. Mater.* **191-194**: 84.

López-Salvans, M., Sagués, F. and Claret, J. (2000). Fingering in thin layer electrodeposition, *the Proceedings of the 1st Latin American School on Materials Instabilities, held in Valparaiso, Chile, Dec 98, Kluwer ublication.*

Lu, Y.-T., Petroff, P. and Metiu, H. (1990). Growth-kinetics simulation of the al-ga self-organization on (100) gaas vicinal surfaces, *Appl. Phys. Lett.* **57**(25): 2683.

Maksimkin, O. (1995). Radiation and radiation-anneal hardening of tantalum, *Phys. Met. Metallogr.* **80**: 592.

Maziasz, P. and et al. (1999). New ods ferritic alloys with dramatically improved high-temperature strength, *J. Nucl. Mater., Proc. 9th Int. Conf. Fusion Reactor Materials*.

McCabe, D. E., Merkle, J. G. and Wallin, K. (2000). Techinical basis for the master curve concept of fracture toughness evaluations in the transition range, *Fatigue and Fracture Mechanics:30th Volume, ASTM STP* **1360**: 21.

McCoy, H. (1986). Creep properties of selected refractory alloys for potential space nuclear power applications, *Oak Ridge National Lab Report ORNL:TM-10127*.

Metiu, H., Lu, Y.-T. and Zhang, Z. (1992). Epitaxial-growth and the art of computer-simulations, *Science* **255**(5048): 1088.

Metropolis, N., Rosenbluth, A., Rosenbluth, M., Teller, A. and Teller, E. (1953). Equation of state calculation by fast computing machines, *J. Chem. Phys.* **21**: 1087.

Mughrabi, H. (1983). Dislocation wall and cell structures and long-range internal-stresses in deformed metal crystals., *Acta Met.* **31**: 1367.

Mughrabi, H. (1987). A 2-parameter description of heterogeneous dislocation distributions in deformed metal crystals., *Mat. Sci. & Eng.* **85**: 15.

Nanotechnology Research Directions: IWGN Workshop Report Vision for Nanotechnology Research and Development in the Next decade (1999). WTEC, Loyola College in Maryland.

Neuhauser, H. (1990). Plastic instabilities and the deformation of metals, *Patterns, Defects and Materials Instabilities, Walgraef, D. and Ghoniem, N.M. (Eds.), Kluwer Academic Publishers,Dordrecht*.

Nicolis, G., Dewel, G. and Turner, J. (1981). *Order and Fluctuations in Equilibrium and Nonequilibrium Statistical Mechanics*, Wiley Publishers, New York.

Noronha, S. J. and Farkas, D. (2002). Effects of dislocation pinning on fracture behaviour: atomistic and dislocation simulation, *Phys. Rev. B* **66**: 132103.

Noronha, S. J., Roberts, S. G., Wilkinson, A. J. and Hirsch, P. B. (2003). Factors effecting discrete dislocation models for cleavage from microcracks in ferritic steels, *to be published*.

Odette, G. and Lucas, G. (1983). Analysis of cleavage fracture potential of martensitic stainless steel fusion structures, *J. Nucl. Mater.* **117**: 264.

Odette, G. R. and He, M. Y. (2002). Micromechanical modeling of master curve temperature shifts due to constraint loss, *J. Nucl. Mater.* **307-311**: 1624.

Odette, G. R., H. M. Y. (2000). A cleavage toughness master curve model, *J. Nucl. Mater.* **283-284**: 120–127.

Odette, G. R., H. M. Y. (2002). Micromechanical modeling of master curve temperature shifts due to constraint losl, *J. Nucl. Mater.* **307-311**: 1624–1628.

Osetsky, Y. N., Bacon, D., Serra, A., Singh, B. and Golubov, S. (2000). *J. Nucl. Mater.* **296**: 65.

Osetsky, Y. N., Bacon, D., Singh, B. and Wirth, B. (2002). Atomistic study of generation, interaction, accumulation and annihilation of cascade-induced defect clusters, *These proceedings.*

Perepezko, J. H. and Boettinger, W. (1983). *Mat Res Soc Symp Proc* **19**: 223.

Rehberg, I., Winkler, B., de la Torre Juarez, M., Rasenat, S. and Schopf, W. (1989). *Festkorperprobleme/Advances in Solid State Physics* **29**: 35.

Rice, J. and Rosengren, G. (1968). Plane strain deformation near a crack tip in a power-lasw hardening material, *J. Mech. and Phys. of Solids* **16**: 1.

Rieth, M., Dafferner, B. and Röhrig, H.-D. (1998). Embrittlement behaviour of different international low activation alloys after neutron irradiation, *J. Nucl. Mater.* **258-263**: 1147.

Ritchie, R. O., Knott, J. F. and Rice, J. R. (1973). On the relationship between critical tensile stress and fracture toughness in mild steel, *J. Mech. Phys. Solids* **21**: 395.

Roberts, S. G., Noronha, S. J., Wilkinson, A. J. and Hirsch, P. B. (2002). Modelling the initiation of cleavage fracture of ferritic steels, *Acta Mater* **50**: 1229.

Robertson, J.P.and Klueh, R., Shiba, K. and Rowcliffe, A. (1997). Radiation hardening and deformation behavior of irradiated ferritic-martensitic cr-steels, *in Fusion Materials Semiann. Prog. Report for period ending Dec. 31 1997, DOE:ER-0313:23, Oak Ridge National Lab* p. 179.

Rosenfield, A. R., Shetty, D. K. and Skidmore, A. J. (1983). Fractographic observations of cleavage initiation in the ductive-brittle transition region of a reactor-pressure vessel steel, *Met. Trans. A* **14 A**: 1934.

Rowcliffe, A. and et al. (1998). Fracture toughness and tensile behavior of ferritic-martensitic steels irradiated at low temperatures, *J. Nucl. Mater.* **258-263**: 1275.

Rudy, E. (1969). *Report AFML-TR-65-2, Wright-Patterson Air Force Base, OH.*

Ryazanov, A., Manichev, V. and van Witzenburg, W. (1996). Influence of helium and impurities on the tensile properties of irradiated vanadium alloys, *J. Nucl. Mater.* **227**: 304.

Sass, S. and Eyre, B. (1973). *Philos. Mag.* **27**: 1447.

Schroeder, H. and Ullmaier, H. (1991). Helium and hydrogen effects on the embrittlement of iron- and nickel-based alloys, *J. Nucl. Mater.* **179-181**: 118.

Seul, M. and Wolfe, R. (1992). *Phys. Rev. A* **46**: 7534.

Sharafat, S. and Ghoniem, N. (2000). Comparison of a microstructure evolution model with experiments on irradiated vanadium, *J. Nucl. Mater.* **283**: 789.

Shiba, K., Hishinuma, A., Tohyama, A. and Masamura, K. (1997). Properties of low activation ferritic steel f82h iea heat-interim report of iea round-robin tests (1), *Japan Atomic Energy Research Institute Report JAERITech.*

Sih, G. and Chen, E. (1981). Cracks in composite materials, *Mechanics of Fracture.*

Singh, B. and Evans, J. (1995). *J. Nucl. Mat.* **226**: 277.

Singh, B., Edwards, D. and Toft, P. (2001). *J. Nucl. Mat.* **299**: 205.

Singh, B., Evans, J., Horsewell, A., Toft, P. and Edwards, D. (1995a). Microstructure and mechanical behaviour of tzm and mo-5% re alloys irradiated with fission neutrons, *J. Nucl. Mater.* **223**(2): 95.

Singh, B., Foreman, A. and Trinkaus, H. (1997). *J. Nucl. Mater.* **249**: 103.

Singh, B., Ghoniem, N. and Trinkaus, H. (2002). Experiment-based modeling of hardening and localized plasticity in metals irradiated under cascade damage conditions, *Thesis proceedings*.

Singh, B., Horsewell, A., Toft, P. and Edwards, D. (1995b). Temperature and dose dependencies of microstructure and hardness of neutron irradiated ofhc copper, *J. Nucl. Mater.* **224**(2): 131.

Sivashinsky, G. I. (1983). *Physica* **D8**: 243.

Snead, L., Zinkle, S., Alexander, D., Rowcliffe, A., Robertson, J. and Eatherly, W. (1997). Temperature dependence of the tensile and impact properties of v 4cr 4ti irradiated to low neutron doses, *in Fusion Materials Semiann. Prog. Report for period ending Dec. 31 1997, DOE:ER-0313:23, Oak Ridge National Lab* p. 81.

Snead, L., Zinkle, S., Hay, J. and Osborne, M. (1998). Amorphization of sic under ion and neutron irradiation, *Nucl. Instr. Methods B* **141**: 123.

Soneda, N. and Diaz de la Rubia, T. (1998). Defect production, annealing kinetic and damage evolution in α-fe:an atomic-scale computer simulation, *Philos. Mag. A* **78**(5): 995.

Soneda, N. and Diaz de la Rubia, T. (2001). Migration kinetics of the self-interstitial atiom and its clusters in bcc fe, *Philos. Mag. A* **81**(2): 331.

Steichen, J. (1976). Tensile properties of neutron irradiated tzm and tungsten, *J. Nucl. Mater.* **60**: 13.

Stiegler, J. and Bloom, E. (1971). Void formation in irradiated nickel 270, *Rad. Effects* **8**(1-2): 33.

Stiegler, J. and Farrell, K. (1974). *Scr. Metall.* **8**: 651.

Suo, Z. and Lu, W. (2000). Forces that drive self-assembly on solid surfaces, *J. Nanoparticles Res.*

Tatinen, S., Pyykkoen, M., Karjalainen-Roikonen, P., Singh, B. and Toft, P. (1998). Effect of neutron irradiation on fracture toughness behavior of copper alloys, *J. Nucl. Mater.* **258-263**: 1010.

Trinkaus, H., Singh, B., and Foreman, A. (1997a). *J. Nucl. Mater.* **251**: 172.

Trinkaus, H., Singh, B. and Foreman, A. (1997b). Mechanisms for decoration of dislocations by small dislocation loops under cascade damage conditions, *J. Nucl. Mater.* **249**: 91.

Trinkaus, H., Singh, B. and Woo, C. (1994). Defect accumulation under cascade damage conditions, *J. Nucl. Mater.* **212-215**: 18.

Ukai, S., Nishida, T., Okuda, T. and Yoshitake, T. (1998). R&d of oxide dispersion strengthened ferritic:martensitic steels for lmfbr, *J. Nucl. Mater.* **258-263**: 1745.

Veistinen, M. K. and Lindroos, V. K. (1983). The application of a direct approach in the study of the initiation mechanisms of cleavage fracture in a 26 cr - 1mo ferritic stainless steel, *International Conference on Application of Fracture Mechanics to Materials and Structures* **Frieburg**(Germany): 377.

Voter, A. and Doll, J. (1985). Dynamical corrections to transition state theory for multistate systems:surface self-diffusion in the rare-event regime, *J. Chem. Phys.* **82**: 80.

Walgraef, D., L. J. and Ghoniem, N. (1996). *Phys. Rev. B* **53**: 14782.

Wallin, K. (1993). Irradiation damage effects on the fracture toughness transiton curve shape for reactor pressure vessel steels, *Int. J. Pres. Ves. & Piping* **55**: 61.

Wang, S. and Lee, S. (1990). An analysis of the elastic interaction between and edge dislocation and an internal crack, *Mat. Sci. Engn.* **A130**: 1.

Wang, S.-D. and Lee, S. (1998). Screw dislocations near a subsurface crack, *J. Phys. D: Appl. Phys.* **31**: 602–608.

Wang, Z., Ghoniem, N., LeSar, R. and Sriram, S. (2003). A parallel computer code for simulations of dislocation patterns in fcc crystals, to be sumitted, *Mod. Sim. Mat. Sci, & Engr.*

Westmoreland, J., J.A., S., F.A., S. and P.R., M. (1975). *Rad. Eff.* **26**: 1.

Whitley, J. (1978). Ph.d thesis, Nuclear Engineering Department, University of Wisconsin.

Wiffen, F. (1972). *Proceedings of the International Conference on Radiation-Induced Voids in Metals, Albany, NY, June 1971, CONF-710601, Corbett, J.W. and Iannello, L.C. (Eds.), National Technical Information Service, Springfield, VA* p. 386.

Wiffen, F. (1973). The tensile properties of fast reactor neutron irradiated bcc metals and alloys, *Nuclear Metallurgy* **18**: 176.

Wiffen, F. (1984). Effects of irradiation on properties of refractory alloys with emphasis on space power reactor applications, *Proc. Symp. on Refractory Alloy Technology for Space Nuclear Power Applications, CONF-8308130, Oak Ridge National Lab* p. 254.

Wilkinson, A., Roberts, S. and Hirsch, P. (1998). A.j. wilkinson, s.g. roberts and p.b. hirsch, *Acta Mater.* **46**: 379.

Xu, G., Argon, A. S. and Ortiz, M. (1997). Critical configurations for dislocations nucleation from crack tips, *Phil. Mag. A* **75**: 341.

Yamakawa, K. and Shimomura, Y. (1988). Defects in fission-neutron irradiated mo at high temperature in the joyo reactor, *J. Nucl. Mater.* **155-157**: 1211.

Youngblood, G., Jones, R., Morscher, G. and Kohyama, A. (1997). Creep behavior for advanced polycrystalline sic fibers, *in Fusion Materials Semiann. Prog. Report for period ending June 30 1997, DOE:ER-0313:22, Oak Ridge National Lab* p. 81.

Yu. N. Osetsky, A. S. and Priego, V. (1998). *MRS Symp. Proc.* **527**: 59.

Yu. N. Osetsky, D. J. B. and Serra, A. (1999). *Phil. Mag. Lett.* **79**: 273.

Zinkle, S. and et al. (1998). Research and development on vanadium alloys for fusion applications, *J. Nucl. Mater.* **258-263**: 205.

Zinkle, S. and Ghoniem, N. (2000). Operating temperature windows for fusion reactor structural materials, *Fusion Engineering and Design*.

Zinkle, S. and Snead, L. (1995). *J. Nucl. Mater.* **225**: 132.

Zinkle, S., Robertson, J. and Klueh, R. (1998a). Thermophysical and mechanical properties of fe (8 9%)cr reduced activation steels, *in Fusion Materials Semiann. Prog. Report for period ending June 30 1998, DOE:ER-0313:24, Oak Ridge National Lab* p. 135.

Zinkle, S., Snead, L., Rowcliffe, A., Alexander, D. and Gibson, L. (1998b). Effect of irradiation temperature and strain rate on the mechanical properties of v 4cr 4ti irradiated to low doses in fission reactors, *in Fusion Materials Semiann. Prog. Report for period ending June 30 1998, DOE:ER-0313:24, Oak Ridge National Lab* p. 33.

Figure 16: ISIS computational cluster

Figure 17: ISIS computational cluster racks.

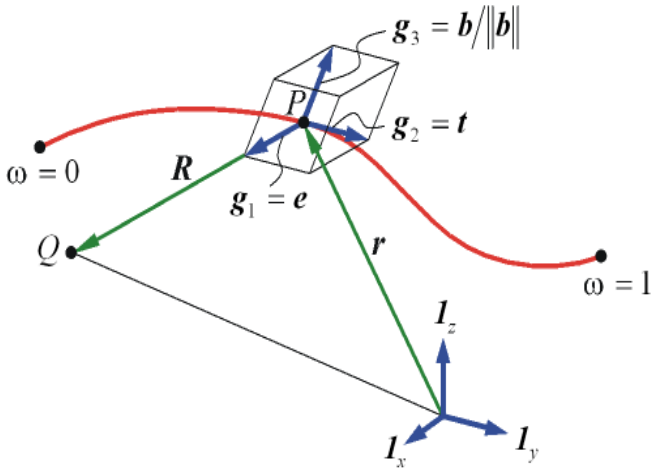

Figure 18: Parametric representation of a general curved dislocation segment, with relevant vectors defined.
After Ghoniem, Huang and Wang (2002))

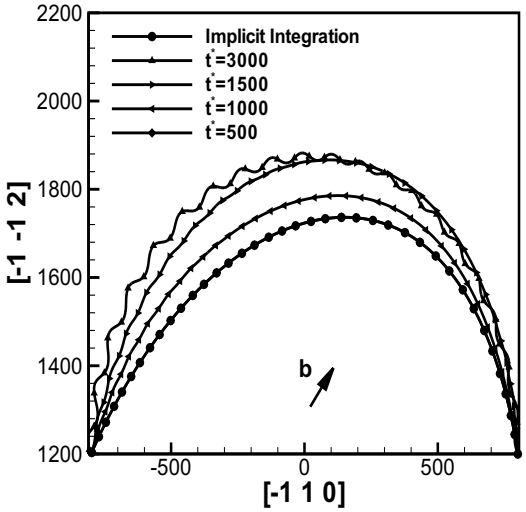

Figure 19: The influence of the time integration scheme on the shape convergence of an F-R source. Here, Burgers vector is chosen as $1/2[\bar{1}01]$ with applied uniaxial stress $\sigma_{11} = 80\ MPa$. (or $\tau/\mu = 0.064\%$)

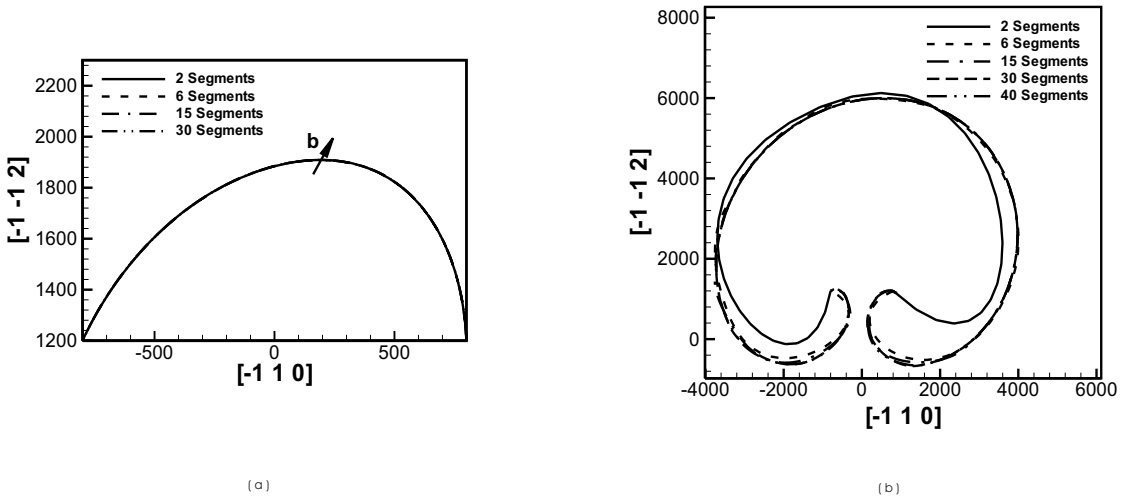

Figure 20: The influence of number of segments on the shape convergence of an F-R source

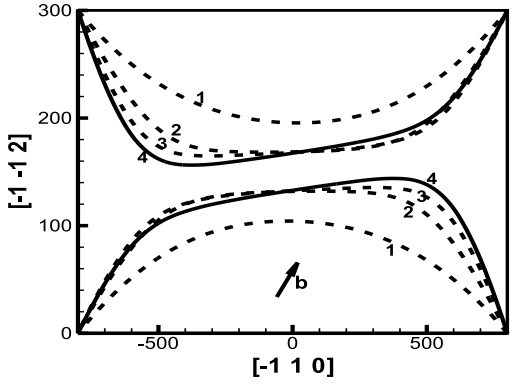

Figure 21: Two F-R source dislocations with the same Burgers vector($\mathbf{b} = \frac{1}{2}[\bar{1}01]$) but opposite tangent vectors gliding on two parallel (111)-planes ($h = 25\sqrt{3}a$ apart) form a short dipole in an unstressed state. The view is projected on the (111)-plane. Time intervals are: (1) 2.5×10^5, (2) 4.75×10^5, (3) 5×10^5 , (4) Equilibrium state

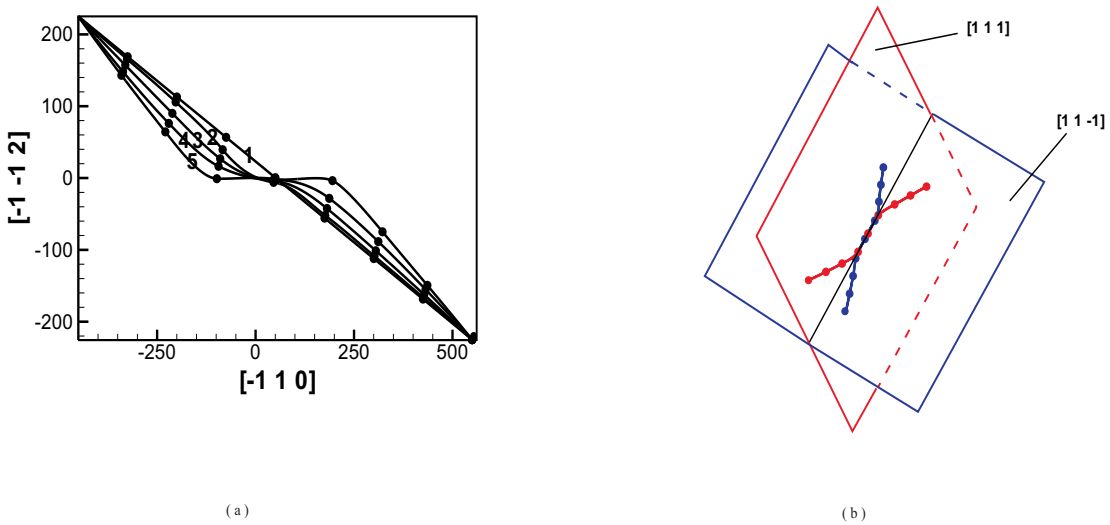

(a) (b)

Figure 22: Dynamics of 2 unstressed F-R sources ($\frac{1}{2}[01\bar{1}](111)$ and $\frac{1}{2}[101](11\bar{1})$) forming a 3D junction along $(\bar{1}10)$, $\mathbf{b} = \frac{1}{2}[110]$. (a) 2D view for the motion of the F-R source $(\frac{1}{2}[01\bar{1}](111)\frac{1}{2}[\bar{1}01](1\bar{1}1))$ on its glide plane(111). Time intervals are (1) initial configuration, (2) 1.5×10^4, (3) 5.0×10^4, (4) 1.3×10^5, (5) Final configuration. (b) 3-D view of the junction

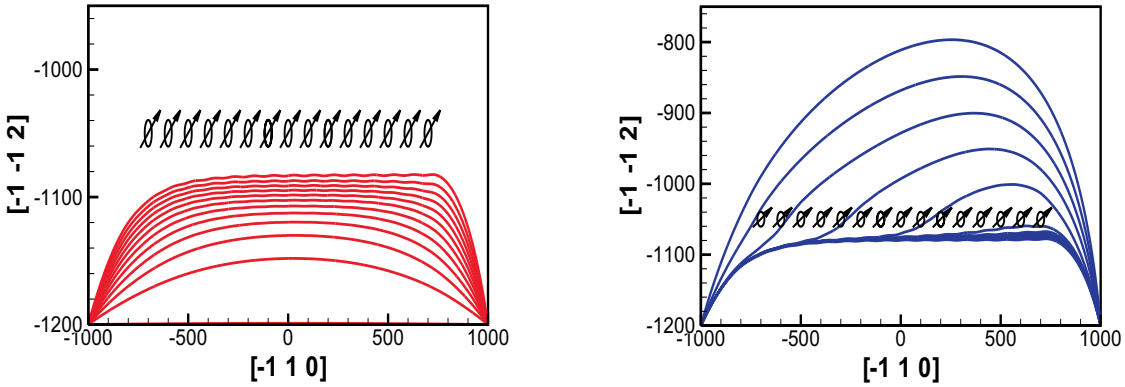

(A) (b)

Figure 23: Dynamics of dislocation *unsymmetrical unlocking* mechanism, from a cluster atmosphere of 15 equally distributed sessile interstitial clusters with diameter 40, stand-off distance 50 and inter-cluster distance 100. (a)Equilibrium state with equal shear stress interval 4MPa($\Delta\tau/\mu = 0.008\%$). (b)Unlocking state at stress state $\sigma_{11} = 120MPa(\tau/\mu = 0.0984\%)$ with equal time interval $\Delta t^* = 1 \times 10^5$.

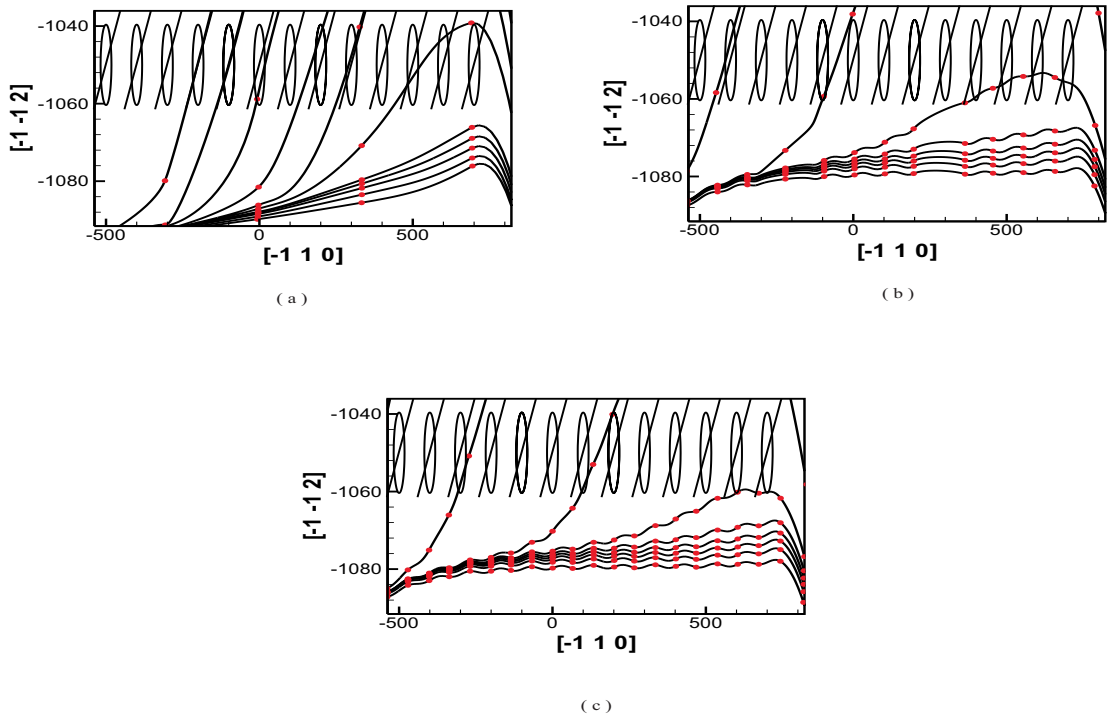

Figure 24: Comparisons of different nodal distribution of the details of unlocking mechanism. (a) 6 Segments. (b) 18 Segments. (c) 30 Segments.

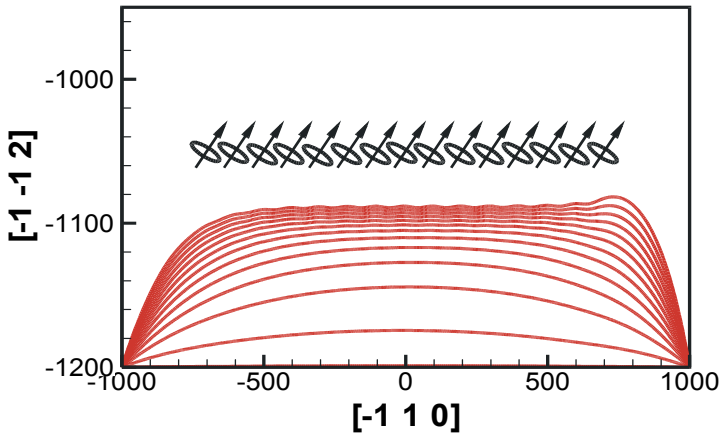

(a)

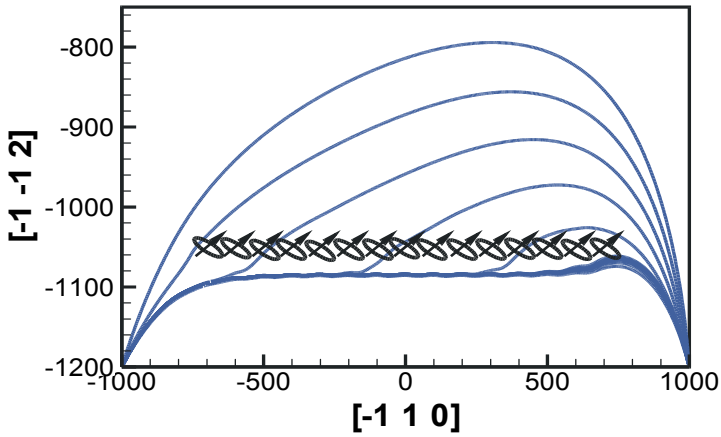

(b)

Figure 25: Dynamics of dislocation unlocking from the stress field of an SIA cluster atmosphere

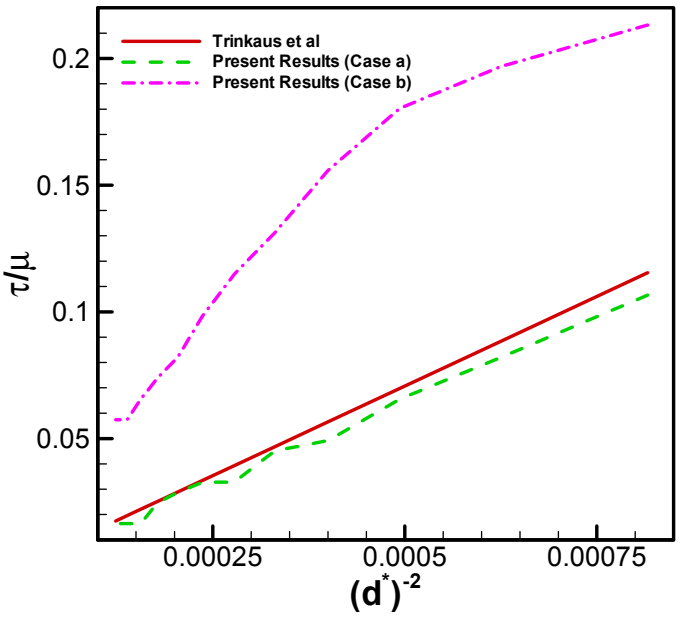

Figure 26: Dependence of the CRSS on the stand-off distance

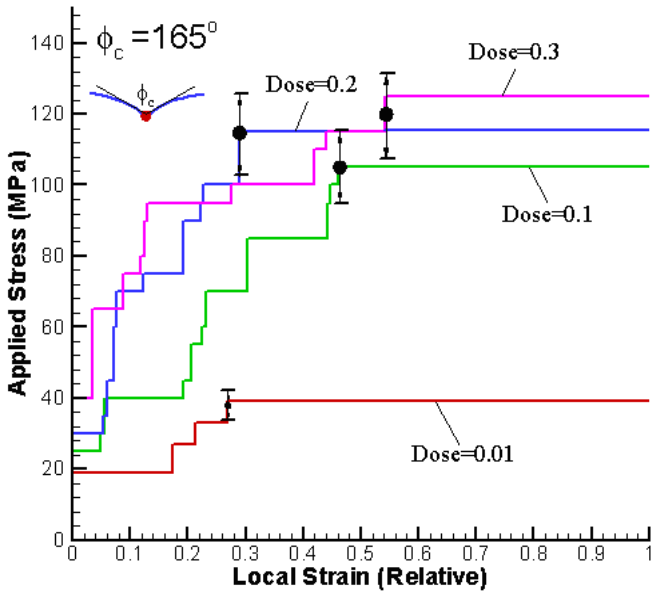

Figure 27: Local stress-strain diagrams at different doses for annealed Cu irradiated at 100 °C

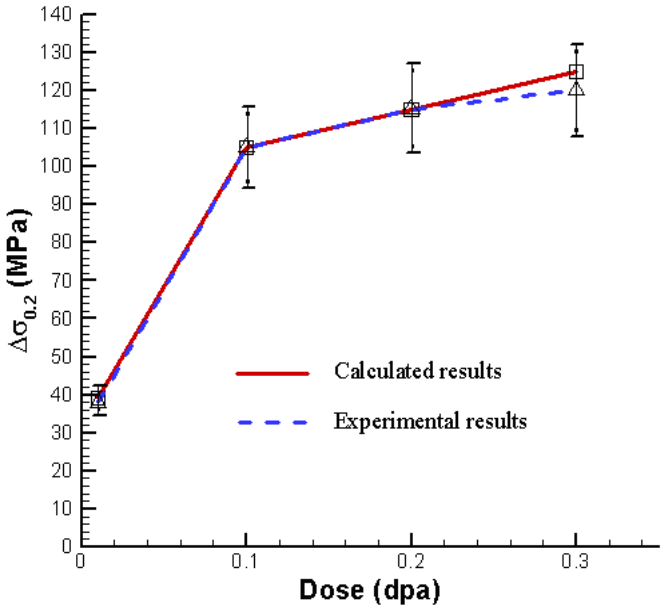

Figure 28: A comparison between results of computer simulations and experimental data for annealed Cu irradiated at 100 °C

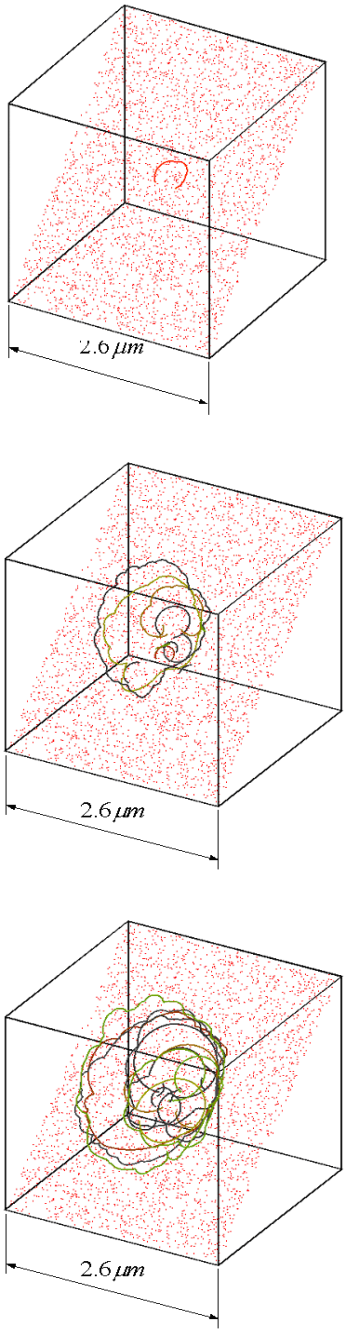
2.6 μm
2.6 μm
2.6 μm

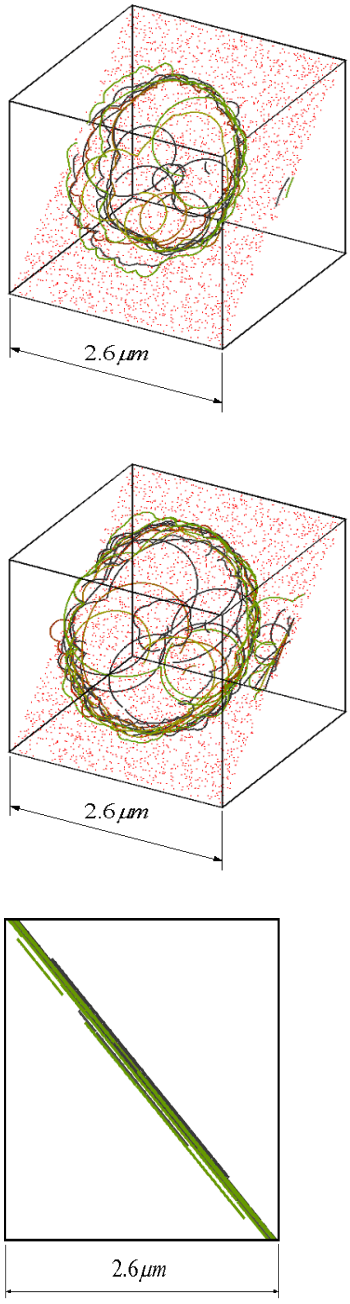

Figure 29: Various stages for the development of a dislocation channel in irradiated Fe. Figures (a-e) show the evolution of dislocation loops as they interact amongst themselves and microvoids on planes parallel to {101}-planes, while Figure(f) shows the dislocation channel edge-on (the $< 0\bar{1}0 >$-direction is towards the viewer

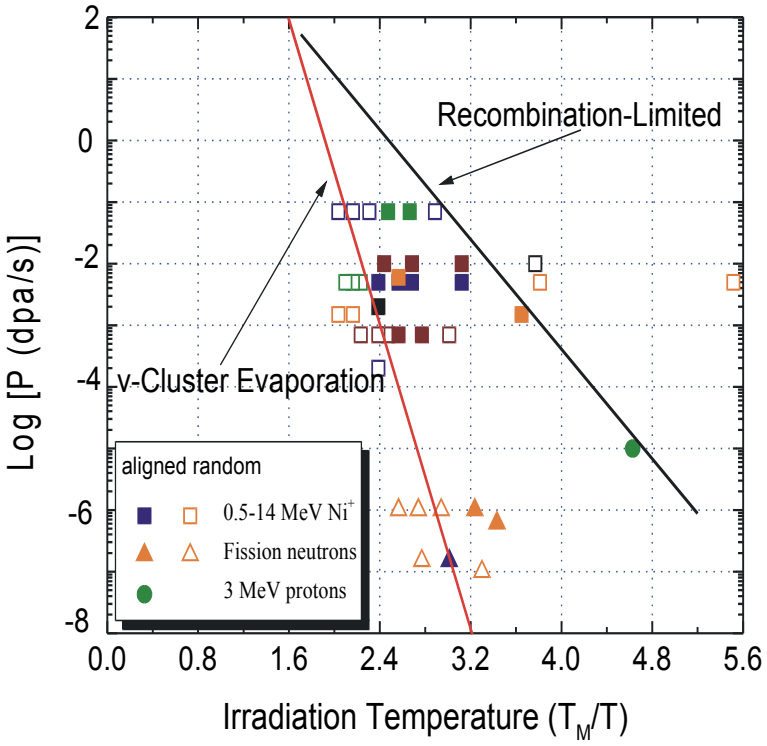

Figure 30: Comparison between experimental data and theoretical predictions for the temperature and dose rate dependence of defect cluster wall observations in irradiated nickel.

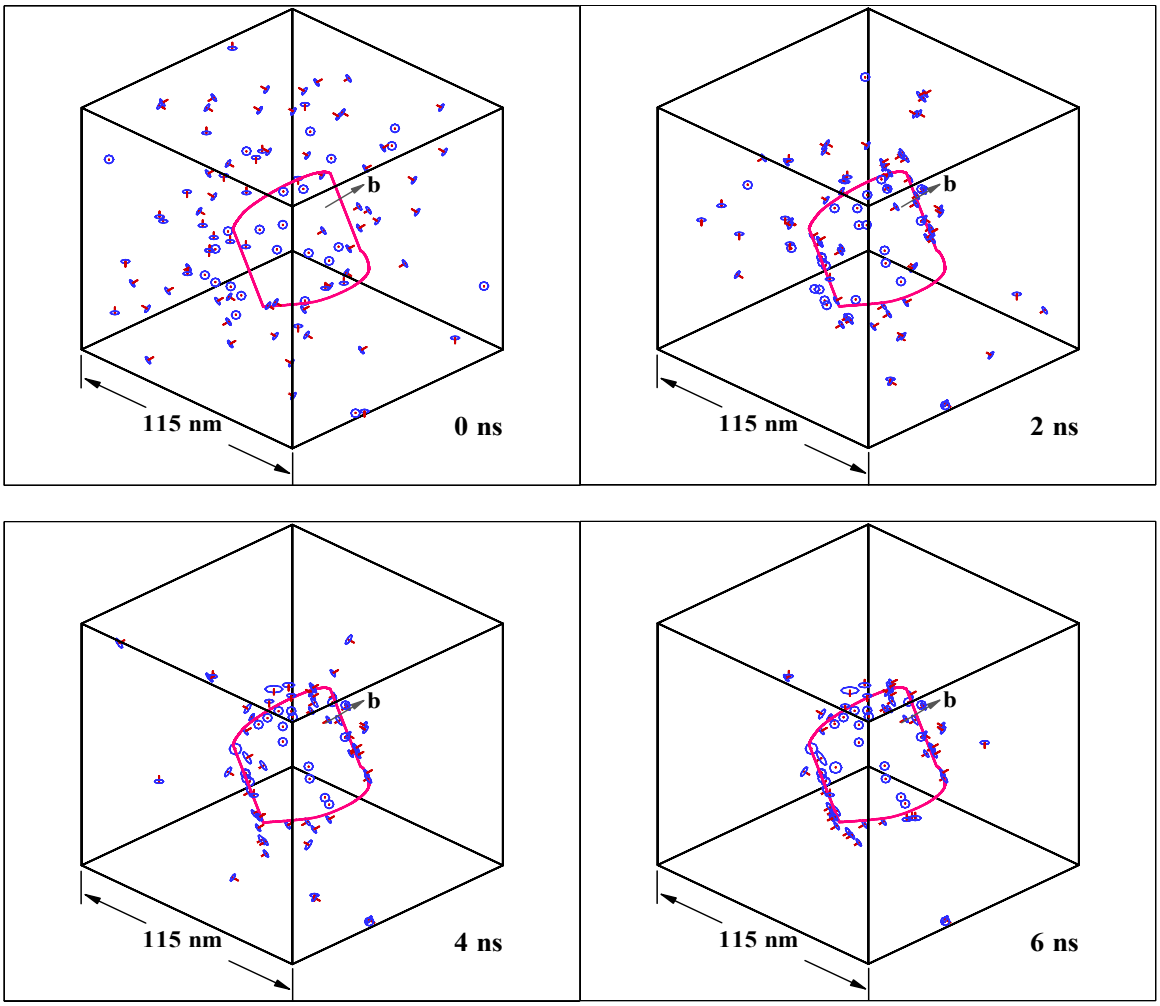

Figure 31: KMC simulation of SIA diffusion and clustering in the stress field of a 3-D dislocation loop. Self-assembled SIA loop *Rafts* are clearly observed on lower left corner, and close to edge orientations of the loop

Figure 32: Thermal analysis showing some detailed variations in structure temperature of a section of the FW/B module.